March 2008

UNIVERSITY OF CANTERBURY
Te Whare Wānanga o Waitaha
CHRISTCHURCH NEW ZEALAND

Organometallics in the Stabilization of Dyed Fibres

A thesis
submitted in partial fulfilment
of the requirements for the Degree of

Doctor of Philosophy in Chemistry

at the

University of Canterbury

by

Neroli Ayling

A Very Clever Brain could catch a Heffalump if he knew the right way to go about it.

- Pooh Bear, A. A. Milne

Table of Contents

Acknowledgements

I would like to thank a number of people who have made it possible for me to pursue higher learning. Firstly, my supervisor Associate Professor Richard Hartshorn, who not only guided me through the sometime turbulent seas of ‘real life’ research but also helped and assisted me in matters of personal growth. I am a better person for having worked under his supervision. Also my co-supervisor Dr Gerald Smith and Industrial Research Limited (IRL) who laid the ground work for my involvement in the project and gave me the financial backing, without which my continued studying would not have been possible.

I would also like to thank the University of Canterbury Chemistry Department as a whole. The willingness to help out students and the technical staff is amazing. Specifically, I would like to thank Professor Leon Philips, Dr Glenn Rowland and Alan Downward for their help with the laser studies and the maths behind the numbers. I would also like to thank Professor Ward Robinson and Dr Jan Waikira for their assistance with X-ray crystallography. In addition, I would like to thank Wayne, Rob and Bruce for keeping things running smoothly and not running away when they saw me coming with something to be fixed.

My time at university would not have been the same without my fellow students. The past and present members of the Hartshorn group: Reuben, Alan, Sarah, Paul, Deborah, Sam C., Andrea, Jocelyn, Ramin, Jana, Eleanor, Hayden, Sam S., Chris and Anna. Thanks also to the Steel group and the members of other Inorganic groups, for

providing a different perspective on inorganic chemistry and sharing their knowledge and expertise.

On a more personal note I have to thank my parents for a number of things, firstly life, which was an important requisite for attending university, secondly unconditional love and support and thirdly, which perhaps I should have mentioned first, money. I would also like to thank my more extended family for spreading out and giving me opportunities to visit all over the country and the world.

Big thanks must go to my friends, Jen, Clair, Emma, Andrea, Kat, Kathryn, Heather, Jodie, Grace, Suzanne, Jarred, Michael and Melissa for keeping me sane and not giving up on me when all my conversations started to steer towards chemistry. Thanks to my friends for reminding me that there is a whole world out there and not just a periodic table.

Most importantly, I would like to thank my husband Gareth. For keeping me grounded in life outside of chemistry. For being my biggest fan and cheerleader. For teaching me how to be an optimist. For keeping me fed and providing for me. Everything I am, and everything I do, is for you.

Abstract

It has been observed that in certain cases the exposure of dyed fibres to aging techniques results in the strengthening of fibres. This thesis explores the hypothesis that the strengthening is due to radical cross-coupling reactions that could be initiated through metal ion mediated photodecarboxylation. The approaches taken in this research include kinetic experiments (using flash photolysis), examination of possible cross-coupling experiments (using species of opposite charge), and the design and examination of small molecule model systems.

A flash photolysis system was developed and used in attempts to determine the rates of photochemical product formation for cobalt(III) amino acid complexes. Lower limits have been established for the rate of product formation in these systems. The lower limits are: 2×10^7 s^{-1} for $[Co(bpy)_2(gly)]^{2+}$; 2×10^7 s^{-1} for $[Co(tpa)(gly)]^{2+}$; and 5×10^6 s^{-1} for $[Co(tpa)(aib)]^{2+}$, where bpy is 2,2'-bipyridine; gly is glycinate; tpa is tris(2-pyridylmethyl)amine; and aib is aminoisobutyrate. In past studies, the rates of a series of cobalt(III) amino acid complexes were reported as being the same, and much slower. It is thought that in these cases it may not be the rate of the formation of product that was being measured, but rather the response time of the electronics that was being observed. In this thesis the results obtained for the rate for the aib complex were somewhat lower than those of the gly complexes. This may imply, for the aib complex at least, the rate of the formation of the metallocycle is being observed (and not the response times of the electronics or other limitations of the instrumentation), but the data is poor and there is considerable doubt about this.

The steady state photolysis of opposite charged species $[Co(bpy)_2(gly)]^{2+}$ and $[Co(EDTA)]^-$ is reported. The reactions were carried out on a small scale in deuterated solvent for NMR spectrometry analysis and also on a large scale for the possible isolation and characterisation of the products. Evidence was found for a different reaction occurring when both complexes were present. The exact nature of the product remains elusive.

A model system was designed in which a dinuclear ligand would bind to two metal centres and a fibre mimic would be later added. Eight ligands are discussed that could potentially bind two octahedral metal centres. They all had a xylene spacing group linking the two polydentate sites together. Five of the ligands have two bidentate binding sites. The other three had two tridentate sites.

The binding sites in three of the bis(bidentate) ligands were based on ethane-1,2-diamine (en). Two of these ligands produced hypodentate monocobalt and sundentate dicobalt complexes. The other two bidentate ligands were based on 2-aminomethylpyridine (ampy). Both of these ligands degraded in the complexation reaction conditions.

The binding sites in the tridentate ligands were all based on tacn. Once again, the principal products isolated were hypodentate systems in which only one metal ion was coordinated by the ligands.

There is a distinct pattern observed in the xylene spaced ligands to form hypodentate complexes with cobalt(III) metal centred complexes. There is evidence of the di-nuclear species from a reaction with a charcoal catalyst in the bis(bidentate) system.

^{1}H NMR spectrometry, ^{13}C NMR spectrometry, elemental analysis, X-ray crystallography and UV-vis spectroscopy were used to study and characterise the complexes and ligands that were prepared in this project.

Abbreviations

Δ	heat
ε	extinction coefficient
λ	wavelength
1D	One dimensional
º	degrees
Å	Ångström. 10^{-8} cm
A	absorbance
aa	amino acidate
A-25	anionic resin
aib	aminoisobutyrate
ala	alaninate
alum	$(K[Al(SO_4)_2]\cdot 12H_2O)$
ampy	2-aminomethylpyridine
asp	aspartate
B_{12}	cyanocobalamin
bpy	2,2'-bipyridine
C	Celsius
C-25	cationic resin
Calc.	calculated
CCD	Cambridge Crystallographic Database
cm	centimetre

CM	carboxymethyl
conc.	concentrated
COSY	2D ^{1}H NMR correlation spectrometry
cpg	2-cyclopropylglycinate
cys	cystinate
d	doublet
DEAE	diethylaminoethyl
dien	N^{1}-(2-aminoethyl)ethane-1,2-diamine
dientt	N,N',N''-tri(p-toluenesulfonyl)N^{1}-(2-aminoethyl)ethane-1,2-diamine
DMF	N,N-dimethylformamide
DMSO	dimethylsulfoxide
DMSO-d	deuterated dimethylsulfoxide
dpa	N,N-(2-pyridylmethyl)glycinate
EDDA	ethane-1,2-diamine-N,N'-diacetate
EDTA	ethane-1,2-diamine-N,N,N',N'-tetraacetate
EDTRA	ethane-1,2-diamine-N,N,N'-triaacetate
en	ethane-1,2-diamine
endt	N,N',-di(p-toluenesulfonyl)1,2-ethanediol
FTIR	Fourier-transform Infrared Spectroscopy
g	grams
glu	glutamate
gly	glycinate
glycol	ethane-1,2-diol
hν	photon of light

HSQCAD	Heteronuclear Single Quantum Coherence Adiabatic
I	transmitted intensity of light
I_o	incident intensity of light
I_a	light measurement of the first sample
I_b	light measurement of the second sample
I_d	light measurement with no analysing beam or laser flash
I_{df}	light measurement with no analysing beam
Im	imidazole
IR	infrared light
IRL	Industrial Research Limited
IUPAC	International Union of Pure and Applied Chemistry
k	rate
K	Kelvin
k_c	rate for ring closure
k_r	rate for radical ring arrangement
k_{-r}	rate for the reverse radical ring arrangement
l	length
L	litre
L	ligand
L-ala	L-alaninate
ln	natural log
LMCT	ligand-metal charge transfer
Log_{10}	log base 10
m	mass

m	multiplet
m	meta
M	mol L^{-1}
M	metal
M^{-1}	L mol^{-1}
mg	milligrams
mm	millimetre
mJ	millijoules
mL	millilitre
m.p.	melting point
M_R	relative molecular mass
nm	nanometre
NMR	Nuclear Magnetic Resonance
NOESY	nuclear Overhauser effect spectrometry
ns	nanosecond
o	ortho
OC-6	octahedral geometry
p	para
pgly	phenylglycinate
pH	$-\log_{10}[H^+]$
phen	1,10-phenanthroline
pn	propylenediamine
ppm	parts per million
R	side group
R_1	refinement factor

s	seconds
s	singlet
S	solvent
t	time
t	triplet
tacn	1,4,7-triazacyclononane
tacntt	N,N',N''-tris(*p*-toluenesulfonyl)-1,4,7-triazacyclononane
TBPY-5	trigonal bipyramidal
Tf	trifluoromethanesulfonate
TMPS	trimethylsilyl-1-propane sulfonate
TMS	tetramethylsilane
tpa	tris(2-pyridylmethyl)amine
tpy	2,2':6',2''-terpyridine
Ts	*p*-toluenesulfonate
UV	ultraviolet light
v	volume
V	volts
val	valinate
vis	visible light
W	watts

Chapter One

Introduction

Chapter 1

Introduction

Background research

Humans are visual creatures. For a long time we have been fascinated with colour. Through the ages it has been used in many ways by both people and nature to warn, distinguish and adorn. Examples of warning can be seen in a number of poisonous frogs and snakes being brightly coloured. This is a way of nature saying do not touch. The use of colour to distinguish can be seen in purple clothes previously only worn by nobility because of the high cost of producing purple dye.[1] Adornment can be seen in the variety of different colours of dyes being made very early in human history presumably for aesthetic purposes. Across the world, native people discovered techniques to decorate and dye their cloths.

Colour, as we perceive it, comes from a small region of electromagnetic radiation with wavelengths between 400 nm and 700 nm (Figure 1-1).[2] When radiation hits an object, it can be absorbed, scattered or reflected. Humans can distinguish between the different wavelengths absorbed, reflected and scattered: absorbing no visible light results in white or colourless substances, absorbing all visible light results in a black substance.[2]

Figure 1-1 Colour and Wavelength Relationship

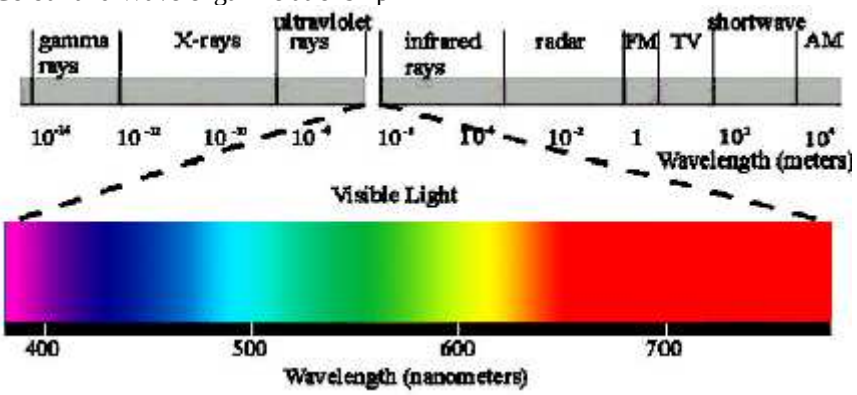

Dyes

Dyes are often organic aromatic compounds, with large conjugated systems.[2] The conjugated π-system means that there is a smaller energy transition between a lower energy orbital and the π* orbitals.[3] This means that light of a longer wavelength can excite an electron into the π* orbital.[4] Ultraviolet light can be used to promote an electron from the lower energy orbital to a higher energy orbital in a carbon-carbon double bond. The lowering of energy in conjugated systems shifts the energy of the transition into the visible region of the electromagnetic spectrum.[3] The dye absorbs the wavelength of light needed for the transitions. These compounds need to be attached to the cloth for the cloth to also be coloured.[5] In some cases, the fibre and dye bond just by coming in contact with one another to make the cloth change colour. These can be both permanent and non-permanent dyes.[6] One such class of non-permanent dyes is direct dyes. The direct dyes are usually long molecules that can lie along the cellulose fibre and make use of van der Waal forces such as hydrogen bonding. The direct dyes are not covalently bonded to the fibre and will bleed with each washing.[6]

Scheme 1-1 Different Binding of Dye and Fibre

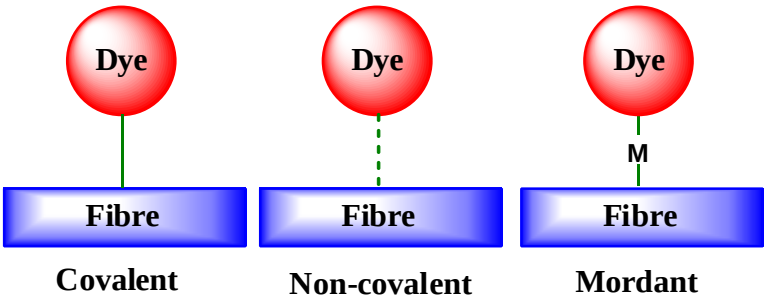

For permanent dyes that bond by just coming in contact with the fibre, ionic dyes can be used. These dyes fall into two broad categories: acid dyes and basic dyes.[6] Acid dyes are anionic and interact with cationic fibres and can be used on protein based fibre. Basic dyes are cationic and interact with negatively charged fibres; again they can be used on protein based fibres.[4] Attachment of the dye to the fibre involves the interaction of the ionic dye and the ionic fibre with opposite charge. Some dyes need a metal to fix themselves to the fibre, to bring out the colour, or both. Mordants are metal ions that are often used as a bridge, binding both to the fibre and to the dye, in order to make the dye permanent.[2]

The metal used can have an effect on the colour as well. The dye produced from the roots of the madder plant (*Rubia tinctorum*) is light red when prepared with aluminium mordant but is purple when prepared with iron.[7] Generally the dye and mordant form five or six membered chelate rings. This metal/dye coordination complex is referred to as a lake. Metals that were commonly used include iron, aluminium and tin. Without the metal present the dye may be removed with washing.

The range of colours available from traditional plant and animal sources is large and varied. Often a range of shades can be achieved by varying the dyeing time. For example Raurekau bark without a mordant metal can produce colours ranging from pale yellow to old gold, depending on how concentrated the solution is and how long the fabric is dyed for.[8] However, a mordant can still be used with Raurekau bark to produce different colours. Alum ($K[Al(SO_4)_2]\cdot 12H_2O$) produces a pinky fawn colour while copper or alum and soda can produce a fawn to dark brown colour; iron produces a deep brown and aluminium and soda produce a tomato shade.[8]

Looking at the archaeological catalogue there seems to be an evolution of colour. The oldest examples of dyed cloth from each region, stretching from Great Britain to East Asia, are in the red range.[9] Whether this is because it was the first, or because the red dyed cloth is long lasting, is yet to be determined. The oldest example of a dyed thread comes from Catal Huyuk which is in modern day Turkey.[9] Red dye came from a variety of sources; it is believed that one of the oldest results from soaking cloth in iron bearing mud like red ochre. There are also animal sources such as kermes (from the unlaid eggs of the scale insect *Kermes vermilio*) and plant sources such as madder (*Rubia tinctorum*), and the bark of various trees including oak or lichens such as litmus.[9]

Blue is usually the next colour, after red, to be discovered, again judging from the age of the blue dyed cloth found. It is presumed that the predominant blue dyes of ancient times are derived from berries. The other main source is what is called indigo blue. The exact source is unknown for each particular piece of cloth because there are several plant sources that contain the dye. In Europe, the source of blue was woad

(*Isatis tinctoria*) in the places where the indigo plant was not available.[7] Yellow usually followed blue but there are almost as many sources for yellow dyes as there are for red.[9] Some of these sources are still used today but are more predominant in cooking than dyeing such as saffron (*Crocus sativus*) and turmeric (*Curcuma longa*). Green was usually the result of combining some other colour with yellow, and was one of the later colours. Purple was sourced from molluscs such as *Murex brandaris* and *Purpura haematostoma*.[9] The initial liquid that comes out of the mollusc is yellowish white and oxidation has to occur (*e.g.* exposure to the air) before it is coloured purple.[9]

Interestingly, the majority of indigenous people all appeared to use metal mordant dyes for their black dye. The dyeing preparation for the Maori people saw them harvest the individual fibres with soaking and beating.[10] They then soaked them in an aqueous solution of a bark extract, followed by drying, rinsing and afterwards immersing in an iron-rich mud, paru.[10] In Tonga, it is sometimes the finished product that is decorated with printing and painting rather than the individual fibres. A brown-black dye is made by boiling a brown dye with some iron containing substance. Modern day sources of iron could include nails or cans.[11] However, traditionally it would have been a mineral source such as swamp mud. Another common source of black dye in Tonga is to add the soot of burnt candlenut (*Aleurites moluccana*) to one of the brown dyes.[12]

As mentioned before, a mordant can be used to fix, bring out, or change the colour of a dye. The Egyptians made use of this last property as a means of decoration. They would apply a different mordant to certain areas of a cloth. Then they would put the

whole cloth into a dye pot.[13] The different mordants would create diverse colours in altered areas. It is postulated that this technique was around in India long before it was used in Egypt and that it was bought from India to Egypt.[14]

Fibres of Interest

Industrial Research Limited (IRL) has an ongoing project exploring ways to increase the durability of cellulose- and protein-based natural fibres. The research includes finding ways to enhance the durability of the fibres with respect to light and thermal damage during and after dyeing. The IRL research is targeted towards the traditional dyeing methods of the Maori people on *Phormium tenax* (*harakeke*) and the natural dyeing of wool.

The chemical basis for the dyeing process involves metal coordination with functional groups, for example, hydroxyl or carboxylate groups, in the natural fibre. The cellulose fibre (Figure 1-2) *e.g. P. tenax*, is made up of β-1,4-glucose chains with available hydroxyl groups for coordination on the 2, 3 and 6 carbons. In addition, there is an amount of hemicellulose (Figure 1-3) which is the easily hydrolysed portion of branched cellulose and contains carboxylic acid groups. Protein based fibres (Figure 1-4) *e.g.* wool have side-chain carboxylic acids (in aspartic acid and glutamic acid) and thiol groups (in cysteine) able to bind a metal ion.[15] Through other coordination sites, the metal also attaches itself to the dye through the dye functional groups. The dye and the fibre are competing with each other to be bound to the metal.

Figure 1-2 Structure of Cellulose

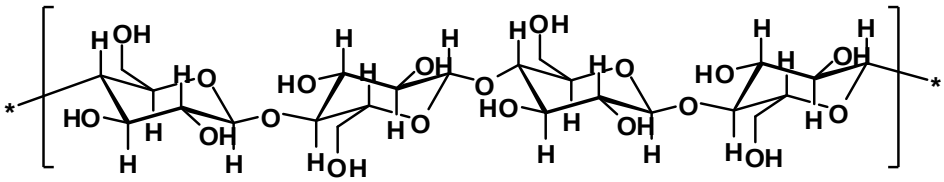

Figure 1-3 Example of the Possible Structure of Hemicellulose

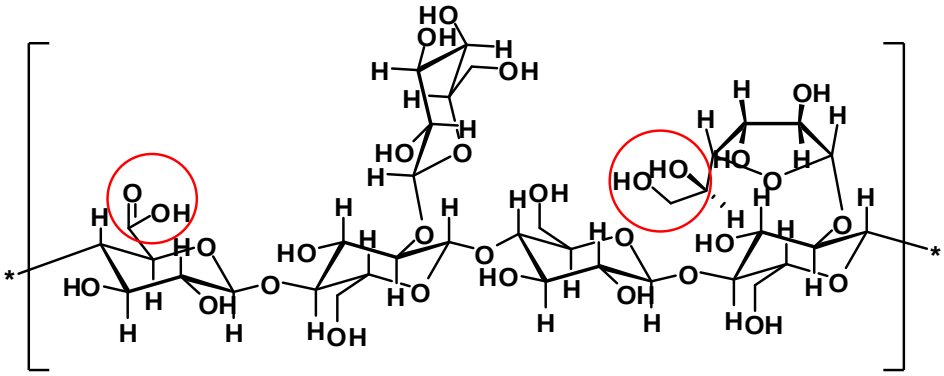

Figure 1-4 Example of a Protein Fibre

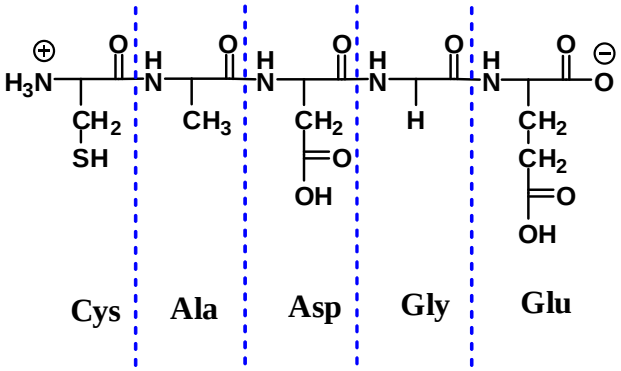

Previous Research

Research has shown that when exposed to an accelerated ageing technique (increased humidity, temperature and/or exposure to light) the fibres that have been prepared with a black iron tannate-dye tend to consume oxygen and produce carbon dioxide.[16] Physically, in most cases, it results in fading, brittleness, weakening and increased hot water solubility.[10] Surprisingly, when proteinaceous fibres (wool) are prepared in such a way that adjacent chains are held close to each other and then exposed to light, there is still loss of carbon dioxide but the overall physical result is a strengthening of the fibres.[15]

The loss of carbon dioxide suggests that decarboxylation is occurring and the quantity has been found to correlate with the extent of fibre degradation.[16] Photoinduced decarboxylations have been observed in metal complexes[17] and, given the involvement of metal ions in mordant dyes, the chemistry in the two systems may be related. The research suggests that the decreased substitution of the fibre chains by the dye is accompanied by an increase of interlocking neighbouring polypeptide chains (Figure 1-5).[15] In these circumstances the loss of carbon dioxide has resulted in the strengthening of the fibres. This gives rise to the notion that the strengthening could be the result of a cross-coupling reaction linking different fibres to each other by covalent bonds, rather than the result of van der Waals interactions. Presumably the two fibres must be close enough to couple with each other. Photochemical reactions often involve radical intermediates, and that may be the case for this system as well, as radical coupling is a well established reaction.[18-22]

Figure 1-5 Increased Substitution of the Metal by the Fibre Holds the Fibres Closer Together

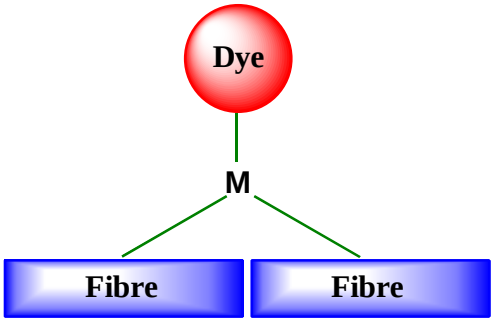

Natural fibres are sufficiently complicated to make study difficult. The fibres of most interest are cellulose (*P. tenax*) and protein based (wool). They are both complex systems with many components. Cellulose is primarily β-glucose but there are areas of hemicellulose which are not well defined or differentiated from cellulose and provide cross-linking between the cellulose chains.[3] Hemicellulose is a hexose and pentose polysaccharide which is easily hydrolysed and contains carboxylic groups. It is predominantly the hemicellulose area that is coordinated to the metal ion.[23] Similarly, peptides are also very complex with many different amino acids but those with a carboxylic side chain (aspartic acid and glutamic acid) or thiol side chain (cysteine) are likely to coordinate to the metal ion.[15] Working with the whole fibre means working with a lot of components that do not contribute to the system of interest and this makes it harder to characterise and analyse the results. Using the whole fibre would require characterisation of the solid phase which is more difficult than studies in the solution phase.

Background Chemistry

Because of the photochemistry involved, the metals used in this study must have two stable oxidation states one electron away from each other. The three most obvious

candidates are iron, copper and cobalt. Iron has two common oxidation states iron(II) and iron(III), and is the metal used in traditional black metal tannate dyes. It makes sense that this could be used.[10] Copper has two common oxidation states copper(I) and copper(II) and is readily available as many salts. Cobalt has two common oxidation states cobalt(II) and cobalt(III) and its inert and diamagnetic nature as the cobalt(III) ion means it can be characterised by NMR techniques.[17] For these reasons cobalt(III) complexes will be the initial area of interest for this work.

Numerous studies of cobalt(III) complex photochemistry can be found in the literature. This discussion will be limited to the photochemistry of cobalt amino acid complexes, as this topic is most relevant to the work described in this thesis. The photodecarboxylation of cobalt amino acid complexes is postulated to proceed through a radical mechanism resulting in a metallocycle (Scheme 1-2).[24]

Scheme 1-2 Mechanism for Photodecarboxylation of Cobalt(III)

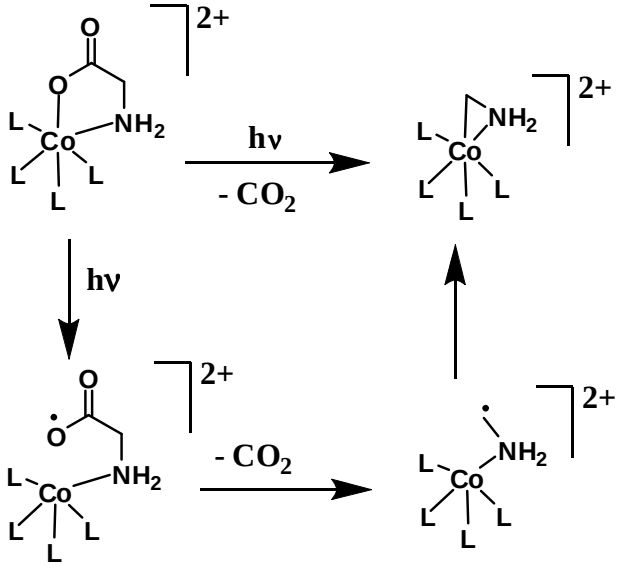

Irradiation with light produces a radical pair, cobalt(II) species and an aminoacyloxy radical. Aminoacyloxy radicals are unstable and decompose to give carbon dioxide and the amino alkyl radical ligand. The cobalt(II) ion is still bound through the nitrogen atom to the amino alkyl radical ligand. The radicals can re-oxidise the cobalt(II) centre and make a Co-C bond and, in this case, a three-membered ring.[25]

Studies by Telfer in 1999, on the UV photolysis of cobalt(III) amino acid complexes with substituents on the α-carbon atom, did not result in stable products containing a metallocycle.[17] The complexes decompose to give carbonyl products, that presumably result from a hydrolysis of an iminium ion. One of the complexes studied was $[Co(bpy)_2(cpg)]^{2+}$, where cpg is 2-cyclopropylglycinate. Cpg was used as a radical clock and the results show retention of the cyclopropyl group in the products. This means that if the reaction did proceed through a radical reaction, the radical has a lifetime of less than 10^8 s^{-1}.[17] The rate of this step has been examined by flash photolysis and reported in 1992 by Natarajan as being 10^3 s^{-1}.[26] This is inconsistent with the results obtained by Telfer. Flash photolysis studies were carried out by Lewis to investigate the rate of formation of the metallocycle in cobalt(III) amino acid complexes.[27] The results obtained led to a rate of 4.6×10^3 s^{-1} for photochemical reaction of the $[Co(bpy)_2(gly)]^{2+}$ complex, which is similar to that of Natarajan's results. There was, however, some doubt about the appropriateness of the experimental setup, and one goal of this research project was to revisit this system.

Formation of metal-carbon bonds similar to those produced in the amino acid photochemistry may have a role in fibre coupling. If two alkyl radicals are in close proximity they can couple together to make a C-C bond. In this case, however, the

radicals are short lived and reactive species, and it is more likely that the radical reacts with the metal centre to form the more stable metallocycle, rather than exist as the radical. If a second alkyl radical is formed it could react with the metallocycle. Thus, binding of metal ions to fibres could lead to cross-linking mediated by free radicals if this kind of chemistry occurs.

There is a literature precedent that may have some relevance to this chemistry. ethane-1,2-diamine-N,N,N',N'-tetraacetate anion (EDTA) has been reported to be formed from the coupling of two nitrilotriacetate anions coordinated to cobalt(III) and subjected to photolysis (outlined in Scheme 1-3).[25] The exact mechanism is not known but two possible intermediates are shown (Figure 1-6). The coupling could occur either as a dimerisation of either species or as a reaction between the two species. An important feature of this system is the fact that two of the cobalt complexes can come close to each other because they are neutral. Most such amino acid complexes are cationic, and electrostatic repulsion would presumably prevent dimerisation, in those cases.

Scheme 1-3 Formation of EDTA through Radicals

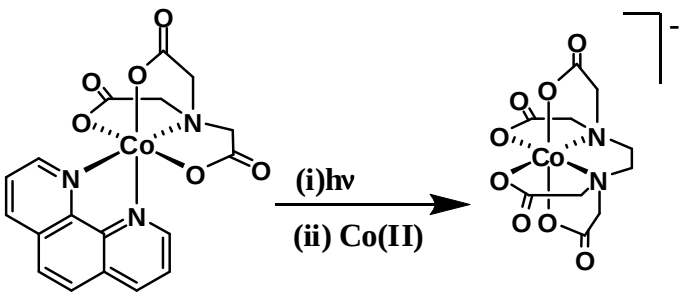

Figure 1-6 Possible Intermediates

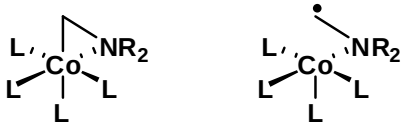

There are two ways to improve on this literature system and model the fibre coupling. The first would be to have opposite-charged species that are attracted to each other. The other would be to design a molecular system in which they are already close to each other, through the use of dinuclear systems (Figure 1-7). This thesis details attempts to explore those possibilities.

Figure 1-7 Example of a Dinuclear Ligand Model System

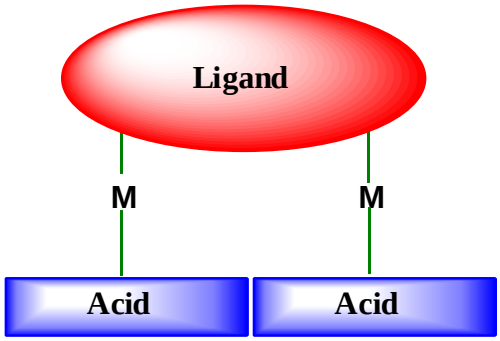

Dinuclear ligands can be made with a known distance between binding sites. It is possible to manipulate how close the metals are by changing the ligand. Small molecules with the appropriate functional groups (*e.g.* carboxylates) will then be added to the complex and treated in attempts to induce photochemical cross-linking reactions that may mimic the intrinsic fibre chemistry. The same reactions that would take place with the whole fibre should, in principle, occur within the model system, but with straightforward spectra and simpler characterisation.

Building and designing a ligand is a fluid process. There is no guarantee that what is predicted and theoretically meant to happen will be what ends up occurring. Polydentate ligands have the ability to bind to a metal through more than one atom. For a variety of reasons this may not be the case and one, or more, donor sites may be left unbound. Constable coined the phrase hypodentate to mean "a ligand in which fewer than the maximum number of donor atoms are involved in the interactions with metal centres."[28] Constable also coined the phrase sundentate to mean the opposite case where all of the donor atoms are involved in interactions with metal centres. The reason for a ligand being hypodentate is due to either steric hindrance or protonation of the ligand that prevents coordination of the ligand to a metal.[29] In the past, hypodentate complexes were accidentally made as a result of unforseen circumstances. Recently, there have been examples of where the complexes were made on purpose.[30] In examples where there are multiple sites for different metals to bind, such as in the dinuclear ligand in this research, there is a possibility that only one of the ligand donor sites will bond to the metal, or, in a few cases that both ligand donor sites will bond to the same metal.

The Metal

Because of the photochemistry involved, the metal used in this study must have two stable oxidation states differing in one electron. As stated before, copper, iron and cobalt metals all satisfy these requirements. Cobalt is a favoured choice for a number of reasons. Cobalt has common oxidation states cobalt(II) and cobalt(III), and its inert and diamagnetic nature in the cobalt(III) state means it can be characterised by NMR techniques prior to the photochemical reaction and after the reaction.[17] Iron and copper also have the option of being diamagnetic; iron(II) low-spin and copper(I). For

this research, however, it is necessary for the higher oxidation state to be diamagnetic because the lower oxidation state is only made transiently in the reaction. For these reasons cobalt(III) complexes were the focus for this work.

Selection of Ligands

The criteria for the ligands were that they were capable of coordinating two metals with a possible site to introduce a fibre mimic on each metal. The fibre mimics, most likely carboxylate ligands, should be close enough that a cross-coupling reaction could take place. Nitrogen type donors were chosen because they are known to bind many different kinds of metals in a range of oxidation states.

Figure 1-8 Ligands Described in this Thesis

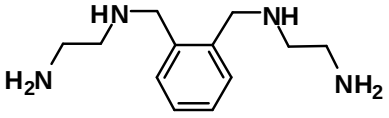

L4.1

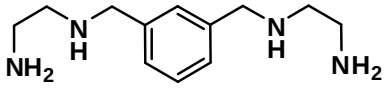

L4.2

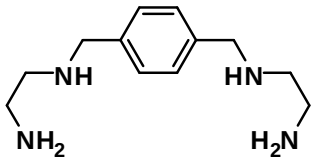

L4.3

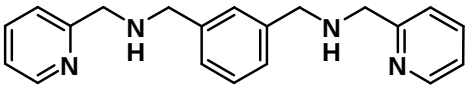

L4.4

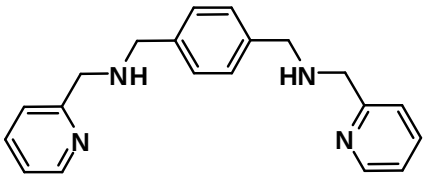

L4.5

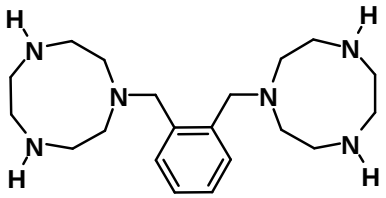

L5.1

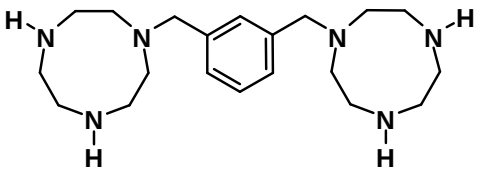

L5.2

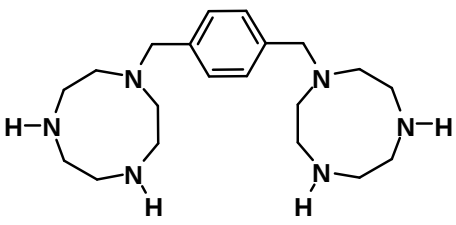

L5.3

A number of ligands were identified as possible suitable candidates for study (Figure 1-8). These were synthesised, and for various different reasons, usually difficulties with synthesis of ligands or complexes, some of those identified were later abandoned. The eight ligands reported in this work are 1,2-, 1,3-, 1,4-bis(2-aminoethylaminomethyl)benzene,[31](**L4.1**, **L4.2**, **L4.3**); 1,3-, 1,4-bis({2-pyridylmethyl}aminomethyl)benzene, (**L4.4**, **L4.5**) and 1,2-, 1,3-, 1,4-bis(1,4,7-triaza-cyclonon-1-ylmethyl)benzene (**L5.1**, **L5.2**, **L5.3**).[32]

Possible Fibre Models

The dinuclear complexes were to be prepared from the ligands chosen and the remaining coordination sites were then to be used to coordinate fibre mimics such as carboxylate containing ligands. The complexes were to be characterised and then subjected to photolysis. The relevant protein sidechain binding sites are likely to be those of aspartic acid and glutamic acid. These both have carboxylic acid functional group that binds to the metal. The fibre mimics were most likely going to be carboxylic acids. As well as being a good fit to the protein based fibres, the acids can imitate cellulose fibres, in particular the hemicellulose region.

When deciding which acid to use, a look at the resulting coupling species that would be generated is helpful. Ideally the R group would be able to support a radical, yield a stable detectable species on coupling and be derived from a carboxylic acid that is commercially available or easily prepared. The acids chosen for this work are 1,5-pentanedicarboxylic acid (pimelic acid), 1,6-hexanedicarboxylic acid (suberic acid), 2-phenylacetic acid and 3-phenylpropanoic acid (hydrocinnamic acid) (Figure 1-9). These four were chosen for two main reasons. The first is that they were inexpensive

and available from commercial sources and secondly that the possible photo product would be easily detectable using NMR spectrometry. Photoinduced coupling in the first two cases may result in cyclic products being formed, while larger and hopefully easily identifiable products will result in the latter cases.

Figure 1-9 Selection of Readily Available Acids

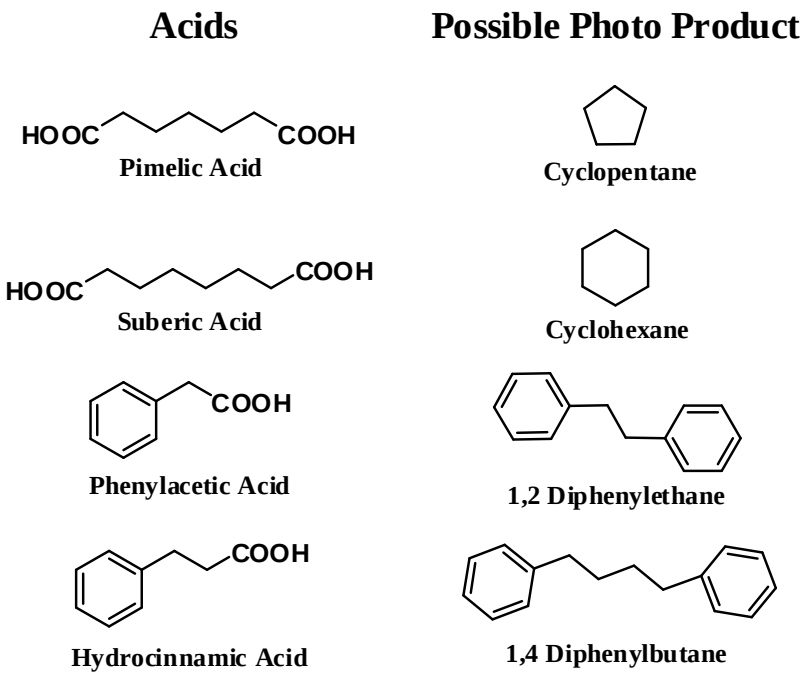

WORK DESCRIBED IN THIS THESIS

The key objective of this project was to understand what is happening at the molecular level in the fibre-metal-dye system. This was approached in three ways. The first way, the subject matter of **Chapter 2**, was to get a better understanding of the mechanism and rate of the reaction, especially in the light of contradictory literature reports. This was done by trying to measure the rate of the photochemical

reaction in an attempt to the resolve this situation. In **Chapter 3** the second approach is discussed, which was to examine whether a cross-coupling reaction could occur between opposite charged species, and to test the ability to predict and detect photoproducts. This was attempted using steady state photolysis methods. This involves following the reaction by NMR spectrometry, or trying to isolate material from bulk reactions. The third approach was to design, synthesise, and study a small molecule model system in order to better understand what might be occurring in the fibres. This is dealt with in **Chapter 4** and **Chapter 5**. These chapters report on the design and synthesis of a section of ligands, and the attempts made to synthesise dinuclear complexes of the ligands.

Chapter Two

Flash photolysis studies

Chapter 2

Flash photolysis studies

INTRODUCTION

Past Research

Being a chemist requires having an innate curiosity of the why and how. Quite often they go hand in hand. To find out why a reaction proceeds the way it does is usually linked to how it proceeds. The how of a reaction is its mechanism. One way in which one can begin to be understand the mechanism is by collecting kinetic data. Flash photolysis studies are a means of collecting such data for photochemical reactions.

This chapter outlines kinetic studies that were undertaken in order to inform discussion of possible mechanisms of photochemical reactions of cobalt(III) amino acid complexes. Using laser flash photolysis, the rates at which the products are formed from photodecarboxylation of $[Co(bpy)_2(gly)]^{2+}$, $[Co(tpa)(gly)]^{2+}$ and $[Co(tpa)(aib)]^{2+}$ can be measured. Through these measurements information about the reaction mechanism and pathway may be inferred and this may provide us with a better understanding of light induced polymer chain cross linking in the fibre.

In the past, photochemical reactions of inorganic compounds were placed into one of three categories; redox reactions, photosubstitution or photoisomerisation. Reactions in which the ligand underwent reaction, but the rest of the complex remained unchanged, were classed as exceptional cases or as part of organic chemistry rather than true inorganic photochemistry. In a review paper in 1988, Poznyak and Pavlovski proposed that reactions of ligands should be considered a fourth reaction category in inorganic photochemistry. That paper summarised the current knowledge up to that point.[24]

The radical pair theory was postulated by Adamson *et al*. and was used to describe the three original photochemical reaction types.[33, 34] Adamson used radical pair theory to explain the photochemical reactions of the complexes $[Co(NH_3)_5X]^{2+}$ (where X = Cl^-, Br^-, I^-, NO_2^-, SCN^-). The complexes were irradiated by light in the LMCT band region. This resulted in the Co-X bond breaking and forming a radical pair of cobalt(II) complex and X. The radical pair can then react further *via* redox, solvation or recombination processes. In the cases where X = NO_2^- or SCN^- the recombination can be through a different atom, which results in isomerisation rather than regeneration of the original complex.

Poznyak and Pavlovski extended the radical pair theory to explain the photochemical reaction of ligands. If ligand X is made up of several atoms or groups it can undergo reaction such as a rearrangement or elimination of a section of the ligand. The review paper details a number photochemical ligand reaction types, concentrating mainly on elimination reactions, such as photolytic elimination of N_2 from azido complexes. The section most relevant to our work was that on photodecarboxylation of

aminocarboxylate complexes to give metallocyclic products. Some metal carboxylates can also be decarboxylated, leading to formation of M-C bonds.

A key result in elucidating this chemistry was the X-ray structure solution of the photolysis product $[Co(bpy)_2(CH_2NH_2)]^{2+}$. This revealed a three-membered Co-C-N ring.[35] Since then, other similar photodecarboxylation products have been isolated. The loss of carbon dioxide and contraction of the chelate ring has been observed for rings of differing sizes. A series of complexes of the type $[Co(en)_2(aa)]^{2+}$ (where aa = glycinate,[36] β-alaninate[37] or γ-aminobutyrate[38]) were photolysed and the reaction products obtained were metallocycles with three-, four- or five-membered chelate rings respectively. The three-membered ring was highly strained and the complex could not be isolated in the solid form. Unlike $[Co(bpy)_2(gly)]^{2+}$ there are no π-acceptor ligands to stabilise the M-C bond.[24] The four- and five-membered rings were less strained and X-ray structures were obtained.

Poznyak and Pansevich proposed a mechanism for the reaction (Scheme 2-1).[36, 39] In this scheme, the radical pair formed is one in which the cobalt(II) atom is still bonded to the aminoacyloxy ligand radical through the amine nitrogen atom. The aminoacyloxy radical decomposes to give carbon dioxide and the corresponding alkyl radical which is then trapped by cobalt(II) and recombines to form the cobalt-carbon bond.

Scheme 2-1 Mechanism for the Photodecarboxylation of $[Co(bpy)_2(gly)]^{2+}$

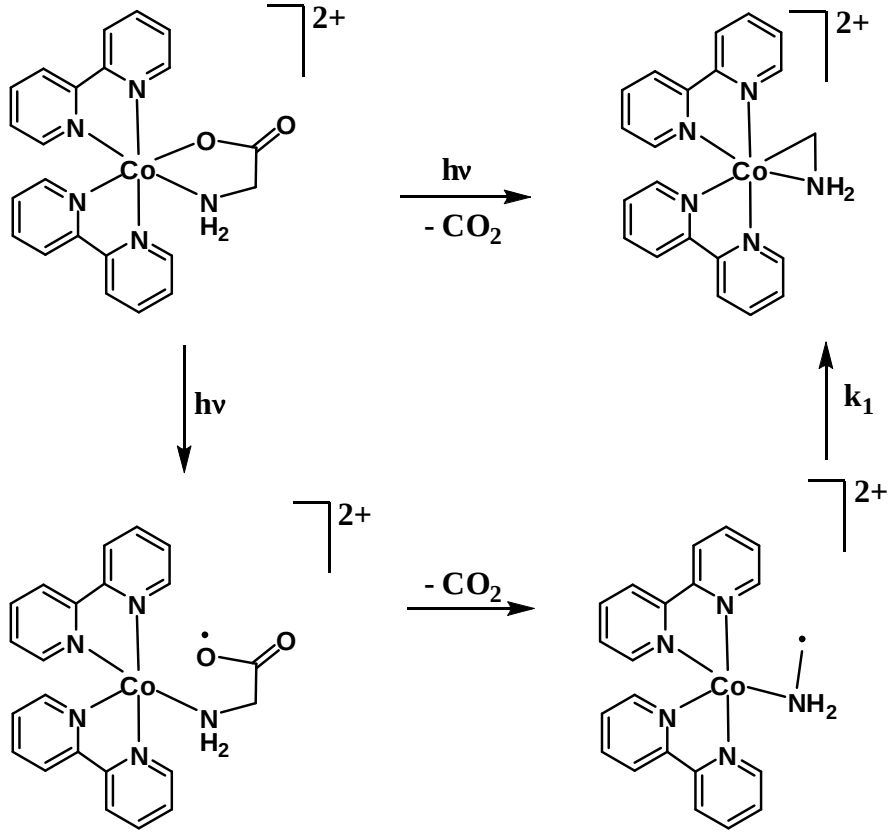

Natarajan and co-workers have done extensive studies on the photolysis of metal-acid complexes. In one of his earlier papers with Ferraudi, copper complexes with amino acids were studied.[40] In this work it was found that some species were produced through secondary reactions between a copper(I) or copper(II) species and a carbon centred radical. A communication in 1989 reported the investigation of $[Co(en)(bpy)(gly)](ClO_4)$ by flash photolysis.[41] It was reported that the rate constant for the formation of a transient species is 8.6×10^4 s^{-1} at pH 3. Steady state photolysis of the complex formed $[Co(en)(bpy)(CH_2NH_2)(H_2O)]^{2+}$ (Figure 2-1). The formation of this complex had been reported earlier by another group.[42]

Figure 2-1 Structure of $[Co(bpy)(en)(CH_2NH_2)(H_2O)]^{2+}$

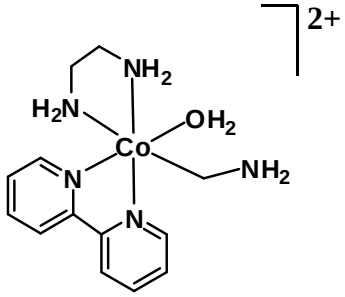

In 1992, Natarajan and Natarajan[26] reported further photochemical studies on a range of cobalt(III) complexes. In their experiments, they used laser flash photolysis to study the kinetics of photodecarboxylation of a number of amino acid containing cobalt complexes. Photolysis of $[Co(bpy)_2(gly)]^{2+}$ resulted in the relatively stable product that had earlier been characterised by Poznyak and Pavlovski being formed. The other complexes studied were $[Co(bpy)(en)(ala)]^{2+}$, $[Co(bpy)(en)(gly)]^{2+}$, $[Co(bpy)(pn)(ala)]^{2+}$ and $[Co(bpy)(pn)(gly)]^{2+}$. With these complexes the resulting species were unstable. These experiments recorded the rates of formation of the metallocycle product.

Natarajan and Natarajan assigned the rate determining step to be the intermolecular reaction of the alkyl radical and the cobalt(II) metal centre shown in Scheme 2-1 as k_1. The rate constant they calculated was around $4 \times 10^3\ s^{-1}$. The paper did not discuss the reasons behind the assignment. Presumably they considered that the first two steps would be fast reactions.

The results that Natarajan and Natarajan obtained, and the assignment of the cyclisation as the rate determining step, is worth further discussion. There are a number of reasons why this conclusion is puzzling.

The first reason is because bimolecular reactions between cobalt(II) metal centres and alkyl radicals have second order rate constants of around 10^8 M^{-1} s^{-1}.[43-49] This is a relatively fast second order reaction. Reactions of this type have been studied in order to model vitaminn B_{12} formation.[50, 51] It seems counterintuitive to propose a similar intramolecular reaction to be as slow as 10^3 s^{-1}.

The second reason is that the rate constant implies a half-life for the cobalt(II) complex with the alkyl radical ligand on the millisecond timescale. Cobalt(II) metal centres are known to exchange monodentate ligands rapidly in aqueous solutions.[52] This would suggest that the radical should be displaced by water molecules on a microsecond timescale.

The third point of concern is the fact that the results for all of the complexes are very similar. If radical recombination is the rate determining step, having different substitution on the radical carbon should change the rate depending on the stabilisation or destabilisation of the radical by the substituent. Radicals have one unpaired electron and are stabilised by groups that would normally stabilise a cation or an anion; such as electron withdrawing groups, electron donating groups or conjugated groups.

Further evidence that this work needed to be revisited is provided by work carried out by Telfer[17] using a radical clock. Telfer synthesised $[Co(bpy)_2(cpg)]^{2+}$ and employed steady state photolysis and ^1H NMR spectrometry to study the photolysis products. The cyclopropylmethyl radical can ring open with a rate constant of 1×10^8 s^{-1} at 298 K, as illustrated in Scheme 2-2. Calculations by Telfer indicated that substitution on the α-carbon atom does not greatly affect the rate, so a similar reaction, with the amine group on the carbon atom should occur at a similar rate.

Scheme 2-2 The Cyclopropylmethyl Radical Rearrangement

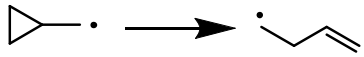

If this ring opening is to occur then the 'normal' reaction of the radical has to be slower that the ring opening. Possible reaction pathways are shown in Scheme 2-3. The product ratio (Ring Opened Products : Ring Closed Products) reflects the ratio of the rate constants (k_r : k_c). If k_r is known, then k_c can be calculated from the product ratio, i.e. the rearrangement rate acts as a clock against which k_c can be measured. In this case, for there to be exclusively ring closed products, k_c has to be much greater than k_r.

No ring opened products were observed. This indicates that a radical on the alkyl carbon is not present for as long a time as predicted by Natarajan. A few possibilities can explain the results. The reaction could proceed at the rate of 4×10^3 s^{-1} but does not go by way of a radical reaction. Alternatively, the reaction could proceed at the rate of 4.0×10^3 s^{-1}, but the cyclization of the alkyl radical is not the rate determining step. Another theory is that the rate is not 4×10^3 s^{-1}.

Scheme 2-3 Possible Reaction Pathways for $[Co(bpy)_2(cpg)]^{2+}$

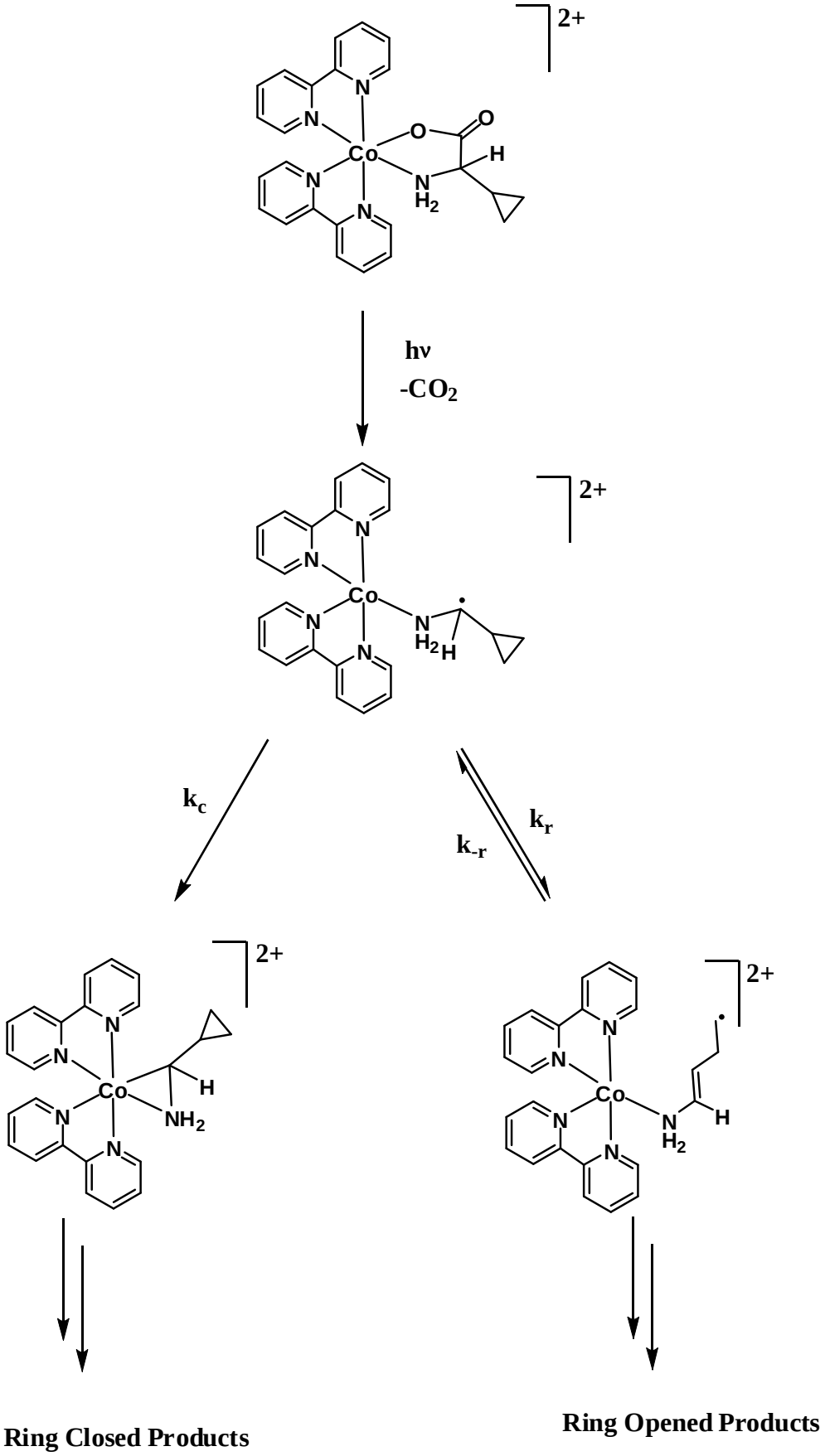

Further work was done by Lewis,[27] who attempted to repeat the work done by Natarajan. The setup that Lewis used was similar to that used by Natarajan. The compounds analysed were all of the type $[Co(bpy)_2(aa)]^{2+}$ where aa is gly, pgly, ala, L-ala, cpg and aib. Upon photolysis some of these produce a stable metallocycle while others produce a transient metallocycle which decomposes to give carbonyl-containing molecules and, eventually, cobalt(II) species.

The rate constant obtained for the formation of $[Co(bpy)_2(CH_2NH_2)]^{2+}$ was comparable to that previously reported and was approximately 4.6×10^3 s^{-1}. The rest of the complexes that form stable metallocycles have slower rates of around 4.0×10^3 s^{-1}. One of the complexes, ($[Co(bpy)_2(aib)]^{2+}$), does not form a stable metallocycle upon photolysis. After the metallocycle is formed it decays. The rate for the formation of the metallocycle was 1.3×10^3 s^{-1} and the decay rate for the metallocycle was 1.3×10^3 s^{-1} The data obtained may have been limited by the slow response time of the electronics used to monitor the reaction spectrophotometrically. Furthermore, the cell containing aqueous solutions of the complexes was found to luminesce on the same time scale as the reaction. These factors mean that any information about the photolysis reaction was likely to be obscured either by the poor response time of the equipment or hidden by the fluorescence of the cell.

Fearing that the main problem was the electronics, the laser set up was changed; preliminary experiments showed that a reaction that was much faster than that observed by Lewis, could be seen.

The compounds used in this work are $[Co(bpy)_2(gly)](ClO_4)_2$, $[Co(tpa)(gly)](ClO_4)_2$, and $[Co(tpa)(aib)](ClO_4)_2$ as seen in Figure 2-2. These compounds were selected for various reasons. It has been observed that upon photolysis, $[Co(bpy)_2(gly)](ClO_4)_2$ produces a relatively stable metallocycle. When bpy is substituted for other ligands such as en the product is less stable. However it is important to see what effect the auxiliary ligands play and if they have any bearing on the rate constant. To test this tpa was also used in some complexes to replace the bis(bpy). The amino acids used were chosen based on what had already been studied and what was readily available. They also have varying ability to stabilise a radical. The two methyl groups on aib as opposed to the two hydrogen atoms on gly should affect the rate of reaction if a radical species is involved in the rate determining step.

Figure 2-2 The Complexes used in the Photolysis Experiments

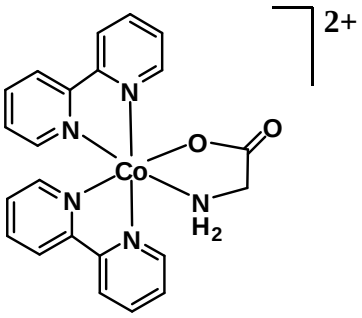

$[Co(bpy)_2(gly)]^{2+}$

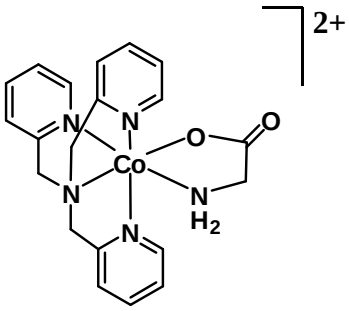

$[Co(tpa)(gly)]^{2+}$

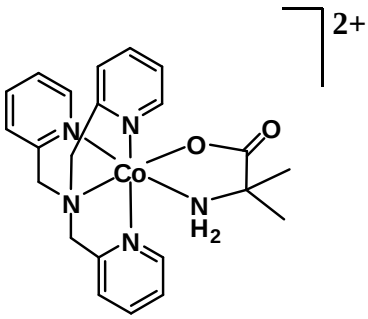

$[Co(tpa)(aib)]^{2+}$

RESULTS AND DISCUSSION

Method and Experimental Setup

Flash photolysis is an experimental technique where a sample is irradiated with a short pulse of light. The sample is then monitored (normally spectrophotometrically) and from the resulting data (change in absorbance as a function of time), rate constants can be derived. For our particular system (shown in Figure 2-3), the coordination compound is irradiated with Ultra Violet light, using a Kr/F laser at 248 nm, thus causing the photodecarboxylation to occur. Simultaneously a monitoring beam is also passed through the sample and the intensity of the transmitted light is measured with a photomultiplier tube. Changes in the photomultiplier voltage measured for this beam can be used to derive changes in the absorbance of the complex. This change is recorded on an oscilloscope. From this data it is then possible to determine an observed rate constant for each reaction.

A schematic of the cell and surrounding set up is shown in Figure 2-4. Pulses of 248 nm excimer laser light are reflected into the cell from above by a specially coated mirror with maximised reflectivity at 248 nm. The laser light passes through a slit which limits the flash to an area of 18 mm x 18 mm. This minimises the effect of light-scattering from the meniscus present at the cell walls.

Figure 2-3 Flash Photolysis Setup (from above)

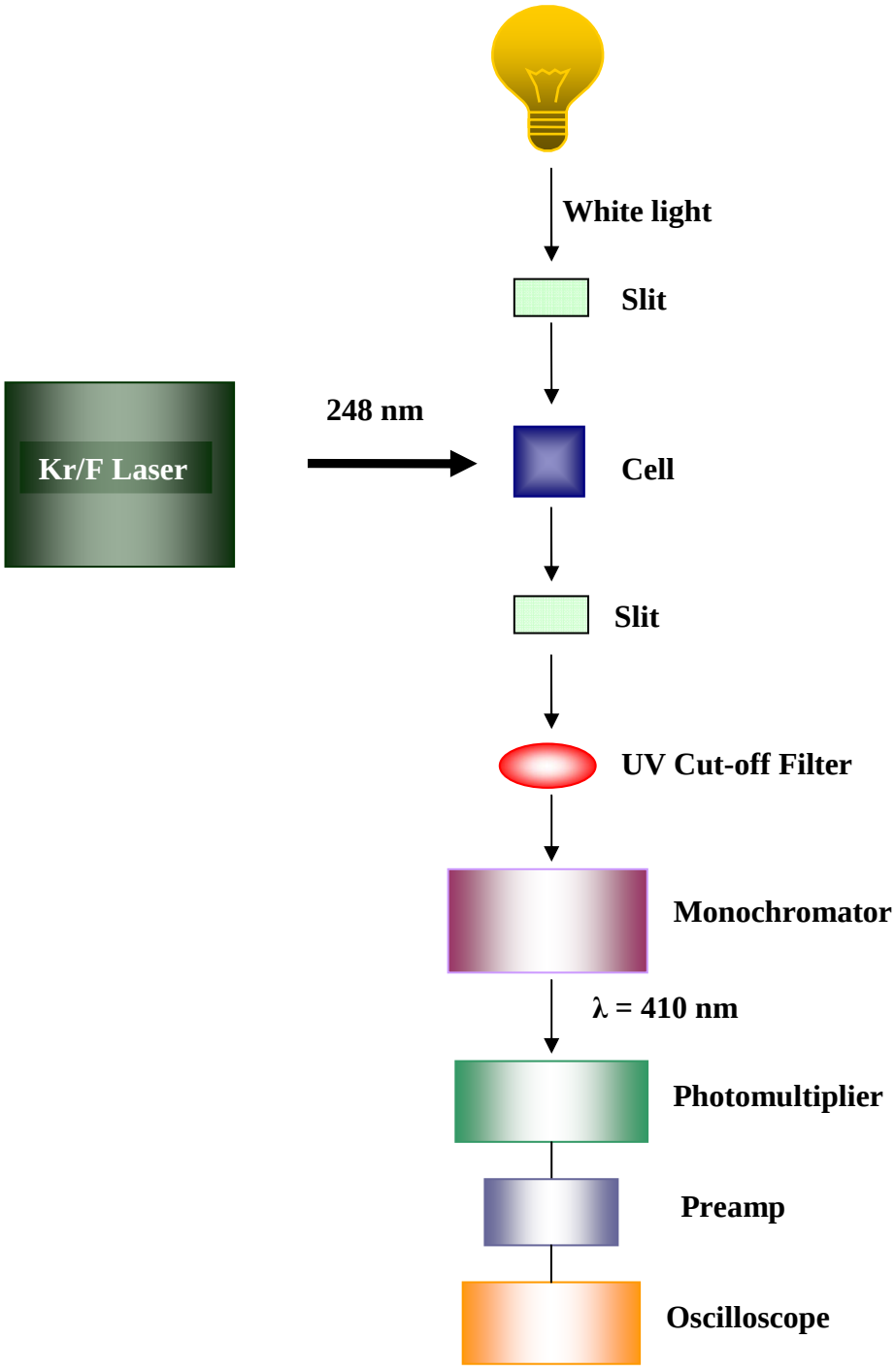

Figure 2-4 Setup showing Laser, Mirror and Cell (from side)

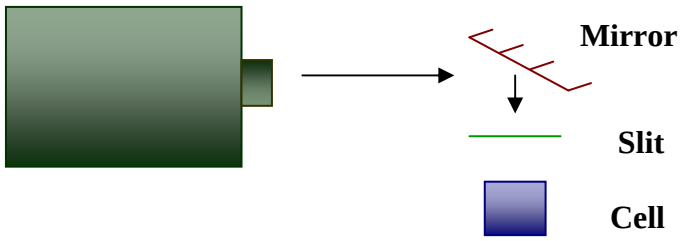

The cell as shown in Figure 2-5 was filled with the aqueous solutions of the required compound. The concentration of the solution was approximately 1 x 10^{-4} mol L^{-1} because this concentration works best for the irradiation and probing beam. After the cell was filled it was placed in position for the experiment.

Figure 2-5 The Cell

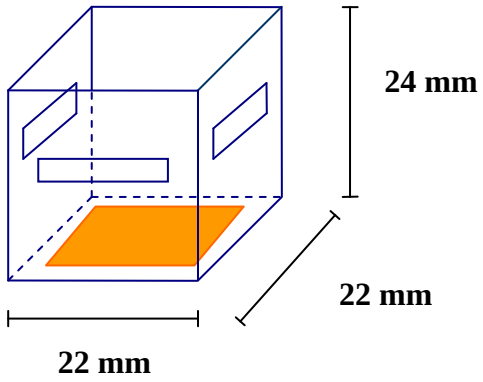

Experimental Discussion

The final set up described in the results section evolved from attempts to limit the interference and noise from various sources. The laser, probe beam light source, oscilloscope and pre-amp all remained the same as those used in earlier experiments. The major changes took place with the cell, the way the experimental components

were linked together, and the procedure. To begin with, the laser was readied after a long period of no use. The optics were cleaned and fresh exhaust gas scrubber was prepared.

The first system utilised was one that was already in place from previous experiments. The procedure followed was as close as possible to that described by Lewis. A quartz cell that was fixed in place was filled with target solution by a syringe system and the laser beam was positioned to hit the side of the cell Figure 2-6.

Figure 2-6 The Original Cell

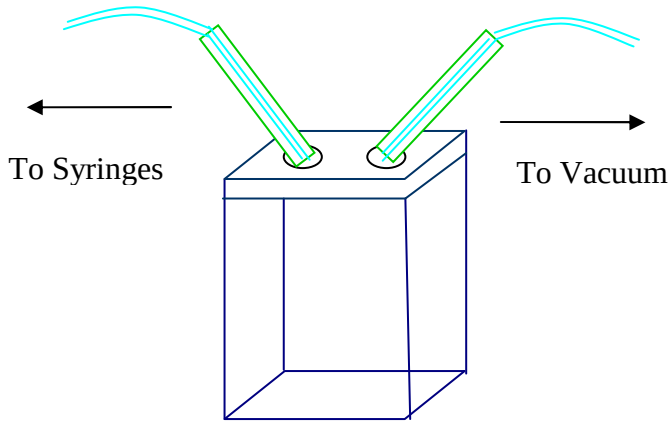

The probe beam was at right angles to the laser beam path. The metallocycle products have a higher absorbance at 410 nm than the starting complexes do. As the reaction proceeds, and more of the complex undergoes photodecarboxylation, the absorbance at 410 nm increases. The reaction is monitored by measuring changes in transmission of probe beam light through the cell as the concentration of absorbing species changes.

The procedure was to have one syringe filled with water and the other with sample. The vacuum tube, used for removing the sample, could be extended into the cell and manoeuvred around inside the cell without disturbing the position of the cell. The tube that came from the syringes could be switched to either the sample or the water syringe. This cell had the advantage that it did not have to be moved to refresh or change the samples. The cell was filled first with water then subjected to a single pulse of 248 nm light from the excimer laser. The oscilloscope was set so that data capture (voltage from pre-amp *vs* time) was triggered by the laser pulse. Data from this "shot" was then saved to disk. The water was then removed with a vacuum. The cell was then filled with sample. Another shot was taken and saved to disk. This was repeated in this manner for as many runs that could be saved to a single 3.5" floppy disk. The data was transferred to a computer where Excel was used to manipulate the results.

All of the initial flash photolysis runs were done with $[Co(bpy)_2(gly)](ClO_4)_2$ solutions unless stated otherwise. This complex was chosen for the set up of the experiment for three reasons. The first reason is that it was one of the compounds used by Natarajan and Natarajan[26] in their experiments and is needed for direct comparison. The second reason is that there was a supply already on hand. Thirdly, it was known that the product of the reaction was sufficiently stable that it could be observed by UV/vis or NMR techniques.

The water shots were taken for a number of reasons. The major reason was to establish the background so any interference intrinsic to the system could be corrected for, such as electronic interference. To do this, the signal from the water shots taken

before and after a sample were averaged and subtracted from the sample shot. Another reason the water shot was taken was to provide a measurement from which to calculate I_o. I_o is needed in order to convert the data from transmission to absorbance using the equation $A = \log_{10} (I_o/I)$. The water shots are also a good way to see if there are changes in the system for reasons unrelated to the sample, such as the degradation of the laser fill. There are also some problems associated with the water shots. Water does not absorb light at the wavelengths of interest so more light of the probing beam passes through the water and is detected. This causes scaling problems in comparing the measurements from the water runs to the sample runs. It also means that the system, when the background is taken, is not the same as in the sample shots.

After collecting some initial data, the cell that Lewis had used previously was re-examined. When the fluorescence of the quartz cell was measured by subjecting the cell to a laser flash with no solution present, it was found that the cell luminesced with a relaxation time around 200 μs, interfering with the data collection. It is supposed that the fluorescence was due to the cell, either, by the quartz itself, or, the glue that was used in the assembly. This was not the only source of error in Lewis's results. There was also a slow response time in the electronics, somewhere between the photomultiplier tube and the oscilloscope. It transpired that, the reaction in question was being completely obscured by the interference of the cell and the slow electronics.

Armed with this knowledge, more experiments were undertaken. At this time another researcher, Rowland, provided valuable assistance. Many aspects of the experimental setup were examined, including the effects of varying the solution concentration and

laser power. As hoped, the concentration of the solution gave no change in the results obtained. At higher laser power the difference in absorbance is more noticeable than at lower laser power. This means that while the shape of the curve, and thus the rate measured, is the same, the precision is increased at higher laser power. This leads to the predictable conclusion that the rate constant is independent of laser power, but the measurement is more reproducible at higher laser power.

After a large amount of data had been recorded it was analysed and considered as a whole. It was clear that the reaction was proceeding rapidly and was at the limits of our electronics. The system improvements were made in the following areas:

- The cables linking system components
- The cell
- Method of filling the cell
- Cell holder
- The photomultiplier
- The procedure

The Cables Linking System Components

The shielding on all the cables was checked and it was found that there was a ringing inherent to the system. It was thought to come about by the electronic signal not all moving on to the next piece of equipment due to a high impedance barrier. Some of the signal echoed back through the cable. This produced an oscillation in the raw signal data. The main problem is that this can distort the signal and lead to recording anomalous data points that have to be accounted for in some way during analysis.

The Cell

Most of the useful kinetic data must be collected immediately after the laser pulse, and this was still being obscured by the cell fluorescence. Experiments were undertaken to find a cell or sample holder that would not interfere with the data collection. The probe beam was positioned just inside the cell, parallel to the face where laser light entered. The samples of interest absorb strongly at 248 nm. Very little light of that wavelength reaches the solution further back in the cell. So the probe beam must be placed near the front of the cell. An optimal distance from the front window to work at can be calculated. The solution must be dilute because of the high extension coefficient at the irradiation wavelength, but to be able to detect notable changes in the absorbance it would be best to measure the highest concentration of product molecules that is possible. In this calculation for the $[Co(bpy)_2(gly)](ClO_4)_2$ system, a value of absorbance was used with $I_o = 2$ and $I = 1$ (which would mean that half of the light had been absorbed) in order to assess how far light was penetrating into the cell. For this system, $\varepsilon = 10{,}000\ M^{-1}\ cm^{-1}$, m = 6.2 mg, $M_R = 644.43\ g\ mol^{-1}$, v = 100 mL.

$$A = \varepsilon cl = \log_{10} I_o/I$$

$$l = A/(\varepsilon c)$$

$$l = 0.3/(10{,}000 \times 9.62 \times 10^{-5})$$

$$l = 0.312\ cm$$

The monitoring beam needs to be set up within 0.312 cm of the laser window in order to get the best concentration of the species being monitored.

One way of minimising interference caused by the cell, such as luminescence and light scattering into the detector, is to avoid the laser light passing through any cell windows before it reaches the sample solution. This led to the idea of the laser flash being reflected onto the top of an open cell system rather than through a side window of a fully enclosed cell.

A mirror that was specially coated to reflect 248 nm light was obtained and the laser, mirror and cell component was set up as in Figure 2-4. A cut-out screen made from copper sheet was added immediately above the cell to prevent light from the laser pulse being incident on either the meniscus or the cell walls, either of which might cause interference.

Through experimentation, it was found that the cell had to be big enough so that the flash was being projected down onto a flat surface and not disturbed by formation of a meniscus near the sides. The analysing beam depth of < 0.312 cm is now measured from the top of the cell rather than the side. It also had to be deep enough that there would be little interference from light reflected from the cell bottom. A competing consideration was that having too large a cell would result in a lot of compound being used unnecessarily. The cell would have to have flat sides on at least two opposing sides for the probe beam to enter and exit. Nothing suitable could be found ready made so the cell had to be constructed.

It was found that regular glass microscope slides were a suitable building material. Four small square pieces each measuring approximately 23 mm x 23 mm were cut from the slide and were assembled in a windmill fashion on a fifth piece of slide. The

glue used was standard super glue which was tested for interference with the measuring equipment, *e.g.* whether it was a source of luminescence, before assembly and none was detected. It was also tested to see if it could withstand exposure to the laser and not degrade.

To further improve the system, the five sides of the cell were painted black inside and out with acrylic paint; this was to minimise any interference from other light sources. An unpainted window was left on each end for the probe beam to pass through. A further window was left on one side so certain aspects of the experiment, such as the fill level, presence of air bubbles and position of the probe beam could be monitored. Unsurprisingly, the paint was found to degrade with laser light. After only a few runs, the paint needed to be reapplied, most notably on the bottom of the cell. To help preserve the paint on the bottom, a small plate of copper foil was placed on the base to reflect any light. While little laser light was expected to reach the bottom of the cell when it was filled with an absorbing solution, almost all of the laser flash reached the bottom when the cell contained water.

Method of Filling the Cell

There were some disadvantages to the overhead irradiation but these were overcome with procedure changes. The main problem was that the system became very sensitive to variations in solution volume. At first, the syringe method of filling was still employed but varying solution depth and the presence of air bubbles were greatly affecting the results obtained. Even when using markings on the side of the cell as a guide the depth of the solution was poorly controlled. This implies that the depth at which the probe beam was passing through the sample was changing between each

fill. This meant that the method of correcting the sample with the water shots was not as valid because the depth of the water was different to the depth of the sample. Filling the cell with syringes also had a tendency to introduce air bubbles. If one of these bubbles found its way into the path of the probe beam, the results were greatly affected and the results meaningless.

In order to avoid this, the cell was filled with a constant volume of solution delivered by pipette. This did mean that instead of the cell remaining stationary the whole time, it would have to be moved out to an open area, be filled and then returned to the exact same position. Standard volumetric pipettes were used initially. It was found that the optimum volume of liquid did not correspond to an exact pipette volume, so an appropriate mark was made on the pipette shaft to ensure the same optimal fill level each time. Two pipettes were needed; one for water and the other for sample. Filling the cell with pipettes also reduced the incidence of air bubbles.

Cell Holder

Now that the cell was being removed to be filled each time, great care was required in making sure the alignment was correct before each run. A wooden block with an indent the same size and shape of the cell bottom was procured. The block was fixed in place to insure the cell returned to the exact same place each time.

The Photomultiplier

Three changes were made to the photomultiplier setup. The monochromator slits were opened wider to their full extent, since we did not require high wavelength specificity.

The second change was that the monochromator was also rotated onto its side so that the slits now lay horizontal. In this position they are in line with the horizontal probe beam. This maximises that amount of light from the probe beam entering the monochromator. The final change to the electronics was that the high voltage supply to the photomultiplier was turned down from 700 V to 350 V. These changes were made to improve the signal to noise ratio.

Change to Procedure

Water shots were eliminated altogether and were replaced by recording the dark voltage (with no probe beam present) at the beginning of each run, and recording a "dark" flash (with sample present in the cell and exposed to a laser flash but with no probe beam) between two sample shots. A UV filter was also placed in front of the monochromator to reduce the effect of light scattered from the flash.

Procedure for rate determination

A number of control experiments are necessary to ensure that the system is able to produce accurate and precise results. The control experiments also provide a useful tool in determining if the system is changing and is a way to determine when the laser fill needs to be changed. How these are used is explained in greater detail when they are used in the mathematical analysis. The general experimental procedure is as follows: a known concentration of the sample solution is put into the glass cell. The first measurement is made with no analysing beam or laser flash (I_d). This measurement will help in determining the base line voltage and is also referred to as the dark measurement. The next measurement is made with the analysing beam and the laser flash (I_a). This is the first of two sample data collections. After that the

system records a laser flash with no analysing beam (I_{df}). This is to correct for any interference in the electronics from the laser and is also referred to as the dark flash. The last measurement in the set is made with the analysing beam and the laser flash (I_b). This is the second sample data collection. Every set of four measurements is carried out on a fresh solution and the cell is emptied and refilled between each set. The results are transferred to a computer programme (Microsoft Excel) for analysis.

Mathematical Analysis for rate determination

The raw data is supplied from the oscilloscope as time dependant amplified voltages that are proportional to intensities. The raw data is graphed as in Graph 2-1. Even from looking at the raw data of the sample shots it can be seen that there is a change in the system after the laser pulse. After the laser pulse the intensity of the light passing through the system goes down. This means that the sample is absorbing more of the light. Furthermore, the drop in intensity occurs very rapidly (fractions of microseconds), much faster than is consistent with the literature values for rate constants for these compounds.

The start of the laser pulse is identified visually and the data is shifted so that time equals zero on the rise of the laser pulse. This gives a new set of time values that is used from now on. The exact voltage value is of little importance. The interest lies in the difference between the intensity of the data collections (I_a and I_b) and the intensity of the dark (I_d). The data was corrected for this by subtracting the dark measurement from each of the shots.

Graph 2-1 Raw Data

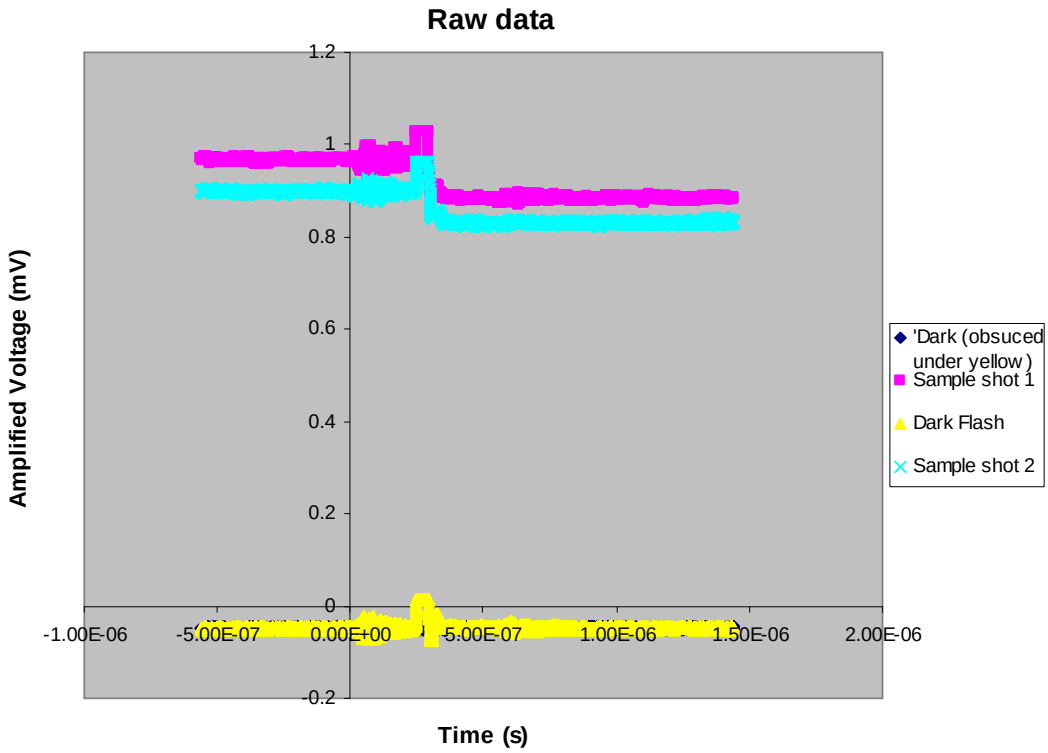

The dark flash (I_{df}) is performed with the analysing beam turned off. Everything else in the system is as in would be in a sample shot. This can account for the luminescence interference created by the system that is unavoidable. The types of interference that could be occurring are light scattering and fluorescence. To correct for this the dark flash is subtracted from the data collections. The corrected data is then graphed (an example is shown in Graph 2-2).

The data is then transferred into absorbances using the formula $A = \log_{10} (I_o/I)$. I_o is calculated on the premise that it is approximately equal to the light coming in before the laser is flashed on the sample shots. This is explained visually in Graph 2-3. The average is taken over this time. An error is introduced in this assumption.

Graph 2-2 Corrected Data

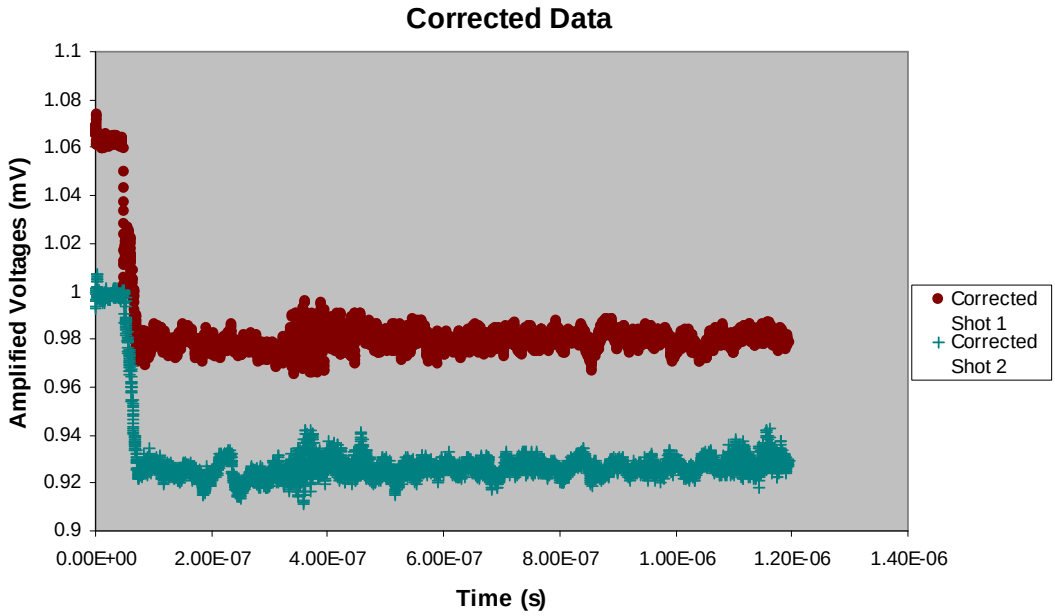

This data is then graphed with the absorbance having a running average over a fixed number of points and from this we can estimate a minimum rate constant. In this estimation we assume that the reaction begins at t equals zero. If it begins after that it would give a faster rate so it should not interfere with the minimum rate that we are reporting.

Graph 2-3 I_o Calculation

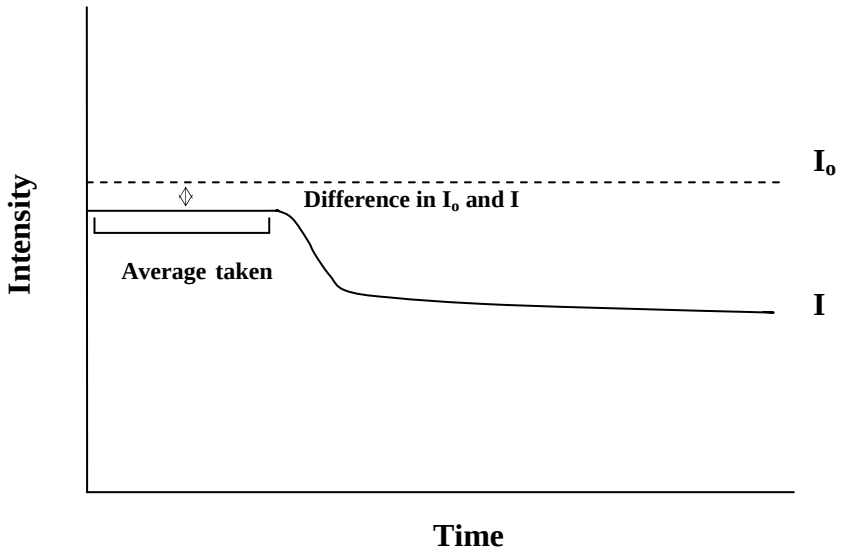

In a reaction A ⟶ B where [A] is the concentration of A, [B] is the concentration of B, $A_o = B_\infty$ is when all A has been converted to B. [A] + [B] = B_∞ The following equations can be derived.

$$\mathbf{d[A]/dt = -k[A]}$$

$$\mathbf{[A] = A_o\, e^{-kt}}$$

$$\mathbf{[A] = B_\infty\, e^{-kt}}$$

$$\mathbf{B_\infty - [B] = B_\infty\, e^{-kt}}$$

$$\mathbf{((-[B] + B_\infty) / B_\infty) = e^{-kt}} \qquad \mathbf{(1)}$$

$$\mathbf{\ln (B_\infty - [B]/ B_\infty) = -kt}$$

In a textbook case a graph of ln (B_∞ -[B]/ B_∞) vs time would be plotted and the slope would be –k. Unfortunately in this real world case the data is not a nice smooth curve but an oscillation over that curve. In some instances the data goes over B_∞ which when placed into equation (1) gives a negative number. To find the least-squares fit the data is squared. This eliminates any problems caused by the negative numbers.

$$\mathbf{((-[B] + B_\infty) / B_\infty) = e^{-kt}} \qquad \mathbf{(1)}$$

$$\mathbf{((B_\infty - [B]) / B_\infty)^2 = e^{-2kt}}$$

The data was then plotted with $\ln((B_\infty-[B])/B_\infty)^2$ along the y axis and t along the x axis. A line of best fit was then applied and the slope of the graph was -2k. From this k was calculated. All of the different runs of the experiment were averaged to get the final rate constant.

Table 2-1 Log Plot of the Data

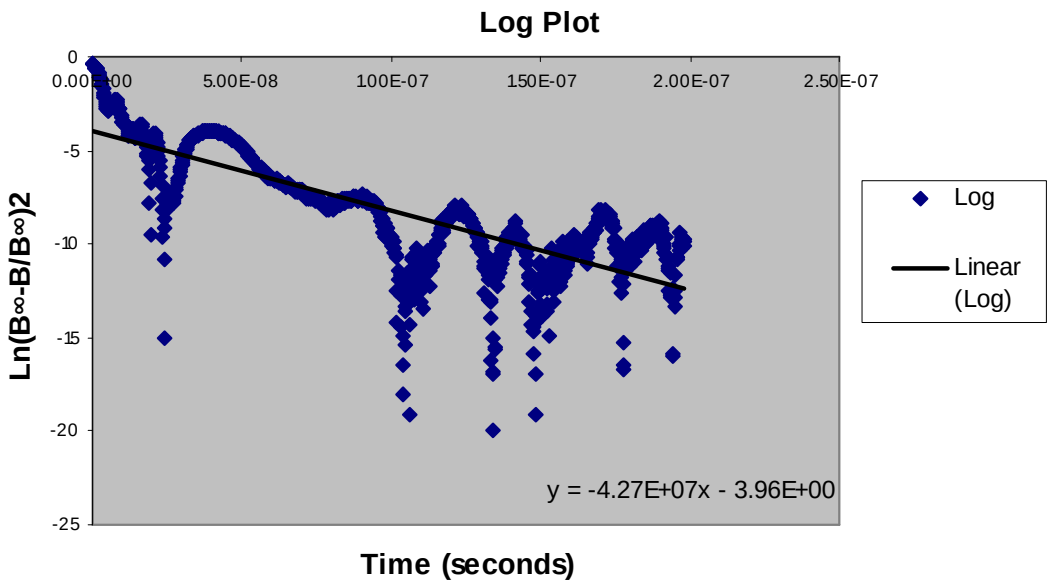

Results for Rate Data

The results of the rate determination are shown in Table 2-2. As stated before, during our research it was observed that the reaction could be proceeding at a faster rate than the electronics can measure. Due to this it was expected that all of the rates would be approximately the same. In the table below that is true for the rates of $[Co(bpy)_2(gly)]^{2+}$ and $[Co(tpa)(gly)]^{2+}$. It is possible that this could be because the similarities of the complexes. The rate for the $[Co(tpa)(aib)]^{2+}$ complex was different.

Table 2-2 Results for Rates

Complexes	**Minimum Rate Constants k/s^{-1}**
$[Co(bpy)_2(gly)]^{2+}$	2×10^7
$[Co(tpa)(gly)]^{2+}$	2×10^7
$[Co(tpa)(aib)]^{2+}$	5×10^6

In complexes where the amino acid derivative was changed (gly and aib) it is expected that there would be a difference in rate due to the stabilisation of the radical. The aib ligand has two methyl groups on the α-carbon. Methyl groups are electron donating and can stabilise a radical more than what a hydrogen atom would. Thus, it is expected that the reaction would be slower. The rates would all be the same, or very similar, if it were the electronics being measured. The rate for the aib complex is slower, but not by much and it is unclear whether this is a significant difference.

These results have far reaching consequences. The rates reported previously from flash photolysis studies had rates of ~10^3 s^{-1} for the same or similar complexes.[26, 27] These results show that the rate is much faster than this. The observations that Telfer made in the radical clock experiments implies the reaction proceeds at a rate faster than 10^8 s^{-1}. Our results provide more evidence to support the idea of such a fast reaction.

This has mechanistic significance. Some proposed mechanisms in the literature have the radical formed from a photodecarboxylation reaction on a $[Co(\mathbf{L})(aa)]^{n+}$ complex participating in further reactions. The fast rate of the formation of the metallocycle suggests that the radical is not present for enough time to participate in the reactions suggested. One such proposed mechanism is the photodecarboxylation of $[Co(EDTA)]^-$ put forth by Natarajan and Endicott.[53]

It had been previously reported that the primary photolysis products from the photolysis of $[Co(EDTA)]^-$ are cobalt(II) species, CO_2 and a radical species. The reported ratio of cobalt(II) : CO_2 : CH_2O is 2 : 2 : 1.[54, 55] Natarajan and Endicott put

forth a mechanism to explain these observations (Figure 2-7).[56] In the mechanism the radical produced from the decarboxylation reacts with another molecule of $[Co(EDTA)]^-$.[56] It was thought that the radical produced attacks EDTA in preference to oxidising the cobalt(II) to cobalt(III).[55]

Due to the observed formation of the metallocycle and the rate of that reaction it is unlikely that such an intermolecular reaction occurs. The mechanism is more likely to follow that which was proposed by Poznyak and coworkers[57, 58] which is analogous to the mechanism they proposed for the $[Co(bpy)_2(gly)]^{2+}$ (Scheme 2-1).[36, 39] The mechanism proposed is that $[Co(EDTA)]^-$ undergoes a photodecarboxylation and produces a three-membered metallocycle ring as shown in Figure 2-8. It is not possible to identify a rate determining step at this time. This would require a more detailed study of the effect of different amino acid substituent groups. If the result for the aib complex is a lower rate, this may imply that metallocycle formation is rate determining.

Production of the final species found by Natarajan and Endicott may then occur under steady state photolysis, by subsequent decomposition of the metallocyclic complex (perhaps photoinduced).

Figure 2-7 Proposed Mechanism of the Photodecarboxylation of $[Co(EDTA)]^-$ as put forth by Natarajan and Endicott

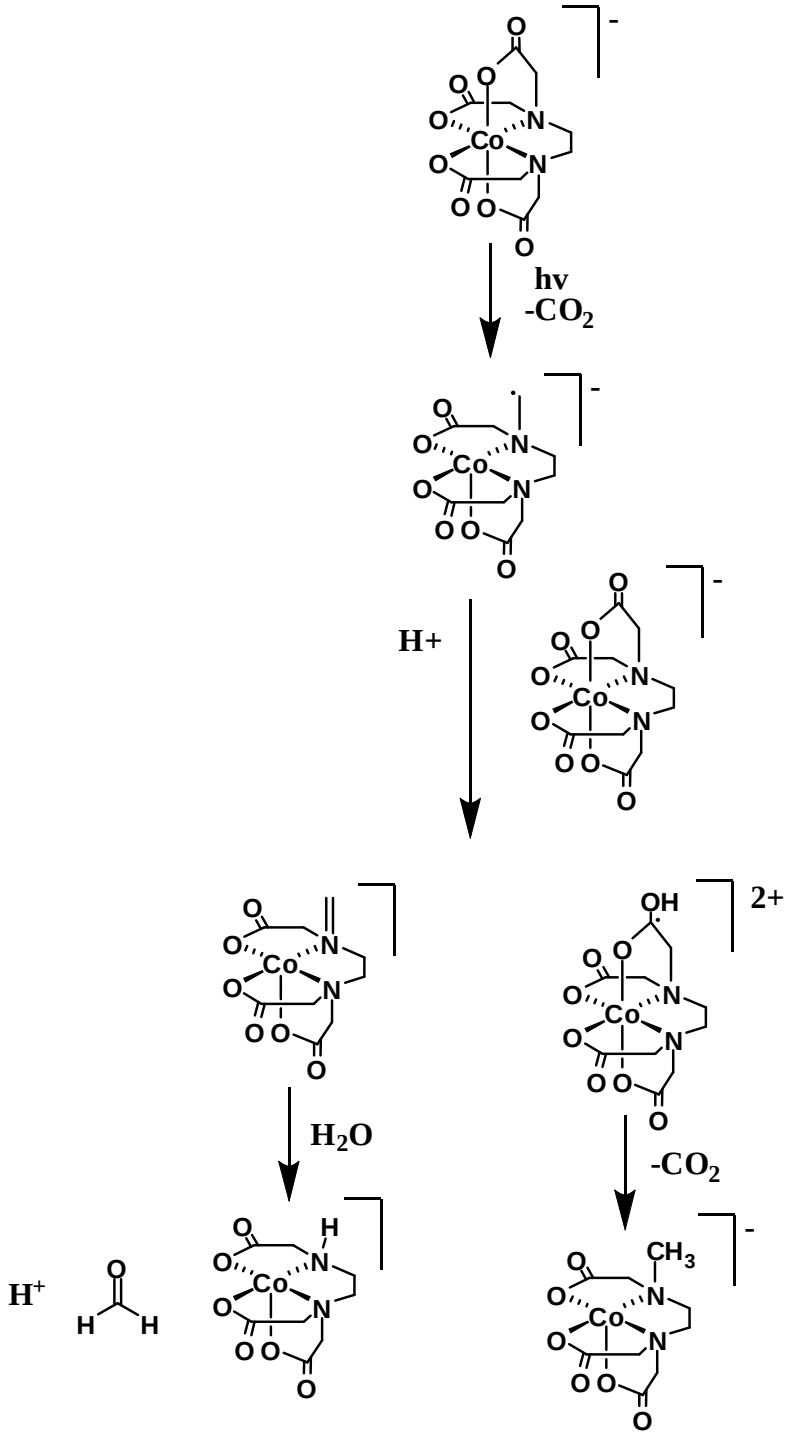

Figure 2-8 Proposed Mechanism for the Photodecarboxylation of $[Co(EDTA)]^-$

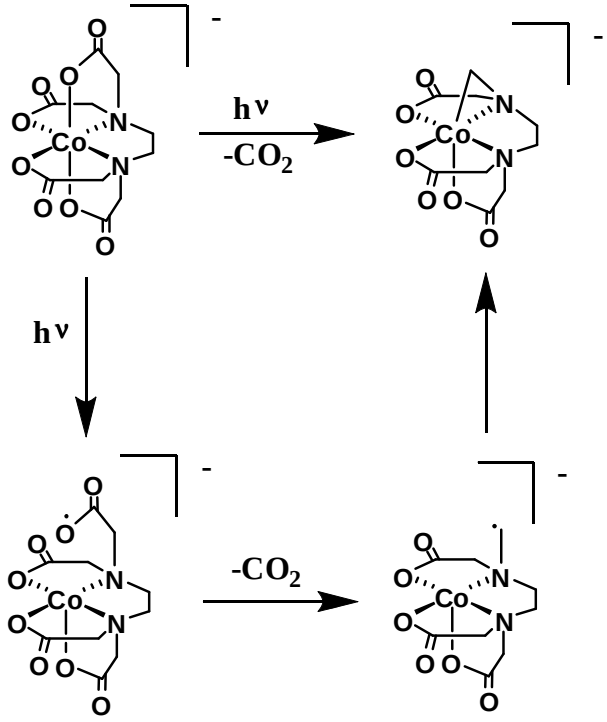

Future work

Exploring the effect of different amino acid substituents may allow assignment of a rate determining step, through comparison of observed rates with expectations of radical stabilising. For example, a more stable radical should result in slower rates if the rate determining step is reaction of the radical or faster rates if the rate determining step is radical formation. The experiment calls for faster times to be able to be recorded and analysed so that such substituent effect can be measured. For this a system with a laser with a shorter pulse width could be used. The electronics used also has to have a fast response time to deal with the fast reaction rate.

SUMMARY

In this chapter the design and set up of a new laser system is described. The new system was used to investigate the formation of the metallocycle from the photodecarboxylation of $[Co(L)(aa)]^{2+}$ complexes. The results of these experiments have produced a lower limit for the rate of formation of the metallocycle of 10^7 s^{-1}.

We are now confident that the rate of the formation of the metallocycle product is fast, with a lower limit of 2×10^7 s^{-1}. From previous work it was determined that any radicals in the system are short lived. It is not clear which step is the rate determining step. The results for the aib complex gave a slower rate which may imply that the rate determining step is that of the radical forming the metallocycle.

Chapter Three

Steady state photolysis

Chapter 3

Steady state photolysis

INTRODUCTION

Sayings and clichés are not always backed up by science; in fact they are sometimes quite contrary to it. For example while the saying goes ‘two wrongs don’t make a right’, the multiplication of two negative numbers does make a positive number. However one saying that is backed up by science is the basis of this chapter: ‘opposites attract’. Positive charges repel each other, as do negative charges; whereas a negative and a positive charge are drawn to each other. Such attractions have been identified as the reason for heteronuclear covalent bonds being stronger than homonuclear bonds. This observation led to Pauling to come up with the concept of electronegativity.

A polymolecular chemical reaction relies on the species involved coming close to one another in order to interact with each other and react. The likelihood of them coming in contact with one another, and reacting, is dependant on many factors, such as the concentration, the temperature (speed of the molecules), time (the more time they have, the more likely they are to react with each other), etc.

An important factor in two species coming close is the relative charge of the species involved. If, in a two species system, both reactants have the same charge, for example they are both positively charged, the positive charges will repel each other. Furthermore, in a polar solvent such as water there will be a solvent sphere with the δ- negative end of the water molecules being attracted to the positive species. The higher the charge the more solvent the ion will attract, the bigger the solvent sphere will be and the solvent molecules will also be more tightly bound. The solvent spheres may keep the species further apart and hinder, or prevent, them from reacting with each other (Figure 3-1).

Figure 3-1 Solvent Sphere of Two Positively Charged Species

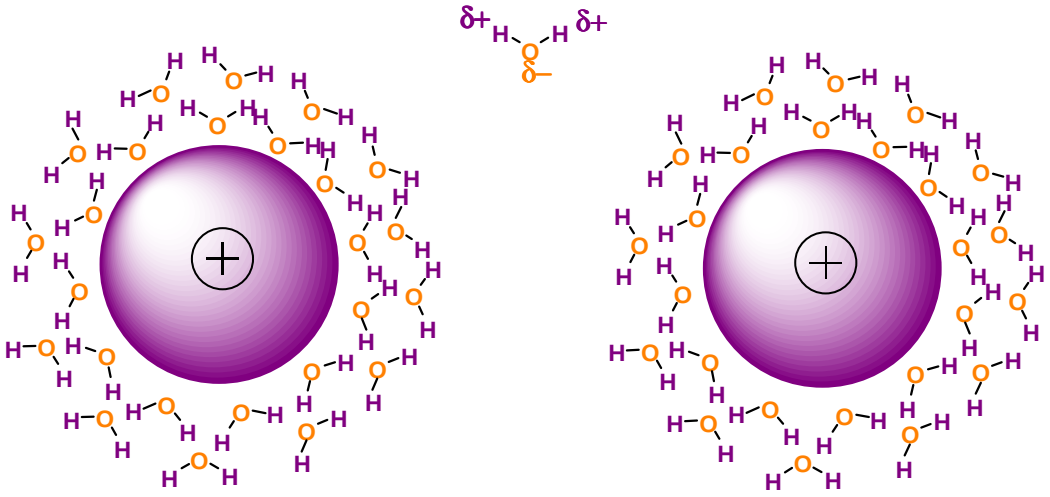

There are a number of ways to manipulate the system to ensure that species react together. One is to manipulate the reaction conditions so that the concentration, pressure and temperature are higher, ensuring that there are a lot of species moving rapidly and the chances of them coming in contact with each other is high.[59, 60] An additional way is to hold the reacting species in place close to each other. This can be achieved by tethering them to a surface,[61-63] or holding them within a molecular frame work *e.g.* cages;[64-66] or building them into the same molecule.[67] A further way to

promote reaction, and is the focus of this chapter, is to have the two ions draw close to each other by using species of the opposite charge (Figure 3-2).

Figure 3-2 Solvent Sphere Species with the Opposite Charge

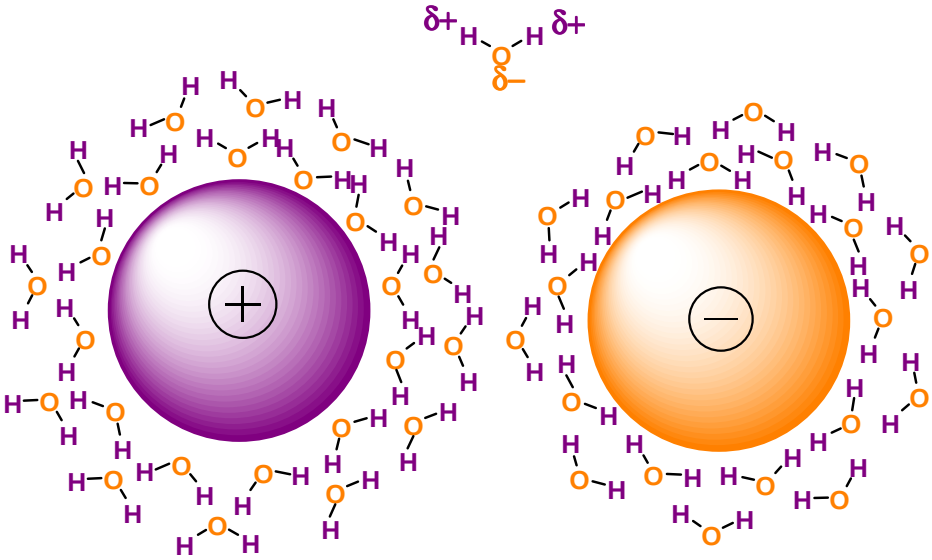

As mentioned in **Chapter 1**, there is a literature precedent in the synthesis involving two neutral complexes reacting together. This is in the formation of an ethylenediamine-tetraacetate anion (EDTA) from the coupling of two nitrilotriacetate anions coordinated to cobalt(III) and subjected to photolysis (outlined in Scheme 1-3).[25] The exact mechanism is not known but two possible intermediates are shown in Figure 1-6. The coupling could occur as a dimerisation of either of the intermediates, or, as a reaction between the two intermediates. An important feature of this system is the fact that two of the cobalt complexes can come close to each other because they are neutral. Most such complexes are cationic, and electrostatic repulsion would presumably prevent dimerisation, in those cases. In this chapter, we explore whether other examples can be found.

Past Work

In 1999, Telfer, carried out a number of NMR experiments in both D_2O and DMSO-d_6.[17] The steady state photolysis (254 nm) experiments were performed on D_2O solutions of a series of $[Co(bpy)_2(aa)]^{2+}$ complexes. Where bpy is 2,2'-bipyridine; and aa is alaninate (ala), valinate (val), phenylglycinate (pgly) or aminoisobutyrate (aib), shown below in Figure 3-3. ^1H NMR spectra was used to identify the photolysis products. The changes in the ^1H NMR spectra upon irradiation of the $[Co(bpy)_2(aa)]^{2+}$ complexes indicated that a complex containing a Co-C-N metallocycle was not present.[17] The metallocycle that formed was unstable. They decomposed to give carbonyl compounds and other species.

Figure 3-3 The $[Co(bpy)_2(aa)]^{2+}$ Complexes used in Telfer's Experiments

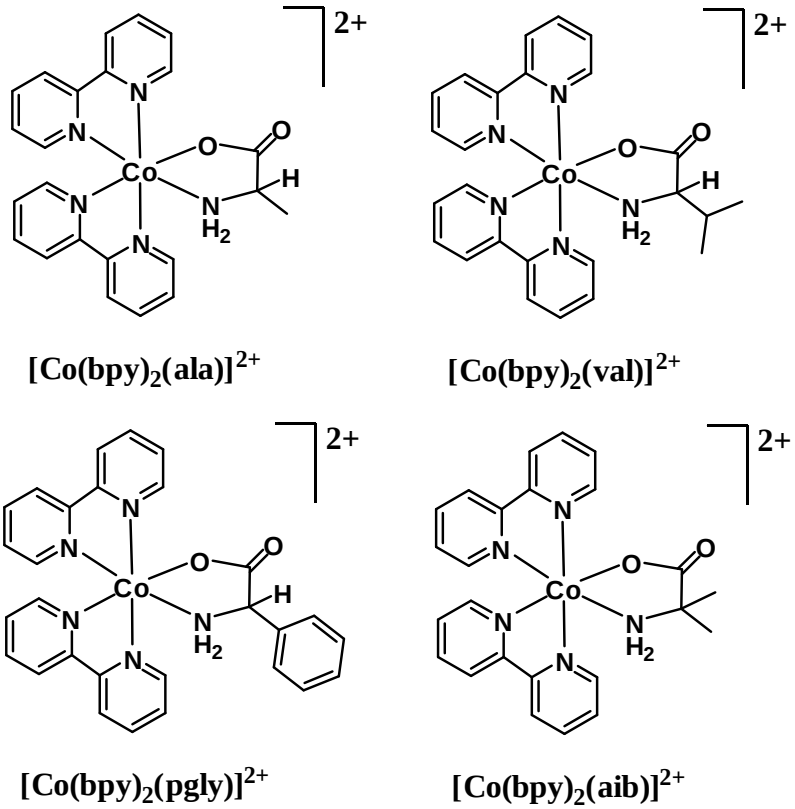

D_2O Photolysis

The photolysate from the photolysis of the complexes in D_2O, produced a number of different components. Free amino acid, $[Co(bpy)_3]^{3+}$, and free bpy were identified by ^1H NMR spectrometry. Carbonyl compounds were also detected amongst the photolysis products. The carbonyl compound detected, closely related to the aa present in the original complex, as shown in Table 3-1. Acetaldehyde, 2-methylpropanal, benzaldehyde and acetone were identified following photolysis of the ala, val, pgly and aib complexes respectively. The hydrated forms of acetaldehyde and 2-methylpropanal were also present.

Table 3-1 Relationship Between aa and Carbonyl Detected

Starting Complexes aa	Carbonyl Compound Detected
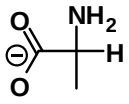 ala	 Acetaldehyde
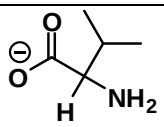 val	 2-Methylpropanal
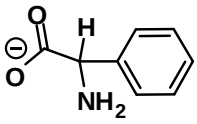 p-gly	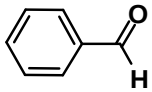 Benzaldehyde
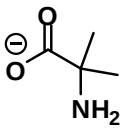 aib	 Acetone

The groups on the carbonyl compound match the groups on the carbon next to the amine. If the expected photodecarboxylation to give a metallocycle has taken place, then reductive elimination would give an imine, and on subsequent hydrolysis, a

carbonyl compound. A suggested mechanism for the production of carbonyl compound is shown in Figure 3-4.

There was some indication that paramagnetic cobalt(II) ions were present and they interacted with the bpy and free amino acid as well as broadening the peaks in the ^{1}H NMR spectra. The addition of DCl to the neutral photolysates resulted in large increase in the integrals of the free bpy and free amino acid signals in the ^{1}H NMR spectra. The interaction of the paramagnetic cobalt(II) ion with the bpy and free amino acid is likely to reduce the intensity of their ^{1}H NMR peaks. The acid also helps in reducing the broadening of the peaks due to cobalt(II) species.

DMSO-d_6 Work

The results of the photolysis of $[Co(bpy)_2(aib)]^{2+}$ in DMSO were found to produce: (1) *trans*-N-$[Co(aib)_2(bpy)]^+$ (Figure 3-5); (2) acetone; (3) free amino acid; (4) free; bpy, and (5) cobalt(II) species. The products (except cobalt(II) species) were detected by ^{1}H NMR spectrometry. Poor signal to noise ratios and poorly resolved peaks were generally encountered when NMR spectrometry of the DMSO-d_6 photolysates were obtained directly. However, addition of DCl solved this problem. The difficulties in obtaining a direct spectrum of the photolysate may well be caused by the presence of paramagnetic cobalt(II) ions. The interaction of cobalt(II) ion with the protonated species would be lessened by the addition of DCl.

Figure 3-4 Suggested Mechanism for Production of Carbonyl Compounds

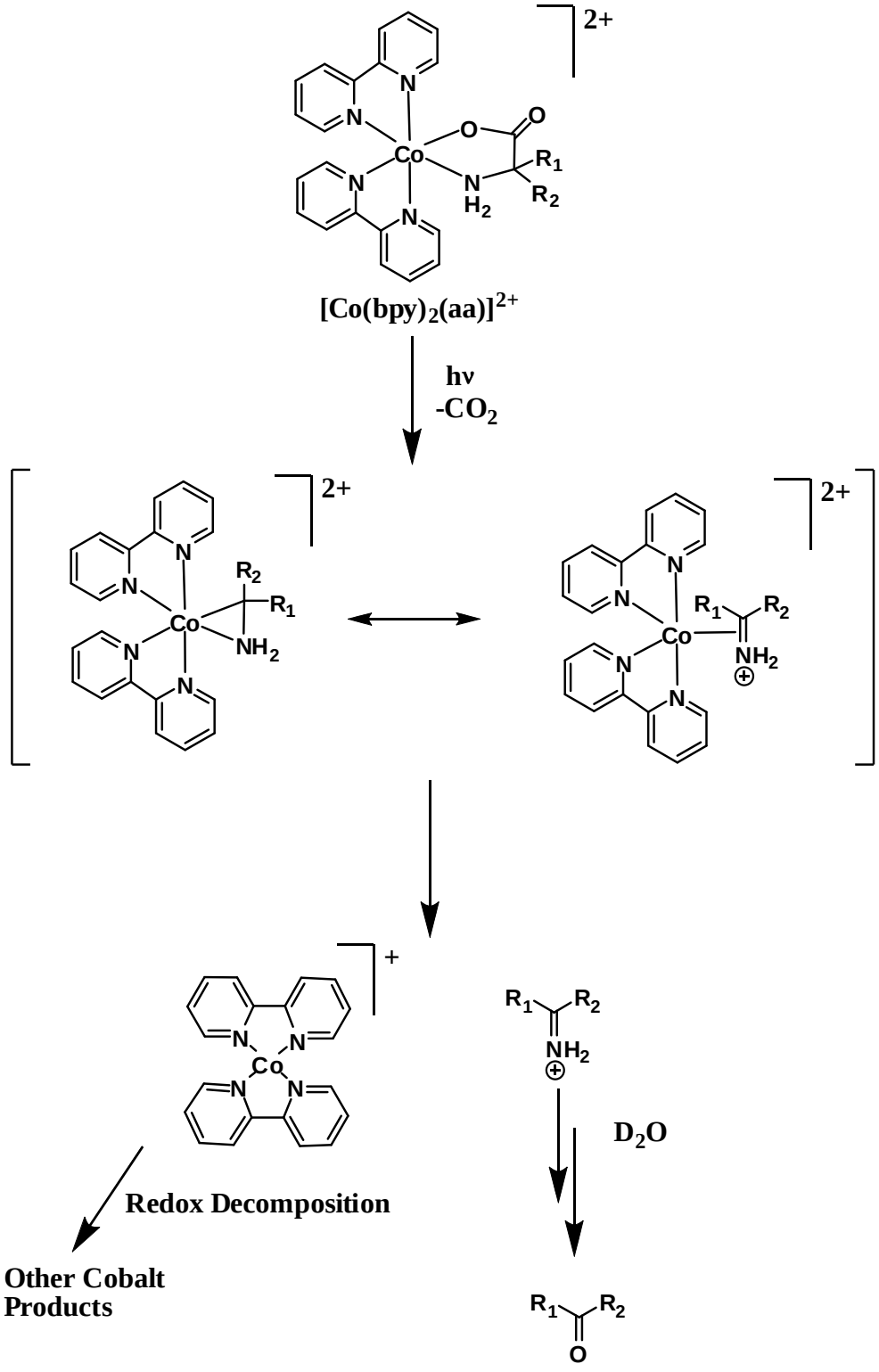

Figure 3-5 A Product of the Photolysis of $[Co(bpy)_2(aib)]^{2+}$ in DMSO

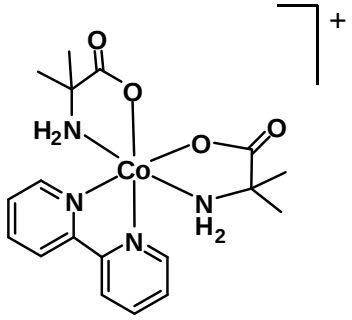

$[Co(aib)_2(bpy)]^{2+}$

The carbonyl compound, in this case acetone, is still present in the photolysate indicating that the same reaction has occurred initially. The end product distribution however is different. $[Co(bpy)_3]^{3+}$ was not detected in the DMSO photolysate. Spiking experiments demonstrated that it would have been detected if it was there. It was noted that $[Co(bpy)_3]^{3+}$ was rapidly formed when the DMSO photolysate was added to DCl and the concentration increased over time.

UV irradiation of $[Co(bpy)_2(gly)]^{2+}$ in DMSO gave a similar product distribution to the aib complex. Formaldehyde could not be detected, but signals attributed to trans $[Co(gly)_2(bpy)]^{+}$, uncomplexed gly and bpy were identified in the ^1H NMR spectrum. There was no evidence of the metallocycle which can be isolated from aqueous solution. It has previously been noted that this complex is unstable in a number of non-aqueous solvents.[68]

Figure 3-6 A Product of the Photolysis of $[Co(bpy)_2(gly)]^{2+}$ in DMSO

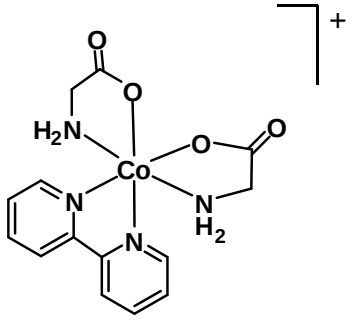

$[Co(gly)_2(bpy)]^{2+}$

$[Co(bpy)_3]^{3+}$ *vs.* $[Co(aa)_2(bpy)]^{+}$

An observation by Telfer[17] was that in DMSO the product $[Co(aa)_2(bpy)]^{+}$ is observed (which is not present in D_2O) and a product that was predominantly formed in D_2O, $[Co(bpy)_3]^{3+}$, is present in a lesser amount. This was investigated further with electrochemistry. The conclusions drawn were that the equilibrium of the cobalt(II) species was the key. In the aqueous solution the species $[Co(bpy)_3]^{2+}$ predominates the equilibrium. Even though it is harder to oxidise than $[Co(bpy)_2(aa)]^{2+}$, there is a large amount of it and O_2 is a powerful oxidant in aqueous solution. In DMSO on the other hand, the equilibrium is dominated by the $[Co(aa)_2(bpy)]^{+}$ species and that is the species present in the largest amount when it is oxidised.[69]

Past Bulk Experiments

Large scale experiments are employed in the hopes of isolating material for further and extensive characterisation, instead of just detecting it by techniques such as NMR spectrometry. The products from a photolysis experiment maybe short lived or highly reactive so time is of the essence in separating the products. Another consideration is

the concentration. The solutions have to be concentrated enough that there is enough material to collect, purify and examine.

[Co(EDTA)]$^-$

In the past in was found that [Co(EDTA)]$^-$ lost some of its optical activity when it was placed in front of intense white light. This was attributed to a redox decomposition process.[70] Further investigation indicated cobalt(II) ions, CO_2 and a radical species as the primary products of the photolysis of [Co(EDTA)]$^-$.[56] Poznyak and coworkers[57, 58] have shown that upon photolysis [Co(EDTA)]$^-$ undergoes a photodecarboxylation and produces a three-membered metallocycle ring as shown in Scheme 3-1.

Scheme 3-1 Decarboxylation of EDTA

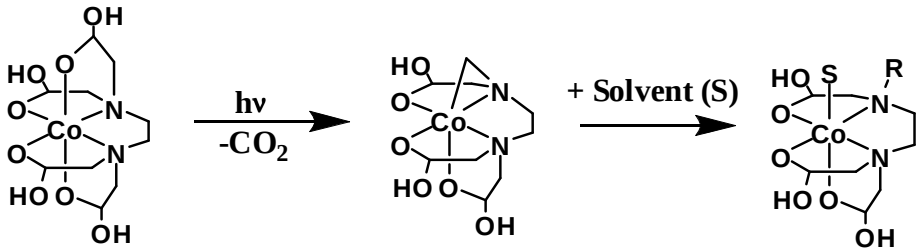

In later experiments, it was shown that the metallocycle degrades with the loss of one of the arms to [Co(EDTRA)H_2O] in neutral solutions at room temperature, where EDTRA is ethane-1,2-diamine-N,N,N'-triaacetate.[57] This was confirmed by studying a range of cobalt EDTA complexes at -40^{o}C. The product isolated was a complex of EDTRA with the three membered metallocycle. The hydrolytic cleavage was confirmed in neutral solutions at room temperature.[71]

Premise of What We Hope to Achieve

In these experiments, the idea is to take two cobalt complexes containing a carboxylic acid group, with opposite charge and photolyse them. The resulting metallocycles could then react together to form a new species.

The two compounds chosen for this work are $[Co(bpy)_2(gly)]^{2+}$ and $[Co(EDTA)]^-$ (Figure 3-7). They are used in the form of the perchlorate salt and the sodium salt respectively. The reason behind this selection is because the photoreactions of both these species and the products made have been studied and reported previously, both in the unpublished results within the research group, and by others.

Figure 3-7 Molecules to be Studied

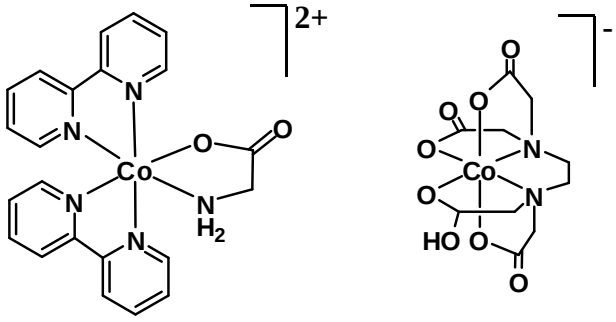

The reaction that is predicted to occur is that both species would undergo a photodecarboxylation which would produce a radical centre on each molecule. The radical could then go on to react further either intramolecularly, by forming a metallocycle with the metal centre, or, intermolecularly with the radical species of the opposite charged species. From the results in **Chapter 2**, it is more likely that the metallocycle is formed rapidly and any further reaction would result from the metallocycle itself.

Based on the hypothesis outlined above, a suggestion for a possible product is shown in Figure 3-8. This would result in a reaction between a positive reactive species (the radical or the metallocycle) and a negative reactive species (the radical or the metallocycle). If these species do react together they would form a bond between the α-carbon on the former glycinato and the α-carbon on the arm of the former acetic acid. This would then form a new ligand **L3.1**. If the reaction happened between the radicals, the cobalt metal centre would likely still be a labile cobalt(II) ion. In this case the likely outcome would be that the metal would easily exchange ligands and the ligand would be coordinated to only one cobalt metal centre (Scheme 3-2). A literature search found only one reference to 4H.**L3.1**.[72] No metal complexes of the ligand have been cited previously.

Figure 3-8 Possible Products

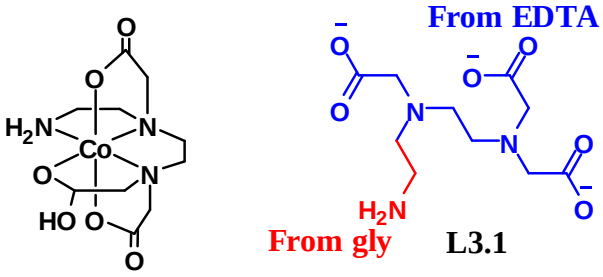

The research consisted of two main strategies. The first was to monitor any change in the reaction and the formation of products by doing small scale photolysis reactions in D_2O. The second strategy was to do large scale photolysis in the hopes of isolating some of the products; this work was carried out in water with an immersion lamp. The two complexes $[Co(bpy)_2(gly)]^{2+}$ and $[Co(EDTA)]^-$ were both subjected to steady state photolysis on their own. The reactions were monitored by NMR spectrometry and UV/vis spectroscopy. The reaction was repeated with the two complexes in the

same solution and again the resulting products were analysed by NMR spectrometry and UV/vis spectroscopy.

Scheme 3-2 Possible Combination of Radicals

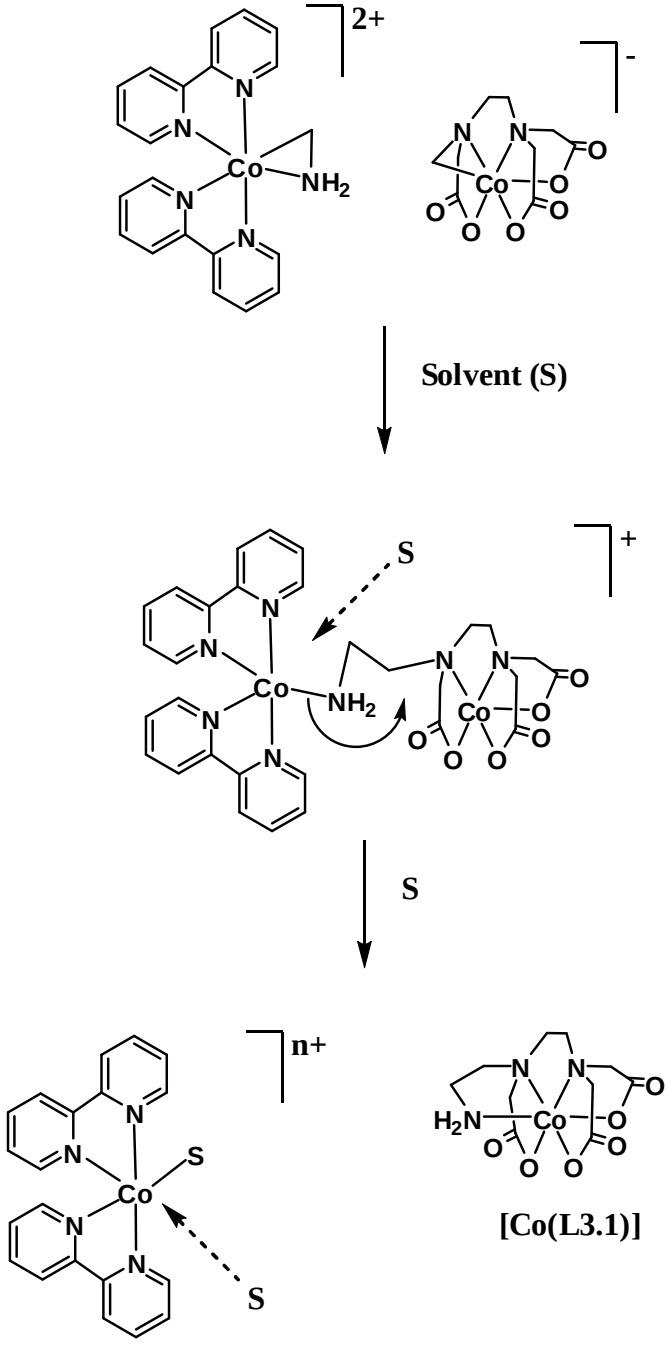

RESULTS AND DISCUSSION

NMR Photolysis

Millimolar solutions of both complexes were prepared in D_2O; TMPS was added as an internal reference for the carbon spectra. They were photolysed with a high-pressure mercury lamp. The samples were kept cold during this time by immersing in an ice-water bath. The solutions were photolysed for one hour at 200 W. Sometimes, after photolysis, a few drops of dilute DCl solution were added. The addition of the DCl acidifies the solution so the species that usually interact with the cobalt(II) ions would be protonated. This lessens the interactions that those species have with the paramagnetic cobalt(II) ions in the solution. The ^{1}H and ^{13}C NMR spectra were obtained.

Control samples where each of the complexes was photolysed on their own were also performed as a reference to determine if what was observed was a direct adding of the two product spectra. A number of spectra of the unphotolysed solutions were taken but it was not taken for every sample due to time restrictions.

As expected there were some solvent issues. $[Co(bpy)_2(gly)]^{2+}$ was only partially soluble in D_2O unless slightly warmed (~30^{o}C). Once the solution cooled down orange crystals formed in the vial which NMR spectrometry and X-ray crystallography proved to be $[Co(bpy)_2(gly)](ClO_4)_2.H_2O$ (Figure 3-9). The crystal structure of this compound has been reported previously.[73] Due to the earlier reporting of the crystal structure only a short collection time was needed to check the cell

against known cell parameters which were obtained through the Cambridge Crystallographic Database (CCD). The picture shown is from the database.

Figure 3-9 The X-Ray Crystal Structure of $[Co(bpy)_2(gly)]^{2+}$

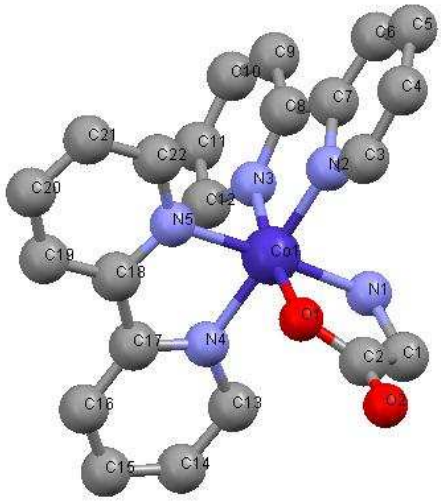

If a solution of $[Co(bpy)_2(gly)]^{2+}$ and $[Co(EDTA)]^-$ was heated all material dissolved, however, the NMR spectra becomes a lot simpler. The change is very obvious with fewer peaks in the aromatic region of the ^{13}C NMR spectrum. The once complex region containing sixteen carbon atom peaks becomes simpler and contains two sets of five aromatic carbons. The aromatic region of the spectrum is what would be expected of a mixture of $[Co(bpy)_3]^{3+}$ and free bpy. In the non-aromatic region of the spectrum there are peaks for $[Co(EDTA)]^-$ and free gly.

Due to the low solubility of $[Co(bpy)_2(gly)](ClO_4)_2$, the concentration was halved for half of the reactions. Even if the compound does not completely dissolve the solubility was not seen as a problem. The concentrations of the reactive species needed to be kept low to prevent unforseen reactions occurring. The only area where

this could be a problem is in the relative concentrations of the positive and negative reactive species.

The peaks and regions of particular interest in the ^{13}C NMR spectrum are the carbonyl peak region, the aromatic region and the region that a metallocycle could appear. In the carbonyl region, if the $[Co(EDTA)]^-$ undergoes a decarboxylation then peaks should increase in number from the two peaks of equal height shown in the unreacted complex. This is because if one of the EDTA arms loses CO_2 then the complex will no longer be as symmetrical. In addition to the new peaks, there will still be the original two peaks from the unreacted material in the photolysate. In the aromatic region, if $[Co(bpy)_2(gly)]^{2+}$ undergoes a reaction, the number of peaks should increase. This is because there will be the aromatic peaks from the new compound and the peaks from the unreacted material. In the unreacted compound there are 16 aromatic peaks. Logically this would double if a metallocycle is formed. A peak should appear ~70 ppm, which is due to the carbon atom in the three-membered ring, if a metallocycle has been formed and is still present.

$[Co(bpy)_2(gly)]^{2+}$

A clear ^{13}C NMR spectrum of $[Co(bpy)_2(gly)]^{2+}$ in D_2O, even before photolysis, is hard to obtain. To get a good spectrum with defined peaks above the noise the sample has to run for at least 48 hours. After photolysis with the generation of paramagnetic species, this time increases dramatically, even with the addition of DCl to interact with the paramagnetic species. It is conceivable, due to the look of the spectrum after 24 hours, that it would take at least a week, which in an active research university is not practical.

$[Co(bpy)_2(gly)]^{2+}$ was photolysed by itself in D_2O. Changes in the ^1H NMR spectrum were observed. The most obvious change was in the appearance of the spectra. The sharp doublets broaden and in some cases the peaks themselves are noisy, even after the addition of acid. The baseline and the spectrum as a whole have a lot more noise associated with them. In one of the spectra there is a simplifying of the aromatic region. In the ^{13}C NMR spectrum of the same experiment the only five peaks distinguishable from the noise are in the right ratio and separation for $[Co(bpy)_3]^{3+}$. This cannot be confirmed by chemical shift because the reference peaks are not able to be distinguished from the noise.

In short, to support the notion that a metallocycle had formed the number of aromatic peaks had to have doubled from 16 to 32. There was an increase in the number of aromatic peaks but only by five. These five peaks are probably from free bpy or $[Co(bpy)_3]^{3+}$, which has been generated by these experiments before.[17] These observations fit in with what has been seen before, although there is no firm evidence to say for certain that the expected reaction is taking place, the same conditions are being used as was used previously and there is nothing to suggest otherwise.

$[Co(EDTA)]^-$

A clear ^{13}C NMR spectrum of unphotolysed $[Co(EDTA)]^-$ could be obtained in 30 minutes. A reasonable ^{13}C NMR spectrum of the photolysate could be obtained in a 48 hour run. When the $[Co(EDTA)]^-$ was photolysed by itself in D_2O the resulting NMR spectra again become more noisy and it takes longer to acquire a suitable spectra. The ^1H NMR spectrum is limited in the information it provides. The peaks

between 3.4 - 4.1 ppm in the unphotolysed solution are nicely separated. In the spectra of the photolysate they all become one peak between 3.4 – 4.8 ppm, even after the addition of DCl. The ^{13}C NMR spectrum of the unphotolysed solution shows five distinct peaks, two at ~185 ppm that correspond to the carbonyl carbon atoms and three between 65 – 68 ppm that correspond to the CH_2 carbon atoms. The two carbonyl peaks are the same height and the three CH_2 peaks are the same height. All peaks represent two equivalent carbon atoms. In the spectrum for the photolysate the number of peaks in both regions increase and the heights are no longer the same. In the 65 – 68 ppm region there is one tall peak at 65.8 ppm and then a further three peaks of varying heights. Likewise at ~185 ppm the number of peaks have increased. The exact number is hard to say due to the noise associated with the spectrum.

$[Co(bpy)_2(gly)]^{2+}$ and $[Co(EDTA)]^-$

When $[Co(bpy)_2(gly)]^{2+}$ and $[Co(EDTA)]^-$ were photolysed together in D_2O there were marked changes in both the ^1H and ^{13}C NMR spectra. In the ^1H NMR spectrum three distinctly new peaks were seen in the aromatic region of the spectrum. The new peaks are at 7.95 ppm, 7.84 ppm and 7.44 ppm. These peaks could be due to $[Co(bpy)_3]^{3+}$ peaks or the free bpy that had been previously seen. Also in the range of 3.4 – 4.4 ppm there is an increase in complexity but the number of peaks is hard to determine. One peak at 3.65 ppm seems to have disappeared but it could just be hidden in the peak at 3.70 ppm because the latter has broadened. In the ^{13}C NMR spectrum five new peaks were seen in the aromatic region. They were at 158.9 ppm, 133.9 ppm, 130.1 ppm, 129.9 ppm and 127.0 ppm. Even though the exact chemical shift does not correspond to $[Co(bpy)_3]^{3+}$ or to free bpy, the number, spacing and relative heights suggest that it is a bpy based compound. Additionally there was a new

peak at 42.7 ppm which is close to the shift for the non carbonyl gly carbon at 47.6 ppm. This indicates the presence of free gly. There are three other peaks that appear at 65.3 ppm, 64.4 ppm and 63.6 ppm, which have yet to be explained.

Again, the experiments are not conclusive. There is a definite increase in the number of peaks. Once more the five new peaks in the aromatic region corresponds to free bpy or $[Co(bpy)_3]^{3+}$. Even though only three new peaks were observed in the ^1H NMR spectrum where four would be expected for $[Co(bpy)_3]^{3+}$ or free bpy, the fourth peak could be hidden under an existing peak. In efforts to obtain more conclusive results the experiments were repeated in DMSO-d_6. The spectra obtained were unreadable and in most cases no peaks were seen in the ^{13}C NMR spectra for the experiments where $[Co(bpy)_2(gly)]^{2+}$ and $[Co(EDTA)]^-$ were reacted together.

Bulk Photolysis

Aqueous solutions of the complexes of millimolar concentrations were photolysed with an immersable mercury lamp for 80 minutes. The solutions were kept cool by placing the reaction vessel inside an ice-water bath. A bulk sample was prepared and the photolysis was performed in batches of 200 mL. This allowed for consistency in the sample being photolysed and the large bulk sample meant that dilute solution could be used. The concentration of the metallocycle has to be kept low because it has been observed that the metallocycle is not isolated from solutions when the concentration is high. Cationic and anionic columns were used to separate positively charged, negatively charged and neutral species. The batches were combined and chromatographed down a CM Sephadex C-25 (25 x 3 cm) column, a DEAE (diethylaminoethyl) Sephadex A-25 (25 x 3 cm) column, or both.

Both of the columns were eluted with 0.2 M $NaClO_4$. The fractions were collected and the UV/vis spectra were taken. The fractions were then reduced in volume to ~20-50 mL. By that time a precipitate had usually formed. The solids were filtered off and the filtrates were placed into evaporating dishes to see if slow evaporation would yield any crystals. The precipitates formed when the volumes were reduced all turned out to be deliquescent, coupled with the fact they were mostly perchlorate salts added to the problem. The NMR spectra obtained were all saturated with water peaks and product peaks could not be observed.

Again there were three main experiments performed, two control experiments where $[Co(bpy)_2(gly)]^{2+}$ and $[Co(EDTA)]^-$ were photolysed individually and the one where they are photolysed together.

When the $[Co(bpy)_2(gly)]^{2+}$ was photolysed by itself, the colour of the solution changed slightly from the bright orange to a paler orange. Upon immediately running the cationic column the products separated out into two bands. The first was an orange band that was later identified as the starting material $[Co(bpy)_2(gly)]^{2+}$. The second band was yellow and was identified as the product band with the three membered metallocycle $[Co(bpy)_2(NH_2CH_2)]^{2+}$. The structures of these are shown in Figure 3-10.

Figure 3-10 Products from the Photolysis of $[Co(bpy)_2(gly)]^{2+}$

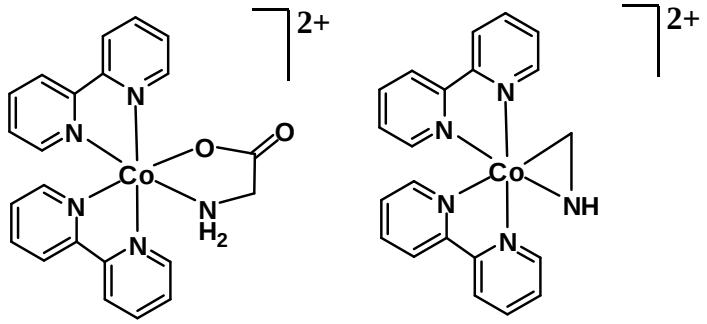

Band 1 **Band 2**

It was found that if there was a delay in the running of the column the number of bands increased to four. The first two bands were found to be the same as stated before (Figure 3-10). An orange starting material band, $[Co(bpy)_2(gly)]^{2+}$, followed by a yellow metallocycle band, $[Co(bpy)_2(NH_2CH_2)]^{2+}$. The third band was also yellow and upon reducing the volume of the fraction a precipitate formed and crystals grew from the filtrate. The material characterised by NMR spectrometry and X-ray crystallography and was found to be $[Co(bpy)_3]^{3+}$ (Figure 3-11). The crystal structure has been reported previously (Figure 3-12).[74] The fourth band was orange and was unable to be characterised. In addition to this, there was also some material stuck to the top of the Sephadex that could not be removed even when 1M $NaClO_4$ and 1M NaCl was run through the column.

Figure 3-11 A Product from the Photolysis of $[Co(bpy)_2(gly)]^{2+}$ with a Delay in Separation of Products

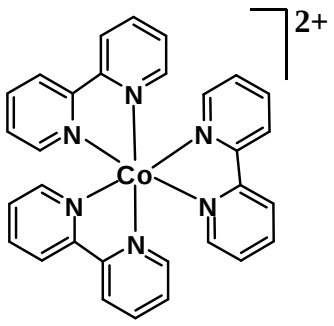

Band 3

Figure 3-12 Crystal Structure of $[Co(bpy)_3]^{3+}$

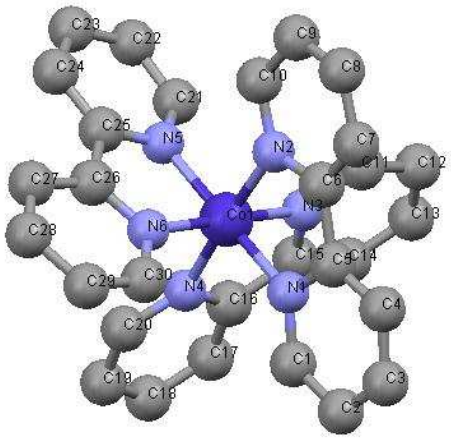

When the $[Co(EDTA)]^-$ was photolysed by itself there was no apparent colour change. Both the starting solution and the final solution were a deep purple. The photolysate was run down an anionic column and the material was separated into one band that stuck to the Sephadex and material that went through the column. The material that stayed on the column was eluted with 0.2M $NaClO_4$ and came off as one band. This was the starting material and made up the bulk of what was recovered (Figure 3-13). The fraction that passed straight through was either neutral or cationic. A theory of what happened to the material is that the EDTA ligand could have lost an arm; which has been reported and seen previously by Poznyak and co-workers.[57, 58, 71]

Figure 3-13 Products from the Photolysis of $[Co(EDTA)]^-$

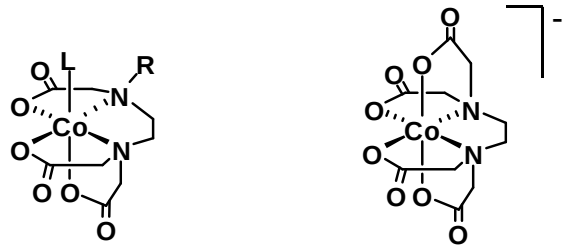

Passed Through Column **Band 1**

A proposed mechanism for what is happening is shown in Scheme 3-3. The deacetylation could proceed in a similar fashion as the production of the carbonyl compounds proposed earlier in the chapter. Except in this case the imine is still bound to the complex because the two R groups are the rest of the former EDTA ligand and is still bonded to the cobalt metal centre.

When $[Co(bpy)_2(gly)]^{2+}$ and $[Co(EDTA)]^-$ were photolysed together there was an obvious colour change from the starting solution to the photolysed solution. The starting solution was a deep purple like that of the $[Co(EDTA)]^-$ solution. After photolysis the colour changed to a pink orange colour. Due to the species of opposite charge, and the thought that the product could be neutral, two columns were run sequentially. The first column that was run was a cation exchange column and the material that passed straight through was then loaded on to an anion exchange column.

Scheme 3-3 Possible Reaction Mechanism

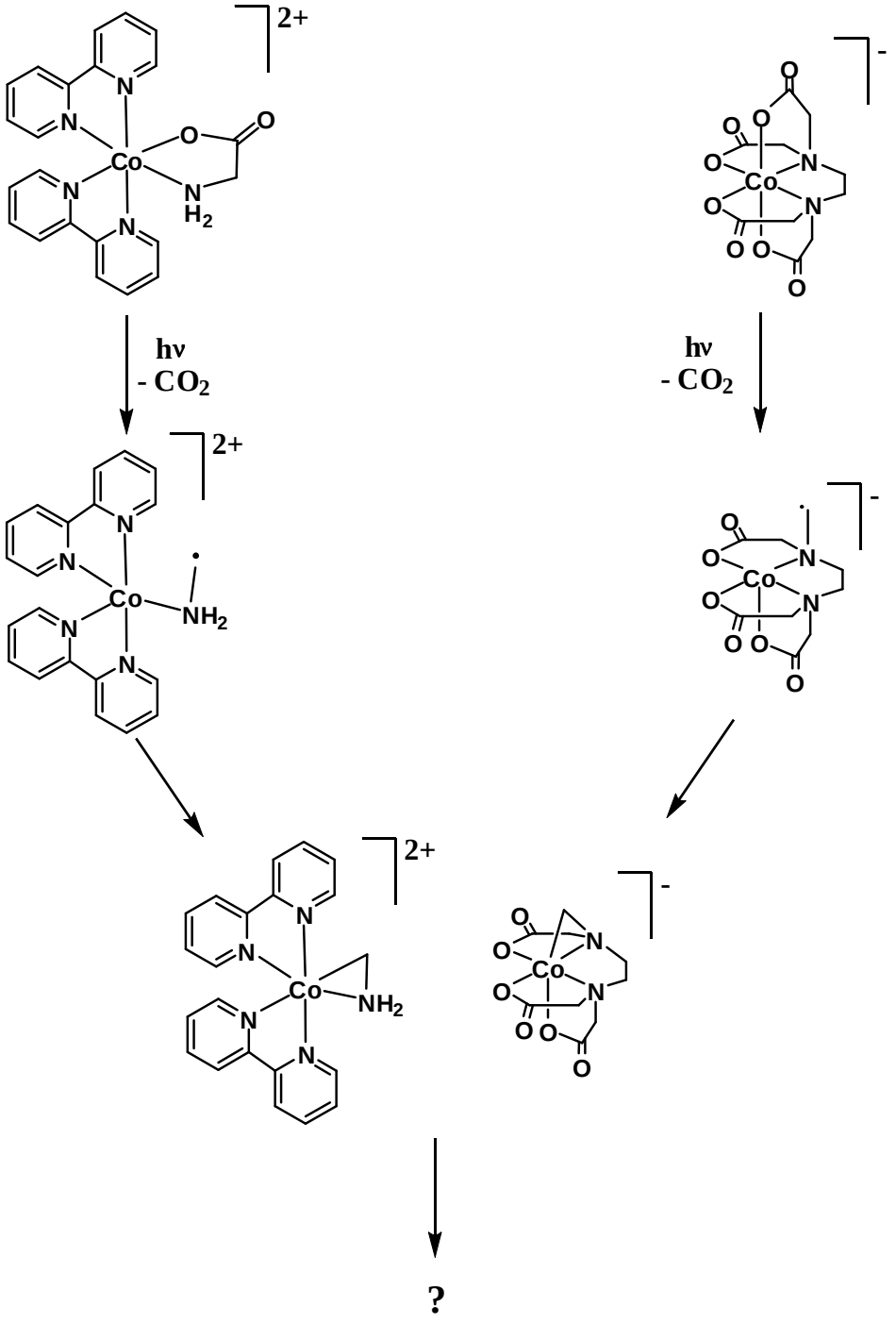

For the cationic column there was a purple fraction that passed straight through the column and then there were three bands (Figure 3-14). The first band was the orange cationic starting material $[Co(bpy)_2(gly)]^{2+}$. The second band was pink and could not

be assigned to a compound. The third band was yellow and was the three membered metallocycle ring $[Co(bpy)_2(NH_2CH_2)]^{2+}$. The anionic column was run and there was only one purple band that turned out to be the anionic starting material $[Co(EDTA)]^-$. No material passed straight through both columns so there was no neutral species detected.

Figure 3-14 Characterised Products from the Photolysis of $[Co(bpy)_2(gly)]^{2+}$ and $[Co(EDTA)]^-$

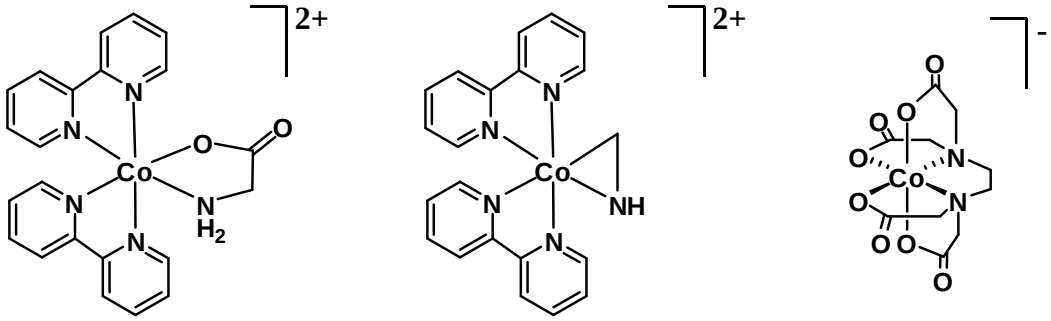

The UV/vis spectra were recorded as soon after the fraction stopped eluting from the column. The fraction was not concentrated in any way and due to this the spectra were often too weak to see peaks in the 400-800 nm region. On occasion the computer software would place an absorbance peak in that area but the presence of a peak could not be confirmed visually. From the control experiments the main absorption bands could be compared to that obtained from the photolysis of the starting materials by themselves. In most cases they matched up exactly. The only band not accounted for by past experiments was the second band from the cationic column. The precipitate is pink and the UV/vis spectrum records peaks at 215.0, 300.1 and 534.9 nm. The colour of the solution and the colour of the resulting precipitate from the concentrating of the solution is pink. The expected complex of **L3.1** has three amine nitrogen donor atoms and three carboxyl acid oxygen donor atoms. Compared to the EDTA complex which

has two amine nitrogen donor atoms and four carboxyl acid oxygen donor atoms, the λ max for the d-d transition will be at a shorter wavelength. The λ max for the d-d transition of the EDTA complex was 540.1 nm. The fact that the wavelength is shorter is promising. However the complex isolated is positively charged which is not what is expected for the cobalt(III) complex of **L3.1**.

Proposal of What Could be Happening

The active species are the two radical species and the two metallocycles. They can react in any combination; the more plausible combinations are the ones in which two species of opposite charge react together. This does not exclude any coupling reactions occurring between species with the same charge. Past research has shown, the same charge does not completely eliminate species reacting with each other it just provides an extra barrier.[75] From there the predicted reaction, based on past literature work, the coupling of the two metallocycles could result in the product **L3.1**.

Crystal structure of Na[Co(EDTA)]

During the course of this research a number of NMR samples of Na[Co(EDTA)] were prepared. One of these samples was left to slowly evaporate at room temperature over several months. The result of this was X-ray crystallographic grade crystals. The space group and unit cell has been reported before.[76] The reporting of the complex was limited to the unit cell dimensions and the crystal system, there was no picture of the complex or discussion of the solvation of the sodium counterion. From the data collected the crystal structure was able to be solved with a R_1 factor of 5.16%. A picture of the complex is shown in Figure 3-15. The cobalt metal centre is in an

octahedral environment with all six sites around bound by the EDTA ligand. The EDTA ligand is coordinated to the metal through four oxygen donor atoms and two nitrogen atoms. Each individual $[Co(EDTA)]^-$ complex is a discreet molecule with no obvious interactions between neighbouring molecules Figure 3-16.

The interesting part of the crystal structure is the counterion shown in Figure 3-17. Each sodium counterion is coordinating to six water molecules, two are terminal and the other four water molecules are bridging. Each sodium ion is bridged to two other sodium ions by two waters between each pair of sodium ions (Figure 3-18). This structure extends as a chain through the crystal. The Na-Na distance is 3.588(15) Å.

Figure 3-15 Crystal Structure of $[Co(EDTA)]^-$

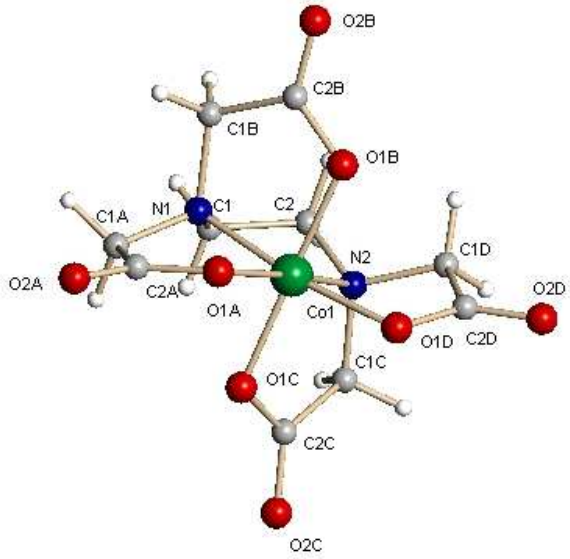

Selected bond lengths (Å) and angles (°) Co1-O1B 1.892(3), Co1-O1C 1.900(3), Co1-N1 1.917(3), Co1-O1A 1.920(3), Co1-O1D 1.922(3), Co1-N2 1.933(3), O1B-Co1-O1C 177.30(13), O1B-Co1-N1 87.72(13), O1C-Co1-N1 94.05(13), O1B-Co1-O1A 91.02(12), O1C-Co1-O1A 87.11(11), N1-Co1-O1A 85.05(12), O1B-Co1-O1D 86.41(12), O1C-Co1-O1D 92.04(11), N1-Co1-O1D 171.53(13), O1A-Co1-O1D 101.15(12), O1B-Co1-N2 94.60(13), O1C-Co1-N2 87.43(13), N1-Co1-N2 90.51(13), O1A-Co1-N2 172.70(13), O1D-Co1-N2 83.88(13).

Figure 3-16 Packing Diagram of Na[Co(EDTA)] Complex

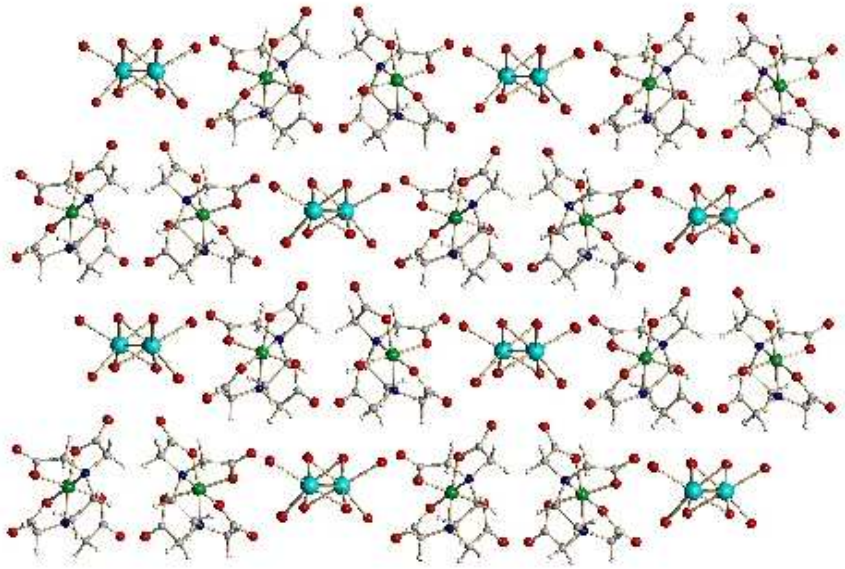

Figure 3-17 Na Fragment

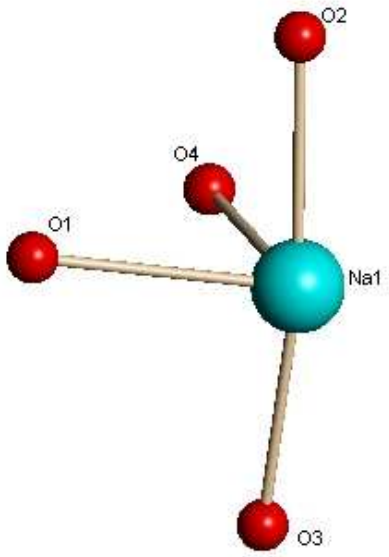

Selected bond lengths (Å) and angles Na1-O1 2.540(4), Na1-O2 2.403(4), Na1-O3 2.410(4), Na1-O4 2.441(4), O2-Na1-O3 170.59(15), O2-Na1-O4 83.59(13), O3-Na1-O4 88.28(12), O2-Na1-O1 81.14(14), O3-Na1-O1 92.89(12), O4-Na1-O1 80.51(12).

Figure 3-18 Extended Structure of the Sodium/Water Chain

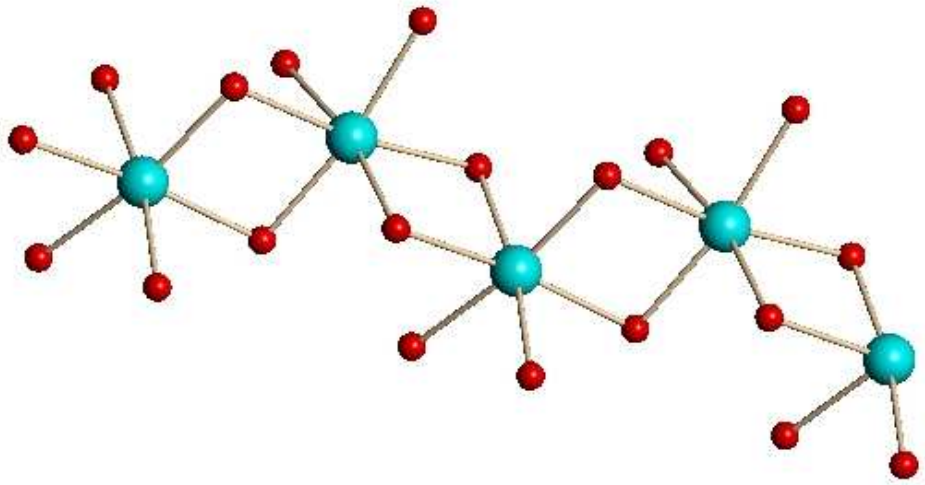

There are other examples of this type of fragment in the literature. In the literature the solvated sodium counter ion can exist as a straight dimer,[77] or as a polymer like that seen in this structure.[78-80]

Crystal Structure of $Ba[Co(EDTA)]_2$

Due to the interesting find with the sodium salt, other salts (barium(II) and hydrogen(I)) of $[Co(EDTA)]^-$ were subjected to a number of recrystallisation techniques in attempts to produce crystals suitable for X-ray crystallography. Unfortunately the crystals obtained for H[Co(EDTA)] were highly twinned and no structural solution could be determined from the X-ray data. There was more success with the $Ba[Co(EDTA)]_2$ salt. Suitable single crystals were grown and the data collected. Since the collection of the data, the crystal structure has been reported in the literature.[81]

The asymmetric unit (Figure 3-19) has two main entities. There is a $[Co(EDTA)]^-$ molecule, which is a discrete complex. There is also a $Ba[Co(EDTA]^+$ unit which is a

polymer that runs through the crystal (Figure 3-20). The barium atom is bridging two $[Co(EDTA)]^-$ molecules and is bonded to them through the carbonyl oxygen atoms on one of the EDTA arms. In addition to the two EDTA oxygen atoms, the barium is also bonded to seven water molecules. The barium motif with the water molecules surrounding it has been reported in the literature before as both the polymeric structure, as seen in this crystal, and also as bridging discreet units.[82-85]

Figure 3-19 Asymmetric Unit of $Ba[Co(EDTA)]_2$

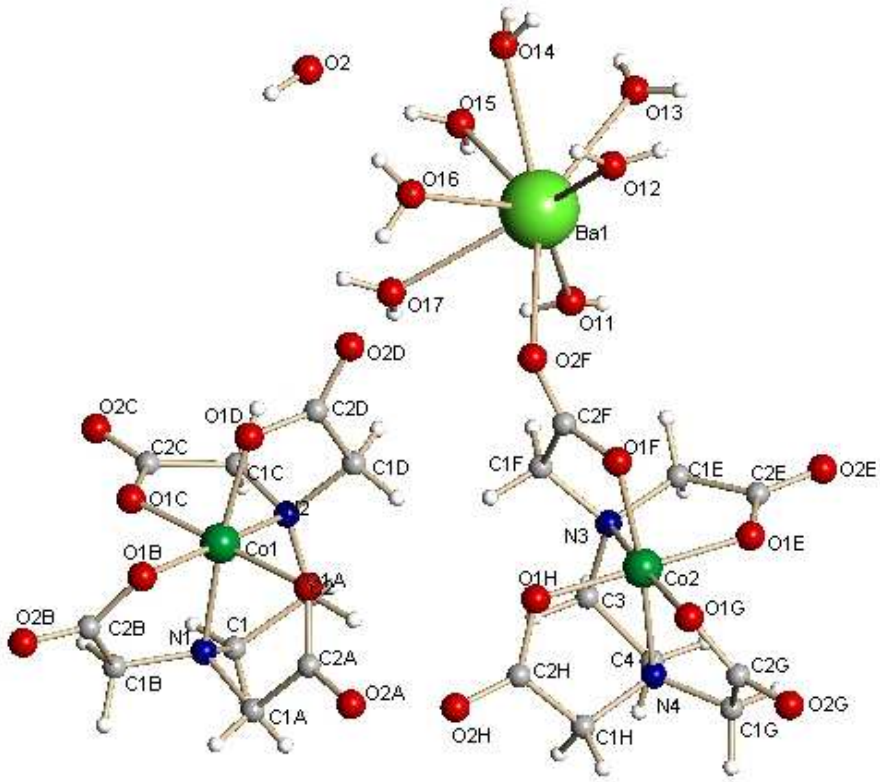

Selected bond lengths (Å) and angles Co1-O1C 1.8857(17), Co1-O1A 1.8925(16), Co1-O1B 1.9134(17), Co1-O1D 1.9143(17), Co1-N1 1.921(2), Co1-N2 1.923(2), Co2-O1H 1.8905(16), Co2-O1E 1.8990(18), Co2-O1F 1.9084(17), Co2-O1G 1.9118 (17), Co2-N3 1.920(2), Co2-N4 1.924(2), Ba1-O12 2.733(2), Ba1-O15 2.7487(19), Ba1-O11 2.791(2), Ba1-O14 2.808(2), Ba1-O2G 2.8290(19), Ba1-O16 2.8322(17), Ba1-O17 2.850(2), Ba1-O13 2.960(2), Ba1-O2F 2.7875(18), O1C-Co1-O1A

177.82(7), O1C-Co1-O1B 86.30(7), O1A-Co1-O1B 91.85(7), O1C-Co1-O1D 90.73(7), O1A-Co1-O1D 88.49(8), O1B-Co1-O1D 100.75(7), O1C-Co1-N1 93.52(8), O1A-Co1-N1 87.42(8), O1B-Co1-N 183.81(8), O1D-Co1-N1 173.98(8), O1C-Co1-N2 86.99(8), O1A-Co1-N2 94.96(8), O1B-Co1-N2 171.35(8), O1D-Co1-N2 84.79(8), N1-Co1-N2 91.16(9), O1H-Co2-O1E 179.02(8), O1H-Co2-O1F 87.25(8), O1E-Co2-O1F 92.22(8), O1H-Co2-O1G 92.02(7), O1E-Co2-O1G 87.27(8), O1F-Co2-O1G 100.60(7), O1H-Co2-N3 94.12(8), O1E-Co2-N3 86.65(8), O1F-Co2-N3 84.50(8), O1G-Co2-N3 172.21(8), O1H-Co2-N4 87.07(8), O1E-Co2-N4 93.53(8), O1F-Co2-N4 172.66(8), O1G-Co2-N4 84.25(8), N3-Co2-N4 91.28(8), O12-Ba1-O2F 79.80(7), O15-Ba1-O2F 141.10(6), O2F-Ba1-O11 86.74(6), O2F-Ba1-O14 136.15(5), O12-Ba1-O2G 71.33(6), O15-Ba1-O2G 132.80(6), O2F-Ba1-O2G, 68.29(6),

Figure 3-20 Extended Structure of $\{[Ba(H_2O)_7][Co(EDTA)]\}^+$ Showing 1D Polymer

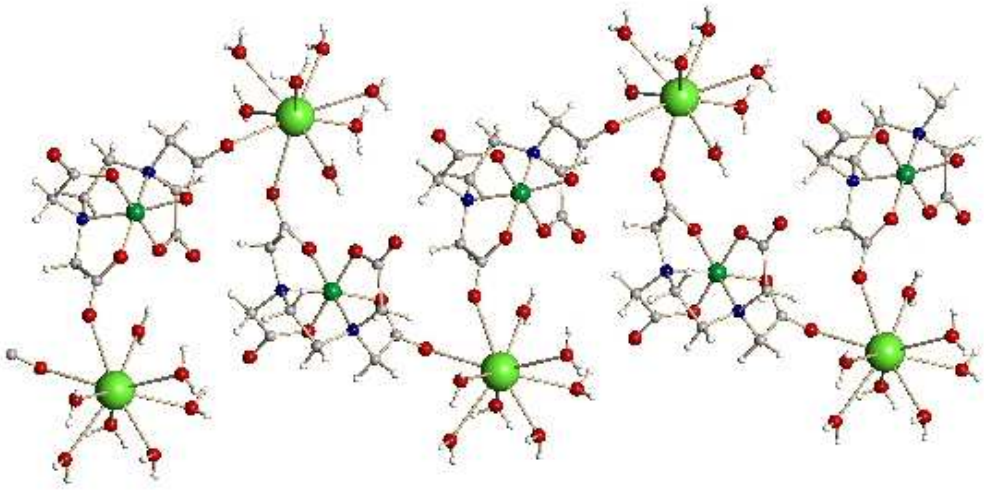

The crystal structure of $[Co(EDTA)]^-$ with a number of counterions have now been reported. The $[Co(EDTA)]^-$ unit in all of the crystal structure stays almost exactly the same. The differences come in the counterion. With the magnesium[86] counterion the magnesium is surrounded by six waters and is a discreet unit unlike the polymeric nature of the barium counterion. The calcium[86] and strontium[81] counterion are similar to that of magnesium ion except that the calcium ion is surrounded by seven water molecules and the strontium ion is surrounded by eight water molecules.

Two other counterions have had crystal structures reported in the literature. The gadolinium counterion has the gadolinium ion surrounded by six waters as well as bonding to four oxygen atoms of the EDTA ligand. Two of the oxygen atoms are carbonyl oxygen atoms and the other two oxygen atoms are atoms that are bonded to the cobalt metal centre.[87] The other crystal structure of the counterion is that of the NH_4^+.[88]

SUMMARY

The premise that species with opposite charges will be inclined to react with each other was tested by having the positive charged $[Co(bpy)_2(gly)]^{2+}$ and the negative charged $[Co(EDTA)]^-$ as reacting species in the same solution. Steady state photolysis has been reported by two different methods. The first method was on a small scale to study the reaction of the starting materials and record any instances of product formation. The other method used was on a larger scale in the hopes of isolating and characterising the products of the reaction.

When the species were by themselves and subjected to steady state photolysis evidence suggested that metallocycles formed. When they were reacted together there was evidence to suggest something new was occurring. The expected result of a neutral complex was not seen. This was especially apparent in the bulk photolysis when there was no coloured material that passed straight through both the cationic and anionic column. There was evidence that a reaction had taken place by the presence of a pink band that was not in either of the two reactions of the starting materials. The UV/vis spectrum of the pink band also did not fit with the starting materials or the known products of the reactions performed on the starting materials.

The crystal structures of Na[Co(EDTA)] and $Ba[Co(EDTA)]_2$ were both obtained. There was interesting characteristics in the water motif that surrounded the counterion. In the case of the sodium ion there was a 1D polymer with bridging waters and in the barium counterion there was a 1D polymer with alternating $[Ba(H_2O)_7]^{2+}$ and $[Co(EDTA)]^-$ connecting through carbonyl oxygen atoms on the EDTA ligand.

Chapter Four

Xylene Bridged Bis(bidentate) Systems

Chapter 4

Xylene Bridged Bis(bidentate) Systems

INTRODUCTION

The key ligands to be discussed in this chapter are a series of five ligands based on a xylene spacer separating two bidentate nitrogen atom donor sites (Figure 4-1). The bidentate sites were based on ethane-1,2-diamine (en) in 1,2-, 1,3-, 1,4-bis(2-aminoethylaminomethyl)benzene,[31](**L4.1**, **L4.2** and **L4.3** respectively**)**. The binding sites in the other ligands were based on 2-aminomethylpyridine (ampy) in 1,3-, 1,4-bis({2-pyridylmethyl}aminomethyl)benzene, (**L4.4**, **L4.5**).

Figure 4-1 Ligands Discussed in this Chapter

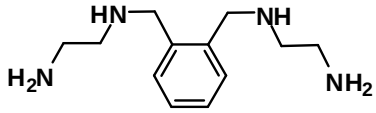

L4.1

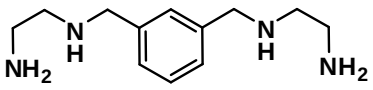

L4.2

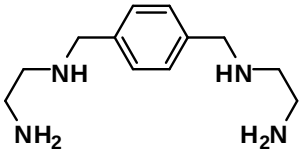

L4.3

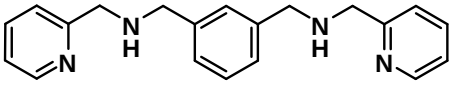

L4.4

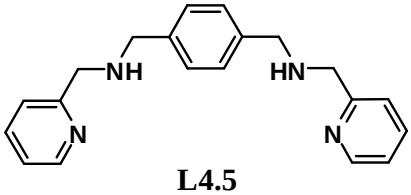

L4.5

This work rose from the ashes of an abandoned approach to dinuclear systems. The original idea for this study was to use flexible bis(polydentate) ligands (**L4.6**) as building blocks to make more rigid bis(pentadentate) ligands (**L4.7**) with two separate binding sites with five donor nitrogen atoms at each site (Figure 4-2). If you used a pentadentate ligand on an octahedral metal centre it is possible that all but one site could be taken up by the ligand. The free site would be used to bind the fibre mimic.

Figure 4-2 Original Synthetic Targets

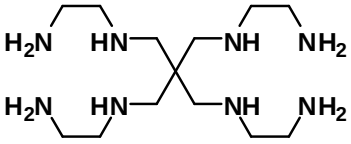

L4.6

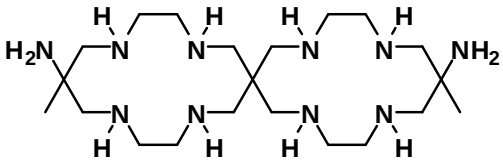

L4.7

The beauty of the **L4.7** system is that the macrocycles are attached to a tetrahedral carbon atom. This means that the planes of the four nitrogen atoms in the two rings are held approximately perpendicular to each other. Building on from this, a system was sought when the binding site were in plane with each other. This could be achieved by using an aromatic spacer group instead of the tetrahedral carbon atom (Figure 4-3). Using a benzene spacer would also mean that the metals, and thus the carboxylate fibre mimics, are held further apart (Figure 4-4).

Figure 4-3 Original Xylene Bridged Synthetic Target

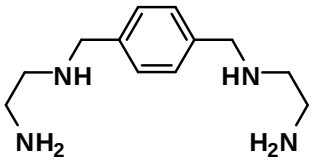

L4.3

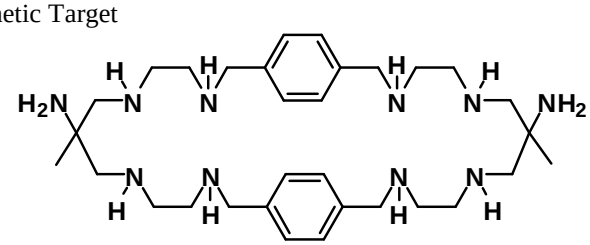

L4.8

Figure 4-4 Difference in the Coordination Planes of **L4.7** and **L4.11**

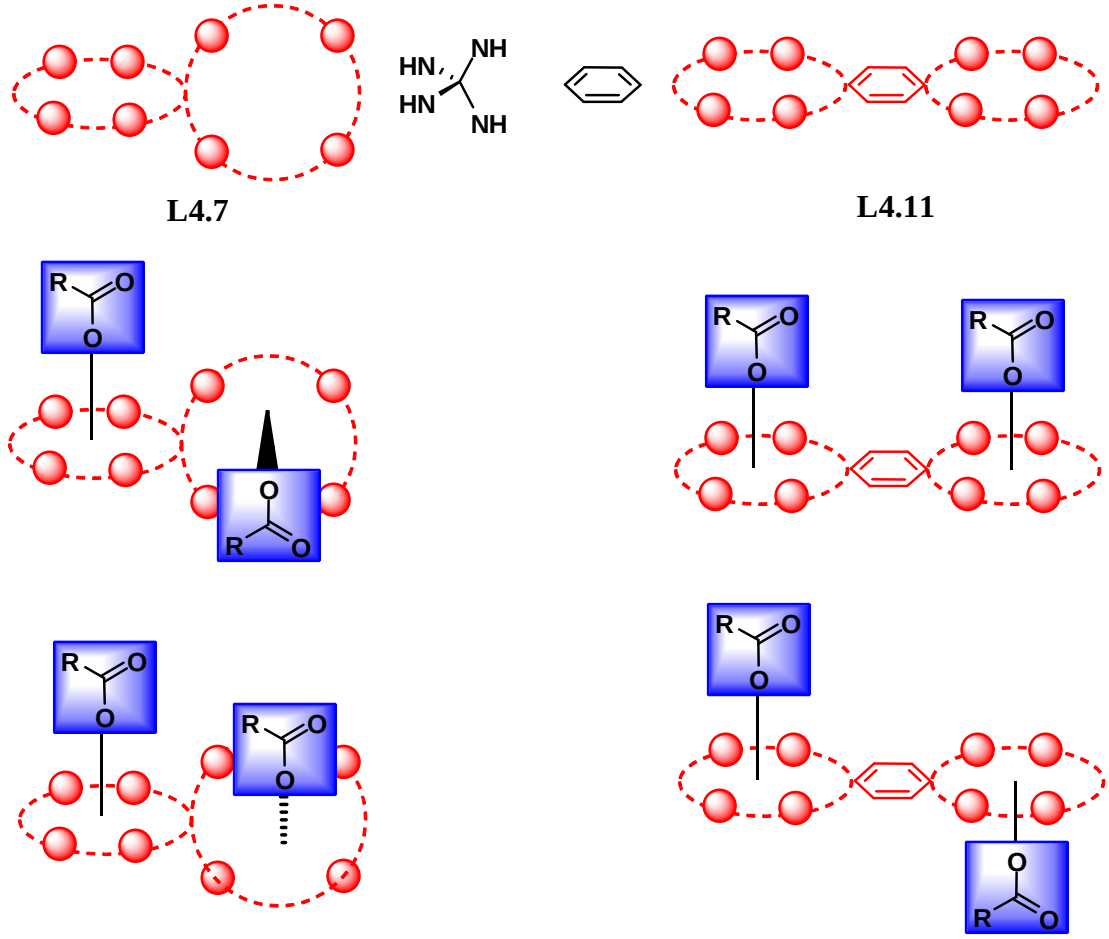

Both **L4.7** and **L4.11** have the potential to bind five nitrogen atoms to each of the two metal centres leaving one site on each of the metal centres for a fibre mimic. 5,5-bis(2-aminoethylaminomethyl)-1,9-diamino-3,7-diazanonane, **L4.6**, is a known compound[89-97] and variations of two different syntheses have been reported.[92, 94-96] A number of metal complexes of **L4.6** have been made including cobalt,[89, 90, 93] nickel,[91, 92, 94, 95] copper[95, 98] and palladium.[95] Base hydrolysis of the cobalt(III) complex has been studied.[89] **L4.6** is also used in the constructing of transfer-promoting dendrimer membranes for separating CO_2 from CH_4.[97]

The two general ways of making **L4.6** are based on the same principle. A 3,3 diethylpentanyl core with a leaving group on each of the four arms is reacted with en. The differences come in the choice of the leaving group. In the first synthesis reported in the literature,[96] the leaving group was bromine. The reaction was carried out under high temperature and the method of purification was distillation. This synthesis has since been modified and improved.[99]

Scheme 4-1 Synthesis of **L4.6**

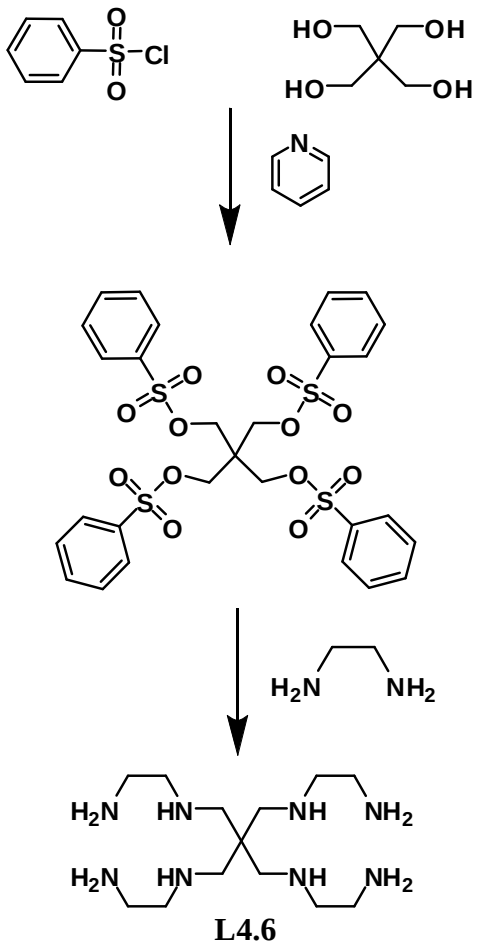

L4.6

Another method, the one employed in this research (Scheme 4-1), started with a pentaerythritol core and underwent functional group conversion to take it from the alcohol substituted, to the tetrakis(benzylsulfonate). With benzylsulfonate as the

leaving group the conditions of the reaction were milder; the reaction is carried out at room temperature. There are four methods of purification reported. The first method isolates **L4.6** as the HCl salt.[92] The second method involves preparing $[Cu_2(\mathbf{L4.6})](NO_3)_4$, which is required for the next step, directly from the reaction mixture.[100] The third method requires the preparation of $[Ni_2(\mathbf{L4.6})](ClO_4)_4$.[92] The final method uses cobalt complexation.[90] In this research the first method was the one employed because the reaction can be easily scaled up and the yields are higher.

A synthesis where the ligand was capped (Scheme 4-2), producing ligand **L4.7** with two macrocycles, has been reported.[100] The synthesis involved coordination of **L4.6** to copper(II) metal and a metal mediated Mannich reaction taking place, to produce $[Cu_2(\mathbf{L4.9})]$. This complex has been further studied by pulse radiolysis.[101] This complex can not be used directly in photolysis experiments for this research and the idea was to react the ligand further, to make a new ligand (Scheme 4-2). The copper was to be removed with a zinc/acid reduction.[102] There was the added benefit of reducing the nitro group to a primary amine and making a pentadentate donor site on each half of the ligand.

In the literature there have not been any reports of **L4.7**. However, the tri-capped ligand **L4.10**, and the cobalt(III) complexes have been reported (Figure 4-5).[103]

Scheme 4-2 Capping Reaction of **L4.6**

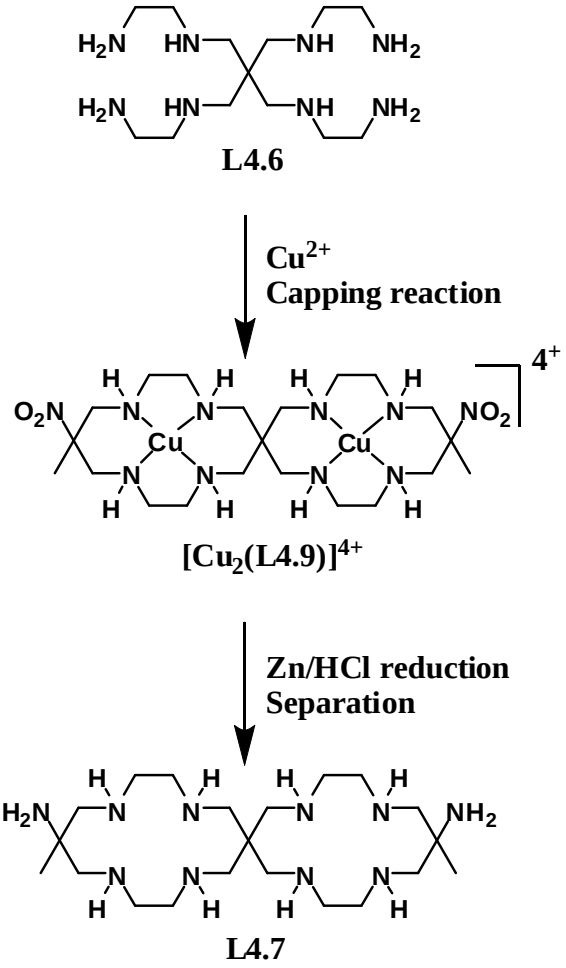

Figure 4-5 L4.10 and its Cobalt Complex

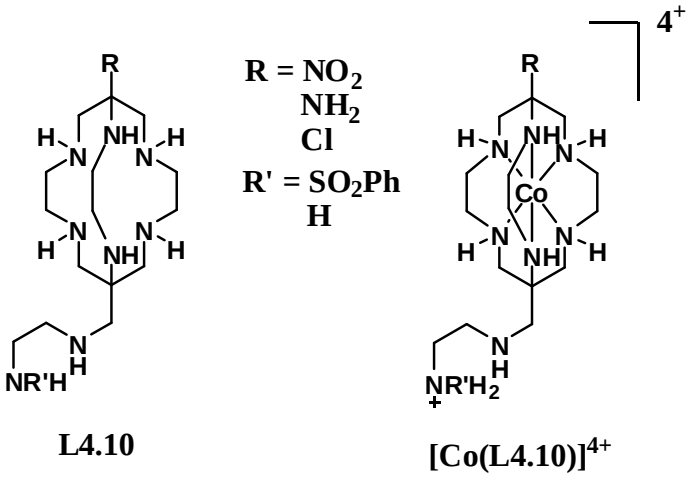

The synthesis that was to be employed to make the capped xylene ligand **L4.8** followed the synthesis for **L4.7** and is outlined in Scheme 4-3.

Scheme 4-3 Proposed Synthesis of Target Ligand **L4.8**

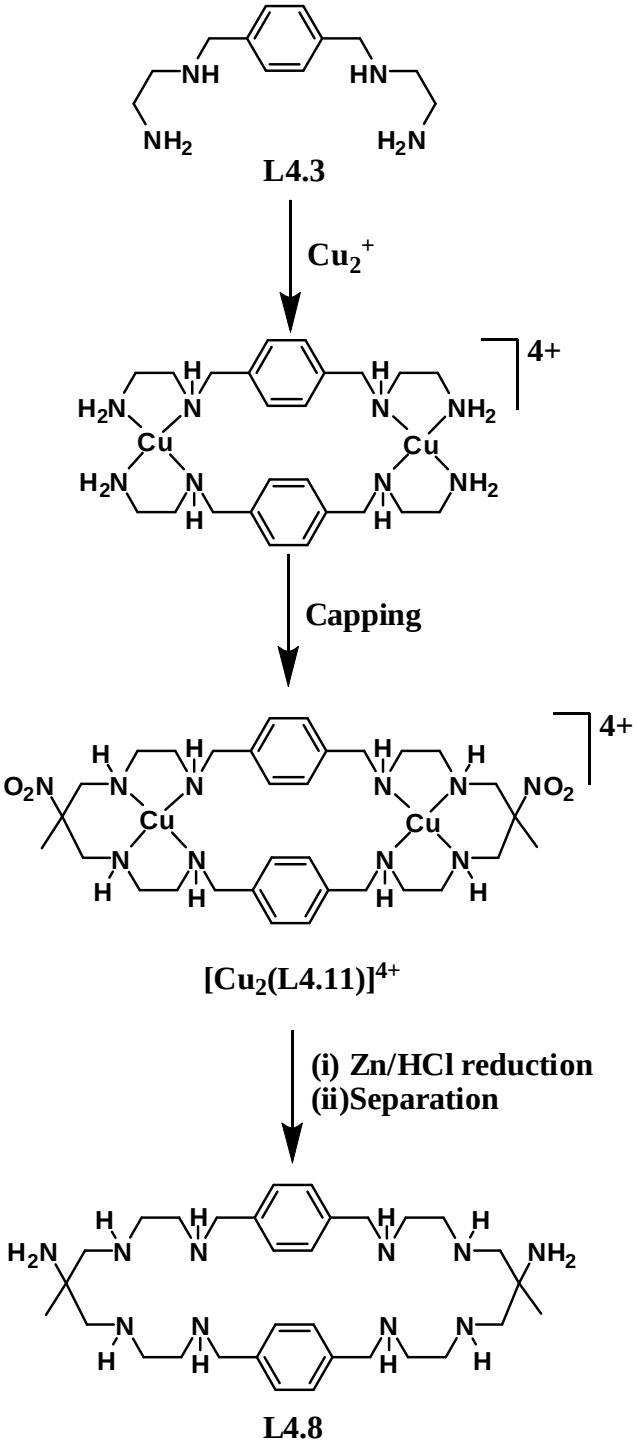

The reactions were unsuccessful for a number of reasons. In the case of **L4.7**, there were problems due to the low yields and poor scale up of the reactions leading up to

and including the capping reaction. For **L4.11**, an insoluble light blue powder was formed in the first step to make the $[Cu_2(\mathbf{L4.3})_2]^{4+}$. It is possible that, in the attempt to make $[Cu_2(\mathbf{L4.3})_2]^{4+}$, a polymer has been made instead of discrete molecules. The extremely low solubility of the product from the $[Cu_2(\mathbf{L4.3})_2]^{4+}$ synthesis supports polymer assignment. Other copper(II) salts and techniques were tried with similar results. It was thought that perhaps a non-coordinating anion, such as perchlorate, would promote discreet molecule formation. Small blue crystals were formed using the H-tube method of growing crystals. They were unsuitable for x-ray diffraction and proved to be just as insoluble as the powder.

While this was disheartening, as considerable time and effort had been invested in pursuit of those systems, there was still potential use for **L4.3**. It was observed that **L4.3** was a ligand capable of binding two metals. For this research, the criteria for the ligands were that they were capable to coordinate two metals with a possible site to introduce a fibre mimic on each metal. The two bidentate binding domains provide two nitrogen donor atoms and can coordinate to a metal ion. This would leave four vacant sites on each octahedral metal atom to bind other ligands. Ideally, three sites will be taken up with a tri-dentate ligand such as tacn. The remaining site will be used to bind a fibre mimic, as in Figure 4-6. This opened up a series of ligands and analogous ligands with different spacing relationships of the arms coming off the benzene ring, and different nitrogen donors (**L4.1**, **L4.2**, **L4.4** and **L4.5**). Ligand **L4.1** has two 2-aminoethyl arms in a 1,2- relationship which raises the possibility of binding both of its bonding sites to the one metal.

Figure 4-6 Possible Binding of **L4.3**

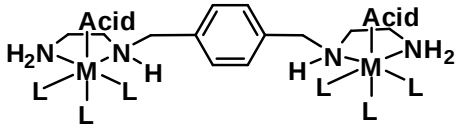

A search of the literature finds that these ligands have not yet been extensively investigated. In 1986, a patent was taken out on **L4.2** and its metal complexes.[104] It was thought that the metal complexes could be used in cancer research due to the fact that the structure of the platinum complex of **L4.2** has similarities to cis-platin, which is a successful chemotherapy drug used against some cancers. Recently, more work has been done.[105] **L4.3** has also been synthesized previously.[106] In 2006, the $[Pt_2(\mathbf{L4.3})Cl_4]$ complex was made.[105] Again, the researchers believe that this complex could lead to new anti-cancer drugs. **L4.12** (see below), a compound related to **L4.2**, having a tertiary amine with two 2-aminoethyl arms instead of a secondary amine with one 2-aminoethyl arm, has been made with dinuclear species of copper and platinum.[107-110] The interaction of the complexes with DNA was studied and the complexes were also studied for anti-cancer properties.

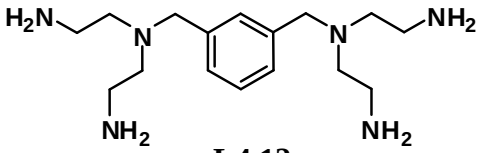

L4.12

RESULTS AND DISCUSSION

Synthesis of Ligands

The syntheses of the ligands are shown in Scheme 4-4. The reactions were carried out at room temperature where α,α'-dibromo-X-xylene (where X is *o* for **L4.1**; *m* for **L4.2** and **L4.4**; and *p* for **L4.3** and **L4.5**) was added portionwise over a number of hours to excess ethane-1,2-diamine (en), in the case of **L4.1**, **L4.2**, **L4.3**; or 2-aminomethylpyridine (ampy), in the case of **L4.4**, **L4.5**. The use of excess en and ampy is to prevent, or at least lessen, the formation of other products and polymers. The polymers and other products occur when two α,α'-dibromo-X-xylene molecules react with the same en, or ampy, molecule. The syntheses could be easily scaled up with little change to the yield.

A larger excess of en was used in the synthesis of: **L4.1**, **L4.2**, and **L4.3**; than ampy in the synthesis of: **L4.4** and **L4.5**. This is due to the fact that ampy is more expensive than en and some of the excess en can be recovered by removing it on a rotary evaporator. Not all of unreacted en can be removed in this way and the product is ultimately separated from the unreacted en (or ampy) and the rest of the reaction mixture by ion exchange chromatography. The ligands are isolated as the HCl salts.

Scheme 4-4 Synthesis of Ligands **L4.1**, **L4.2**, **L4.3**, **L4.4** and **L4.5**

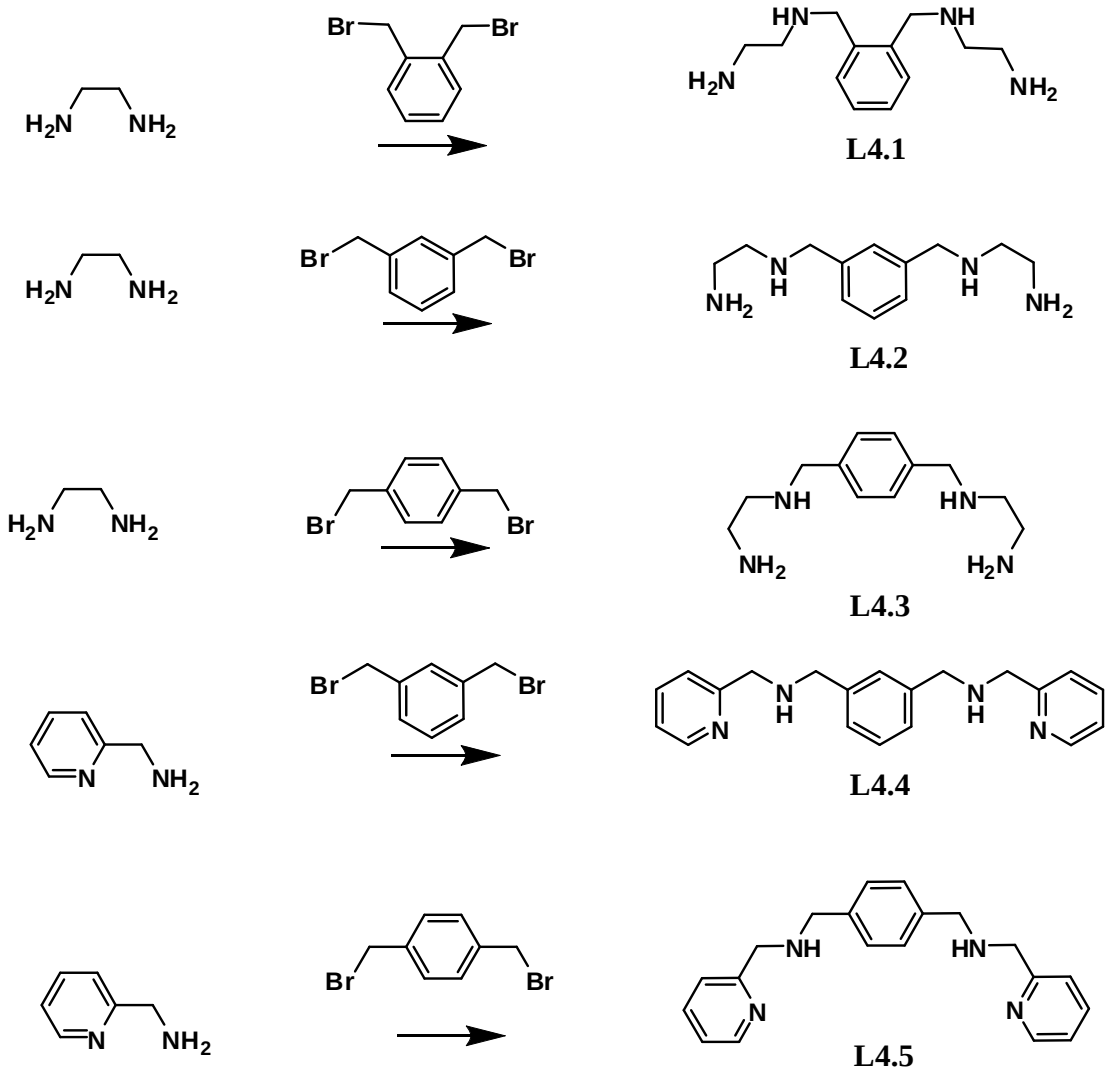

The resin used in the column chromatography was Dowex 50W-x4 (100-200 mesh) cation exchange resin. The bands could not be seen on the column, but once the pattern of elution was established the columns could be completed in a systematic way because of the reproducibility. The reaction mixture was diluted with water and made up to 1 L. The solution was acidified and loaded onto the column. 2.25 M HCl was run through the column and in this fraction the excess en or ampy was collected as the HCl salt. 4 M HCl was then run through the column and this is the fraction where the bulk of the product was isolated.

In the case of **L4.1**, product was contaminated with **L4.13** (Figure 4-7). If required, **L4.1** and **L4.13** can be separated by a silica column eluting with dichloromethane/methanol.[105] The crude material could be used. During the synthesis of **L4.2**, a white precipitate formed during the addition of α,α'-dibromo-*m*-xylene, which was filtered off and through NMR analysis was proven to not be the product. (An elemental analysis of the white powder was taken and the empirical formula $C_{2.5}H_5N$ was calculated. From this, and knowing what the reacting fragments are, it was concluded that it is a mixture of starting materials and possibly some product. Found; C, 44.4; H, 7.8; N, 21.0%).

Figure 4-7 L4.13

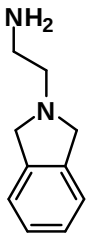

L4.13

The ligands are isolated as the HCl salts. **L4.1**·xHCl is a light yellow powder and has an impurity of **L4.13**·xHCl. The impurity was calculated, by ^{1}H NMR spectrometry, to be 43% of the bulk material by weight, on the assumption that the salts are **L4.1**·4HCl and **L4.13**·2HCl. **L4.2**·xHCl salt is a brown oil and the elemental analysis was unable to be performed. **L4.3**·4HCl is isolated as an off white powder and the elemental analysis is consistent with **L4.3**·5HCl. **L4.4**·xHCl is a brown oil and the elemental analysis was unable to be performed. **L4.5**·4HCl is an off white powder and the elemental analysis is consistent with **L4.5**·5HCl·0.25H_2O.

There are obvious patterns seen in the NMR spectra of the ligands with the same bis(bidentate) binding group. For **L4.1**, **L4.2** and **L4.3** the non-aromatic regions are all similar. In the ^{1}H NMR spectra, there are two peaks associated with the en arms at 3.4 ppm and 3.5 ppm and a peak for the benzylic methylene hydrogen atoms at 4.40 ppm. The integrals for all three peaks are the same. The peaks for the en arms are multiplets and the benzylic methylene peak is a singlet. In the non-aromatic region for the ^{13}C NMR spectra there are also three peaks of equal height. The peak for the carbon atom next to the primary amine is at 38 ppm, the peak for the carbon atom next to the secondary amine is at 46 ppm and the benzylic methylene carbon atom is at 53 ppm.

There are marked differences in the aromatic regions. The spectra for **L4.1** also have the impurity of **L4.13** and are hard to definitively assign, but there is some information that can be obtained. In the ^{1}H NMR spectrum, there is a distinct aromatic region from 7.2-7.8 ppm. Due to the two compounds in the sample, it is expected that there would be four peaks, yet in the spectrum only two are seen. This could be due to one set of peaks being on top of the other. In the non-aromatic region the peaks are too close and are overlapping to get an accurate idea of how many there are.

The ^{13}C NMR spectrum provides a lot more information. The aromatic region has six peaks with three peaks belonging to each of the amine molecules. There are two peaks shorter than the others, that would correlate to the quaternary carbon atoms. In the non-aromatic region there are six peaks, again with three peaks belonging to each of the two ligands. The peaks below 40 ppm are the carbon atoms next to a primary

amine. The peaks between 40-50 ppm are the carbon atoms next to secondary amines and the peaks above 50 ppm are the benzylic methylene carbon atoms.

For **L4.2**, the ^{1}H NMR spectrum shows three peaks in the aromatic region. One of the peaks has an integral twice as big as the other two peaks and is the peak corresponding to the two equivalent hydrogen atoms. The ^{13}C NMR spectrum shows four peaks in the aromatic region with one of the peaks being larger than the other three. The large peak correlates to the two equivalent benzylic carbon atoms with the hydrogen atoms attached. One of the smaller peaks is the two quaternary carbon atoms and the other two peaks are the remaining two carbon atoms.

For **L4.3**, the ^{1}H NMR spectrum shows one peak in the aromatic region it is a singlet and this is due to the fact that all the aromatic hydrogen atoms are equivalent. The ^{13}C NMR spectrum shows two peaks in the aromatic region with one of the peaks being much larger than the other. The larger peak correlates to the four equivalent benzylic carbon atoms with the hydrogen atoms attached. The smaller peak is assigned to the two quaternary carbon atoms.

For **L4.4** and **L4.5** there are also distinct patterns in the NMR spectra. In the non-aromatic region there are two peaks in the ^{1}H NMR spectra which are assigned to the benzylic methylene hydrogen atoms (4.5 ppm) and the pyridylmethylene hydrogen atoms (4.7 ppm). In the aromatic region the pattern of the pyridyl hydrogen atom signals are the same: doublet, triplet, doublet, triplet pattern. The exact assignments of these peaks were assigned using COSY and NOESY spectrometry. In the ^{13}C NMR spectra, there are two peaks in the non-aromatic region which are the benzylic

methylene carbon atoms at 50 ppm and the pyridylmethylene carbon atoms at 54 ppm. In the aromatic region, there are five peaks associated with the pyridyl groups. Four are the same height and these are the peaks correlating to the pyridyl carbon atoms with a hydrogen atom attached to them. The fifth peak is the peak correlating to the quaternary carbon atom. HSQCAD spectrometry was used to confirm the exact assignment of the carbon atoms in the ^{13}C NMR spectra.

The differences in the spectra, between **L4.4** and **L4.5**, are seen in the phenyl peaks. In the spectra for **L4.4**, there are three peaks in the aromatic region for the phenyl hydrogen atoms. Two of the peaks have the same integral while the other peak has an integral twice as big. The ^{13}C NMR spectrum shows four peaks in the aromatic region with one of the peaks being larger than the other three. The large peak correlates to the two equivalent phenyl carbon atoms with the hydrogen atoms attached. One of the smaller peaks is the two quaternary carbon atoms and the other two peaks are the remaining two carbon atoms. For **L4.5** there was one phenyl peak in the ^{1}H NMR spectrum which corresponded to all the hydrogen atoms on the benzene ring which were all equivalent. In the ^{13}C NMR spectrum there were two phenyl peaks. A large peak for the four equivalent carbon atoms with the hydrogen atoms attached and a smaller peak for the two equivalent quaternary carbon atoms.

Crystal Structure of L4.3

Another analysis technique used to characterise **L4.3** was X-ray crystallography. During an attempt to coordinate **L4.3** with iron(II) sulfate some crystals formed upon slow evaporation. The colourless crystals were not that of an iron complex and turned out to be that of the sulfate salt of the protonated ligand. A crystal structure of

$4H^+$[**L4.3**]$(SO_4)_2$ has been solved and refined with an R_1 factor of 3.3%. A picture of the ligand is shown in Figure 4-8. The solvent molecules and counterions have been omitted for clarity.

Figure 4-8 Crystal Structure of **L4.3**

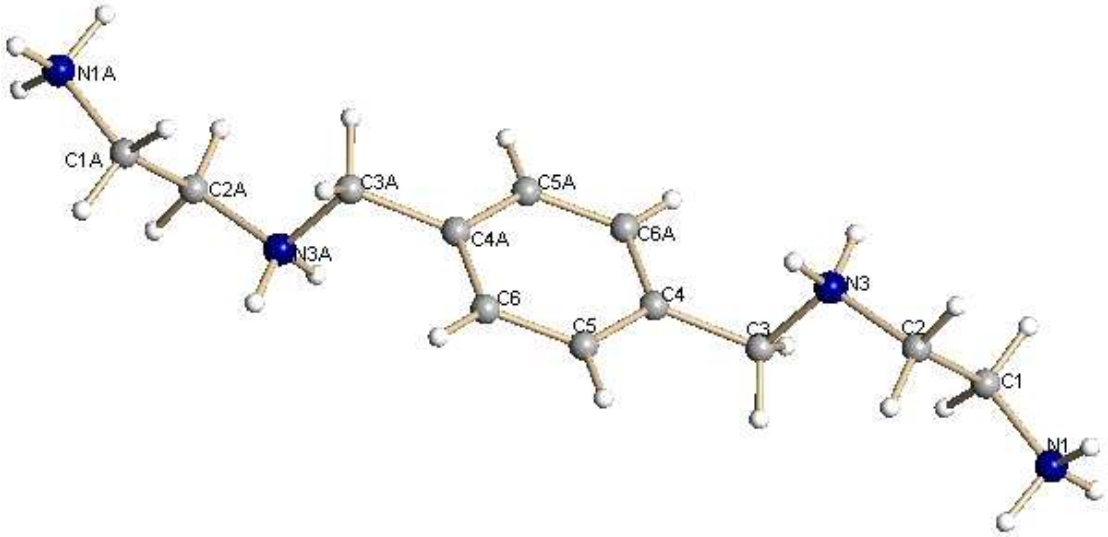

Selected bond lengths (Å) and angles (^{o}) N1-C1 1.482(3), C1-C2 1.521(3), C2-N3 1.494(3), N3-C3 1.511(3), C3-C4 1.509(4), C4-C6 1.395(3), C4-C5 1.399(3), C5-C6 1.385(3), N1-C1-C2 109.27(18), N3-C2-C1 110.86(18), C2-N3-C3113.42(17), C4-C3-N3 110.91(17), C6-C4-C5 119.3(2), C6-C4-C3 120.9(2), C5-C4-C3 119.7(2), C6-C5-C4 120.9(2), C5-C6-C4 119.8(2).

There are some interactions seen in the packing diagrams Figure 4-9. Looking down through the crystal it is possible to view the benzene rings so they line up with each other. Looking at the benzene ring side on in the packing diagram Figure 4-10, it can be seen that the rings are offset between the layers. The distance between one benzene ring and the benzene ring above or below it is 3.55 Å. The en arms of the ligand between each layer of the crystal are off set from each other by approximately 60^o.

Figure 4-9 Packing Diagram of **L4.3**

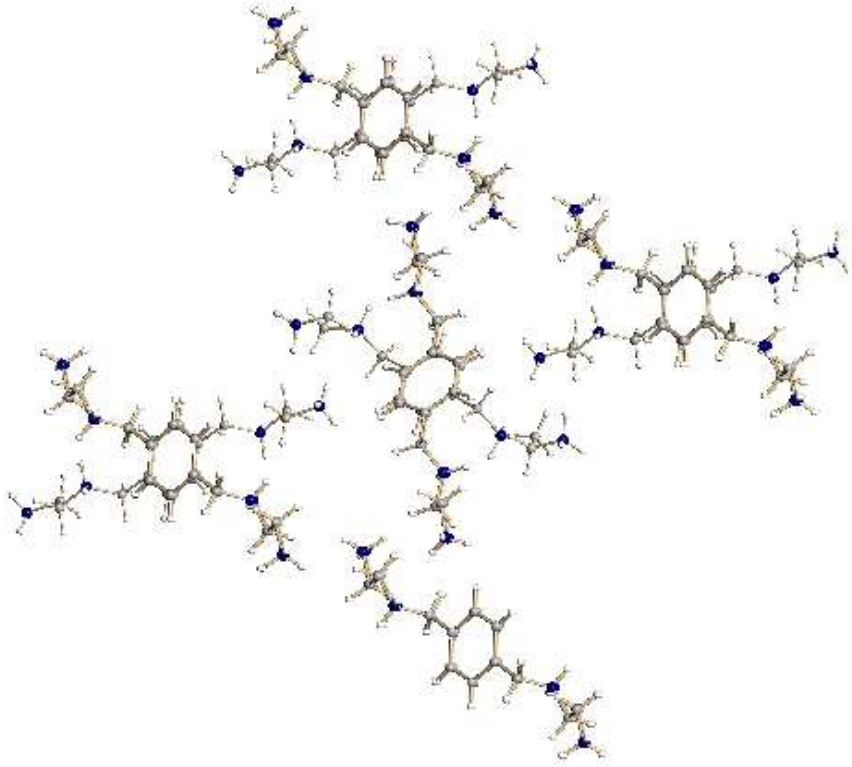

Figure 4-10 A View of **L4.3** Molecules, Side on to the Benzene Ring

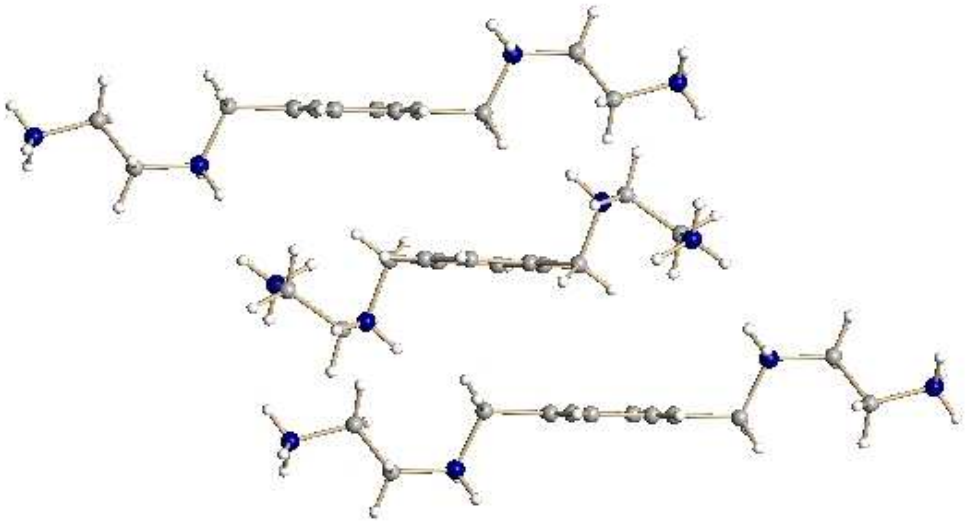

Synthesis of Complexes

The premise for these ligands is that instead of adding additional binding sites to the ligand, the other coordination sites on the metal can be taken up by auxiliary ligands, as in Figure 4-11. In this case, because the work involves octahedral metal centres, the additional ligands need to be tridentate to leave one binding site for the fibre mimic. There are a number of ligands that are tridentate, three of them are shown below. The ligands shown below fall into three broad categories of bonding modes: flexible with the example of N^1-(2-aminoethyl)ethane-1,2-diamine (dien); facial with the example of 1,4,7-triazacyclononane (tacn); and meridional with the example of 2,2':6',2''-terpyridine (tpy). Flexible ligands can bind in either facial or meridional fashion, this leads to the possibility of different isomers. The facial and meridional ligands have built in limitations that restrict the binding and reduce the number of isomers. A facial ligand binds to one of the eight faces of an octahedral metal centre. This means that all of the other binding sites are opposite that ligand. This could influence the strength of the metal-ligand bond due to the trans influence. The meridional ligand runs along the meridian of the octahedral metal centre, and only one of the other binding sites is opposite a meridional ligand.

Figure 4-11 Possible Binding of Complexes

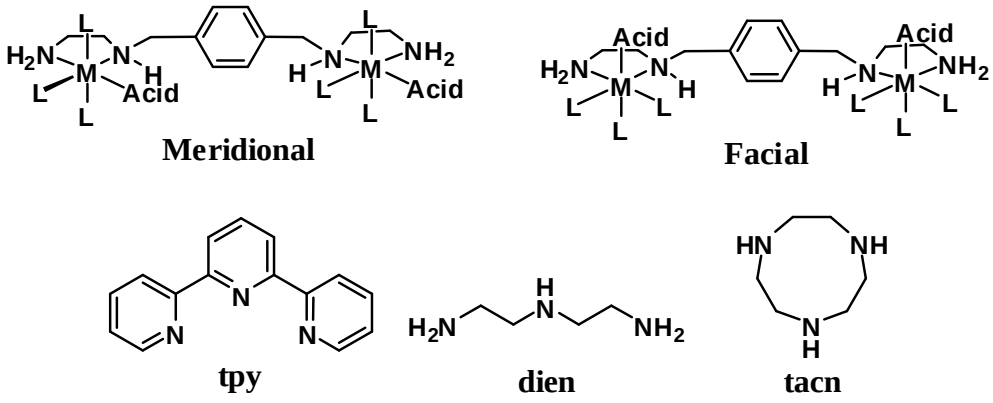

The restricting of isomers simplifies the separation of pure samples, so either a facial or a meridional ligand would be acceptable. Due to previous work, a supply of $[Co(tacn)(NO_2)_3]$ was readily available, so tacn was chosen to be the tridentate ligand. The nitrite ligands in $[Co(tacn)(NO_2)_3]$ were replaced by chloride ligands to make $[Co(tacn)Cl_3]$ using standard methods. The chloride ligands are typically more labile and will undergo substitution reactions more easily than nitrite ligands.[111]

The cobalt complex and the HCl salt of the ligand were added together. In the salt the amine nitrogen atoms are protonated, which means that the lone pair of electrons is unavailable to form a dative bond to the cobalt metal. To activate the ligand, the pH was adjusted to 8; at this pH some of the amine nitrogen atoms deprotonate. The protonated and deprotonated amine species will be in equilibrium with each other; most likely at this pH the primary amine will be deprotonated and secondary amines will still be protonated.[112] The primary amine is free to coordinate to the cobalt metal. After the primary amine is coordinated, the ligand will be close to the metal and when the secondary amine deprotonates (due to the equilibrium) the secondary amine can coordinate.

The reaction mixture was stirred at 80^{o}C. To ensure that the remaining site had a coordinated chloride, the pH was then adjusted to 3 with dilute HCl and the reaction was allowed to continue at 80^{o}C. The reaction mixture was then diluted and a Dowex 50W-x4 (100-200 mesh) ion exchange column was run, eluting with increasing concentrations of HCl. This reaction was performed on **L4.1**, **L4.2**, **L4.3**, **L4.4**, and **L4.5**. The results will be discussed independently, but the chromatographic separations of the mixtures of complexes exhibited some common features.

Occasionally, the first band was collected during the loading of the column. It is a pink fraction and turns to blue upon reducing the volume on a rotary evaporator. The fraction dries to a blue/green powder. The second band is eluted with 1 M HCl and is a pink/purple colour. It also dries to a blue green powder. The third band is eluted with 2 M HCl and is a cherry red colour. It also dries to a blue/green powder. Occasionally there was another fraction that reduced to give a blue/green powder. This was eluted with 3 M HCl and unfortunately sometimes eluted concurrently with other species such as an orange band identified as $[Co(tacn)_2]Cl_3$. The mono-cobalt and di-cobalt complexes, if they were formed, eluted with 4 M HCl and appeared on the column as one band; the mono-cobalt complex being at the start of the band and the di-cobalt complex at the end of the band. The concentration of the eluant was increased to 5 M to remove the last of the di-cobalt band.

The first four bands that dry to give a blue/green powder, which was identified as $[Co(tacn)(Cl)_3]$,[113] are thought to be $[Co(tacn)(Cl)_2(H_2O)]$, $[Co(tacn)(Cl)_2(H_2O)]^{1+}$, $[Co(tacn)(Cl)(H_2O)_2]^{2+}$ and $[Co(tacn)(H_2O)_3]^{3+}$ respectively.

Cobalt complex of 1,4-bis(2-aminoethylaminomethyl)benzene (L4.3)

L4.3 was the first in this series that was made and because of this more work has been done on this ligand, and the resulting complexes, than on the others. The synthesis followed the general synthesis that was described. In attempts to make a di-cobalt complex, the ratio of $[Co(tacn)Cl_3]$ to **L4.3** was 2:1, despite this only the mono-cobalt was isolated. An evaluation of the column fractions is in Table 4-1, in which: **Fraction** is the number of the band that came off; **Concentration** is the concentration

of HCl that the fraction was eluted with; **Colour of the Solution** is the colour of the fraction as it came off the column; **Colour of Product** is the colour of the dried product once all the acid had been removed; and **Yield and % Column Recovery** is the yield in grams and the percentage of what was recovered from the column was in that band. The cobalt complex fraction is highlighted in the table.

Table 4-1 Evaluation of Column Fractions for **L4.3**

Fraction	**Concentration**	**Colour of solution**	**Colour of product**	**Yield and % column recovery**
1	1 M	Purple	Blue	0.46 g 14.1%
2	2 M	Purple	Blue	0.28 g 8.6%
3	3 M	Cherry Red	Blue/Green	0.34 g 10.4%
4	3 M	Orange	Yellow	0.40 g 12.3%
5	4 M	Light Pink	Purple	1.26 g 38.7%
6	5 M	Yellow	Brown	0.52 g 15.9%

Each fraction was taken to dryness under vacuum and further analysis performed on the resulting solid. The fifth fraction eluted with 4 M HCl is $[Co(tacn)(H_2\mathbf{L4.3})Cl]^{4+}$, the mono-cobalt complex, Figure 4-12. A general explanation of what is observed on

the column is that the first three bands are $[Co(tacn)(Cl)_2(H_2O)]^{1+}$, $[Co(tacn)(Cl)(H_2O)_2]^{2+}$ and $[Co(tacn)(H_2O)_3]^{3+}$ respectively. They all become a blue/green powder, which is $[Co(tacn)(Cl)_3]$, when the chloride ion concentration increases as the volume is reduced and they go to dryness. The fourth fraction is $[Co(tacn)_2]Cl_3$. The fifth fraction is $[Co(tacn)(H_2\mathbf{L4.3})Cl]^{4+}$. The sixth fraction is unreacted ligand.

Figure 4-12 Mono-Cobalt Complex of **L4.3**, $[Co(tacn)(H_2\mathbf{L4.3})Cl]^{4+}$

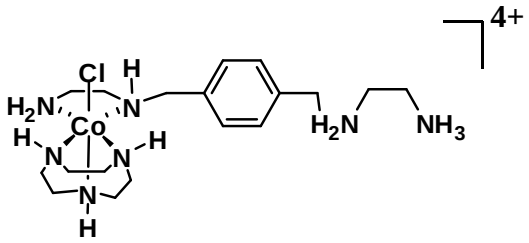

While taking fraction five to dryness it was observed that some material was starting to precipitate out. Methanol was added and more precipitated out. The solid was filtered and the filtrate was still a bright pink colour so it was taken to dryness. By elemental analysis the differences in the filtered precipitate and the residue from when the filtrate was taken to dryness, were in how many water and HCl solvate molecules co-crystallised with the complex. The precipitate that was filtered is a light pink powder $[Co(tacn)(H_2\mathbf{L4.3})Cl]Cl_4{\cdot}2H_2O{\cdot}3HCl$ and by elemental analysis. (Found: C, 32.6; H, 7.0; N, 14.9. Calc for $C_{18}H_{44}Cl_6CoN_7O_2$: C, 32.7; H, 6.8; N, 14.8). The filtrate that was taken to dryness is a dark pink/purple glass $[Co(tacn)(H_2\mathbf{L4.3})Cl]Cl_4{\cdot}3HCl$ and by elemental analysis. (Found: C, 31.2; H, 6.3; N, 14.0. Calc for $C_{18}H_{42}Cl_8CoN_7$: C, 30.9; H, 6.1; N, 14.0).

The complex was also characterised by ^{1}H and ^{13}C NMR spectrometry. To begin with, in the aromatic region there are more peaks than in the spectra for the ligand **L4.3**. This indicates that there is a loss of symmetry. In the aromatic region of the ligand spectrum there was one peak in the ^{1}H NMR spectrum and two in the ^{13}C NMR spectrum. In the complex there are two peaks in this region of the ^{1}H NMR spectrum and four peaks in the ^{13}C NMR spectrum. This indicates that even though the complex is not as symmetrical as the ligand it does retain some symmetry about the benzene ring. In the non-aromatic region of the ^{1}H spectra there are many peaks and it is hard to tell them apart. What was notable was that there were a number of small broad peaks between 5.0-7.4 ppm; these are assigned to amine hydrogen atoms. In the ^{13}C NMR spectrum there is a peak between 30-40 ppm which is where the peak for a carbon atom next to an uncoordinated primary amine should be. There are two peaks in the range of 40-50 ppm which is where the peak for a carbon atom next to an uncoordinated secondary amine or a coordinated primary amine is expected. Between 50-60 ppm there are six peaks for the carbon atoms adjacent to coordinated secondary amines and the benzylic methylene peaks. Some poor quality crystals were grown of the mono-cobalt complex but the data collected from the X-ray crystallography was not of a high enough quality for the structure to be solved.

Another synthesis was carried out with a 1:1 metal to ligand ratio to make the mono-cobalt complex deliberately. As in the same synthesis for **L4.2** the overall result was that there was less unreacted $[Co(tacn)(Cl)_3]$ recovered and a higher percentage yield of the complex. To try and force the synthesis of the di-cobalt species another synthesis was performed where there was a large excess of $[Co(tacn)(Cl)_3]$ available in a 4:1 metal to ligand ratio. No di-cobalt complex was observed and there was more

unreacted [Co(tacn)$(Cl)_3$] recovered than in the previous experiments. Another synthesis was tried in which, instead of starting with the ligand, the reaction started with the mono-cobalt complex. Again no di-cobalt complex was observed and a large percentage of [Co(tacn)$(Cl)_3$] was recovered from the column.

A further strategy was tried in which activated charcoal was added to the reaction mixture and the reaction time was increased. It was noted that the 4 M band was drawn out and had more difficulty eluting from the column than in previous synthesis that had been conducted without the charcoal. The NMR spectra for the beginning of the band were consistent with what has been described for the mono-cobalt complex. The spectra collected for samples from the end of the band were different from the mono-cobalt complex and was identified as $[Co_2(tacn)_2(\mathbf{L4.3})Cl_2]^{4+}$.

In the aromatic region of the ^{13}C NMR spectrum of the mono-cobalt complex, there were two peaks of the same height and these were the two tallest peaks. In the spectrum for the $[Co_2(tacn)_2(\mathbf{L4.3})Cl_2]^{4+}$ complex there is one peak which is much larger than the others. Surprisingly there are three other peaks and not just one other peak. This is not expected or explainable. In the non-aromatic region there should be eight peaks between 50-60 ppm; six for the carbon atoms in the tacn ring and one each for the carbon atom next to the coordinated secondary amine in the ligand and benzylic methylene carbon atom. In the spectrum there are seven peaks but one of the peaks is twice as big as the others indicating that there could be two peaks that happen to be at the same chemical shift. In the region between 40-50 ppm for the $[Co_2(tacn)_2(\mathbf{L4.3})Cl_2]^{4+}$ complex, it is expected that there would be one peak for the carbon atom next to the coordinated primary amine. In the spectrum there is a peak in

that region that is the same height as those in the 50-60 ppm region. There is also a smaller peak. Additional to the peaks described there is a peak at 38 ppm, where you would expect to find a peak for a carbon atom next to an uncoordinated amine. It is worth noting that the spacing between the peaks assigned for the $[Co_2(tacn)_2(\mathbf{L4.3})Cl_2]^{4+}$ complex is different to the spacing seen in the mono-cobalt complex. Further evidence for the di-cobalt complex was in the elemental analysis for the sample. From the NMR spectra it was already known that the sample was not pure but the ratio of carbon atoms, hydrogen atoms and nitrogen atoms was consistent with a di-cobalt complex. (Found: C, 28.5; H, 6.4; N, 13.0%).

Charcoal is often used in the synthesis of cobalt(III) complexes. Most often it is used as a catalyst to facilitate ligand exchange reactions. Presumably, the role of the charcoal is to reduce the cobalt(III) metal centre to a cobalt(II) metal centre. This produces transient cobalt(II) species that can exchange ligands readily and then the metal centre is oxidised back to the cobalt(III) metal centre.

Attempting to Coordinate the Pendant Arm of $[Co(tacn)(H_2L4.3)Cl]^{4+}$

Before the $[Co_2(tacn)_2(\mathbf{L4.3})Cl_2]^{4+}$ synthesis was discovered, the easiest route to dinuclear complexes was thought to be to coordinate a metal to the free arm of the ligand **L4.3** on the $[Co(tacn)(H_2\mathbf{L4.3})Cl]^{4+}$ complex. In an effort to continue with the di-cobalt goal, hydrothermal synthesis was tried. Hydrothermal synthesis is when the components of a crystallisation are put in a tube with a minimum of solvent and sealed. The tube is then heated past the point where the solvent is liquid. The temperature is then lowered in a slow and controlled manner. The premise is that the crystalline state will result from the complexes arranging themselves in an ordered

way. In this experiment the mono-complex was placed in a bomb with an equimolar amount of $[Co(tacn)(Cl)_3]$ or $[Co(tacn)(NO_2)_3]$ and 5 mL of water. The temperature was raised to 170^{o}C and held there for 12 hours and then slowly lowered to room temperature over 48 hours. The results in both cases were black powders with no crystals. Any attempt at the recovery of any starting materials seemed futile.

Attempts to coordinate other metals to the unbound arm of **L4.3** of the mono-cobalt complex were also tried. Due to the nature of the ligand, and the method of isolation, at least one of the amines on the pendant arm is protonated. In order to coordinate to a metal, the amines have to be deprotonated. The usual method of doing this is to raise the pH of the solution to 8. This method creates a problem in the two metals investigated in this manner: copper(II) and nickel(II). Both of these metals form insoluble hydroxide salts. To counter this, a solution was made of the metal in question and then dilute sodium hydroxide was added until precipitation occurred. At that point dilute hydrochloric acid was added until the precipitate dissolved. Then a one equivalence of the $[Co(tacn)(H_2\mathbf{L4.3})Cl]^{4+}$ complex was added. Again sodium hydroxide was added until precipitation and then acid was added. The solution was then put in vials to grow crystals *via* vapour diffusion and evaporation.

In the case of $CuCl_2$ the starting solution was a pale blue and the $Cu(OH)_2$ precipitate that formed was a deep blue. Upon adding the pink $[Co(tacn)(H_2\mathbf{L4.3})Cl]^{4+}$ complex the solution went purple. For the $Ni(NO_3)_2$ the solution started as a very pale green and the $Ni(OH)_2$ precipitation that formed was a light colour that was hard to detect. Upon adding the pink $[Co(tacn)(H_2\mathbf{L4.3})Cl]^{4+}$ complex the solution went pink. The vials for recrystallizations were set up in four different conditions; three were vapour

diffusions defusing in acetone, methanol or ether; and the other was slow evaporation. In both cases the addition of the $[Co(tacn)(H_2\mathbf{L4.3})Cl]^{4+}$ complex resulted in a colour change to the metal salt solution. A change in colour is usually a good indicator of a chemical change occurring. In this case however, the resulting colour change could be accounted for by adding the two colours of the two separate solutions; blue solution + pink solution = purple solution, pale solution + pink solution = pink solution. At this time, no crystals formed, and due to the paramagnetic nature of the metals, NMR techniques would not help clarify what is transpiring.

The arm free for coordination could conceivably be used as a ligand for square planar metals. The ligand, **L4.3**, has already been used to make the $[Pt_2(\mathbf{L4.3})Cl_4]$ complex. Starting with a square planar metal that already has a coordinated ethane-1,2-diamine (en), attempts were made to coordinate it to the $[Co(tacn)(H_2\mathbf{L4.3})Cl]^{4+}$ complex. The two metal complexes used were $[Pt(en)Cl_2]$ and $[Pd(en)Cl_2]$. The platinum and palladium complexes had to be changed from the chloride to the more reactive nitrate. This was done by adding silver nitrate and, in the case of platinum, heating, and then filtering off the precipitated silver chloride. The $[Co(tacn)(H_2\mathbf{L4.3})Cl]Cl_4$ complex also had to be treated with silver nitrate and the silver chloride filtered off to prevent there being any free chloride that could take the platinum and palladium complexes back to the starting complexes. Despite this, upon standing, out of the solutions grew long yellow needles very much like those of $[Pt(en)Cl_2]$ and $[Pd(en)Cl_2]$. As well as the yellow crystals a pink/purple precipitate was also formed. There was not enough of the precipitate to confirm that it was the $[Co(tacn)(H_2\mathbf{L4.3})Cl]^{4+}$ complex.

Many recrystallizations of [Co(tacn)(H_2**L4.3**)Cl]Cl_4 were set up with different conditions and metal salts to try to get a crystal structure. The different techniques tried were vapour diffusion and evaporation. A range of different metal salts was tried. The iron(III) salt $FeCl_3$, and the copper(II) salts $Cu(CH_3COO)_2$, $CuCl_2$, and $Cu(NO_3)_2$ were tried because these metals have a stable oxidation state one electron below. This is needed for the proposed photochemical reactions to take place. When these were unsuccessful, other metal salts were tried to see if they would turn out to be more productive: $Ni(NO_3)_2$, $NiCl_2$, $ZnSO_4{\cdot}7H_2O$, $ZnCl_2$, $FeCl_2$, $FeSO_4$, $Fe(CH_3COO)_2$, CuI, CuO, CuSCN. There were a few crystals formed but they all turned out to be the metal salt. The mono-cobalt complex often ended up as either a pink, viscous and glutinous smudge or small round translucent pink discs on the bottom of the vial. The discs were not crystalline.

Other Metals with L4.3

Ligand **L4.3** was further investigated by trying to coordinate it to metals other than cobalt metal salts. The metal salts tried were: $Ni(NO_3)_2$, $NiCl_2$, $ZnSO_4{\cdot}7H_2O$, $ZnCl_2$, $FeCl_2$, $FeCl_3$, $FeSO_4$, $Fe(CH_3COO)_2$, $Cu(CH_3COO)_2$, $CuCl_2$, $Cu(NO_3)_2$, CuI, $CuClO_4$, CuO, Cu_2O CuSCN. The results of the complexation often ended in insoluble powders that were difficult to analyse. Techniques tried to grow crystals were evaporation, vapour diffusion, H-tubes (liquid diffusion), layering (liquid diffusion) and hydrothermal synthesis.

Model Study

The synthesis of $[Co_2(tacn)_2(\mathbf{L4.3})Cl_2]^{4+}$ came at the end of the experimental time. The mono-cobalt complex had been made a year previously. With the $[Co(tacn)(H_2\mathbf{L4.3})Cl]^{4+}$ complex further studies were done. An endeavour to coordinate a carboxylic acid to the mono-cobalt complex was undertaken. The $[Co(tacn)(H_2\mathbf{L4.3})Cl]Cl_4$ complex was treated with trifluoromethanesulfonic acid (TfH) and was heated at 40^oC under vacuum. The thick reaction mixture was then slowly added to dry ether. A precipitate formed and was collected by vacuum filtration but was not allowed to get completely dry. The still wet solid was then dried in a vacuum desiccator. The solid was hygroscopic and did not remain solid, it went to a pink viscous oil. This oil was then dissolved in dry ethanol, and an excess amount of sodium acetate was added. The reaction was then left to stir overnight and the reaction mixture was taken to dryness. The resulting solid was characterised by ^1H and ^{13}C NMR spectrometry. In addition to the peaks expected in the $[Co(tacn)(H_2\mathbf{L4.3})Cl]^{4+}$ complex, there were two methyl peaks in both of the spectra. In the ^{13}C spectrum there was also two peaks above 180 ppm for the carbonyl carbon atom and there were four peaks in a 1 : 3 : 3 : 1 ratio equally spaced apart which is indicative of a Tf group. There are two sets of peaks for the acetate group. One set of peaks are of a comparable height to the complex peaks and are further down field than the larger peaks. These downfield peaks correspond to the bound acetate. The presence of both unbound acetate and Tf means a number of counterion combinations are possible. The complex was dissolved in ethanol and the excess sodium acetate was filtered off and the NMR spectra were recollected. The spectra still show unbound acetate as well as the bound acetate and the Tf peaks.

Cobalt Complex of 1,3-bis(2-aminoethylaminomethyl)benzene (L4.2)

Before the success of the charcoal synthesis, the general reaction was followed (as outlined earlier). In attempts to make a di-cobalt complex the ratio of $[Co(tacn)Cl_3]$ to **L4.2** was 2:1 A Dowex column was run and eight bands were seen and collected. An evaluation of the fractions is in Table 4-2.

Table 4-2 Evaluation of Column Fractions for **L4.2**

Fraction	**Concentration**	**Colour of solution**	**Colour of product**	**Yield and % column recovery**
1	1 M	Purple	Blue	0.12 g 8.8%
2	2 M	Purple	Blue	0.24 g 17.6%
3	3 M	Cherry Red	Blue/Green	0.15 g 11.0%
4	3 M	Orange	Yellow	0.14 g 10.3%
5	4 M	Pale Yellow	Brown	<0.001 g ~0%
6	5 M	Pale yellow	Brown	<0.001 g ~0%
7	6 M	Purple	Purple	0.62 g 45.6%
8	6 M in ethanol	Purple	Purple	0.09 g 6.6%

The seventh and eighth fraction are $[Co(tacn)(H_2\mathbf{L4.2})Cl]^{4+}$ (Figure 4-13). The eighth fraction was impure. There was no evidence to show that the di-cobalt complex had been made although there was another band that stuck to the top of the Dowex column. Attempts were made to isolate it by removing the stained resin and making a slurry with 6 M HCl. The colour of the resin did not lighten and upon filtering and taking the filtrate to dryness there was no residue on the flask.

Each fraction was taken to dryness under vacuum and further analysis performed on the resulting solid. Once again, the first three bands are $[Co(tacn)(Cl)_2(H_2O)]^{1+}$, $[Co(tacn)(Cl)(H_2O)_2]^{2+}$ and $[Co(tacn)(H_2O)_3]^{3+}$ respectively. They all become a blue/green powder which is $[Co(tacn)(Cl)_3]$ The fourth fraction is $[Co(tacn)_2]Cl_3$. The fifth and sixth fraction had too little material to be analysed using NMR techniques. They are possibly unreacted ligand or degraded ligand. The seventh and eighth fraction are $[Co(tacn)(H_2\mathbf{L4.2})Cl]^{4+}$, as in Figure 4-13. The eighth fraction was impure. There was another band that stuck to the top of the Dowex resin. Attempts were made to recover it but were unsuccessful.

Figure 4-13 Mono-cobalt Complex of **L4.2** $[Co(tacn)(H_2\mathbf{L4.2})Cl]^{4+}$

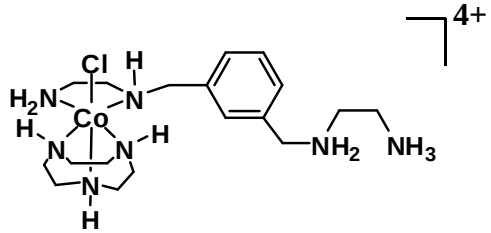

The $[Co(tacn)(H_2\mathbf{L4.2})Cl]^{4+}$complex was characterised by ^{1}H and ^{13}C NMR spectrometry and elemental analysis. As with $[Co(tacn)(H_2\mathbf{L4.3})Cl]^{4+}$ complex, there is a loss of symmetry going from the ligand to the mono-complex and in the non-

aromatic region the same number of peaks with approximately the same chemical shift as are seen for the $[Co(tacn)(H_2\mathbf{L4.2})Cl]^{4+}$ complex as are in the $[Co(tacn)(H_2\mathbf{L4.2})Cl]^{4+}$ complex. There is a difference in the aromatic region. In the ^{1}H NMR spectrum, there are three peaks in the aromatic region, with one of the peaks having an integral twice as big as the other two. It was expected that there would be four peaks with the same integral. Two of the peaks could have the same chemical shift. In the ^{13}C NMR spectrum, there are six aromatic peaks with two peaks being smaller that the other four peaks. These smaller peaks are the quaternary carbon atoms. From the elemental analysis it was found that the isolated product was $[Co(tacn)(H_2\mathbf{L4.2})Cl]Cl_4 \cdot 2H_2O \cdot 3.5HCl$ (Found: C, 28.7; H, 6.4; N, 13.4%. Calc for $C_{18}H_{46.5}Cl_{8.5}CoN_7O_2$: C, 28.7; H, 6.2; N, 13.1%).

A second synthesis was carried out to deliberately make the mono-cobalt complex $[Co(tacn)(H_2\mathbf{L4.2})Cl]Cl_4$. The total recovered unreacted $[Co(tacn)(Cl)_3]$ was 19.3% compared with 37.4%. There was also no $[Co(tacn)_2]Cl_3$ isolated.

Following the success of the charcoal synthesis with **L4.3**, the charcoal synthesis was tried with **L4.2** to try to make the di-cobalt complex. The column behaviour was such as has been described previously. The band that was being eluted with 4 M HCl broadened and while the beginning of the band was the mono-cobalt complex, $[Co(tacn)(H_2\mathbf{L4.2})Cl]^{4+}$, the spectra for the end of the band was different and indicated the presence of a di-cobalt complex. The ^{1}H and ^{13}C NMR spectra, the non-aromatic region is similar to the non-aromatic region of $[Co_2(tacn)_2(\mathbf{L4.3})Cl_2]^{4+}$ complex. The only definite exceptions is that in the ^{13}C NMR spectrum there are no peaks below 40 ppm where the carbon atom next to an uncoordinated primary amines

are and only one peak between 40-50 ppm where the carbon atoms next to coordinated primary amines, or, next to uncoordinated secondary amines are. From this it is clear that both en arms of the ligand are coordinated to the cobalt(III) metal. The aromatic region in the ^{1}H NMR spectrum shows three peaks; one with the integral twice as big as the other two. The larger peak is assigned to the two equivalent benzene hydrogen atoms. The aromatic region in the ^{13}C NMR spectra shows four peaks. One is larger that the other three. This peak is the two equivalent benzene carbon atoms with hydrogen atoms attached. The complex was also analysed by elemental analysis and the ratios obtained are consistent with a di-cobalt complex (Found: C, 26.4; H, 5.6; N, 12.4%).

Cobalt Complex of 1,2-bis(2-aminoethylaminomethyl)benzene (L4.1)

L4.1 was the last in this series that was made. The synthesis followed the charcoal synthesis that was described above; in attempts to make a di-cobalt complex. The ratio of $[Co(tacn)Cl_3]$ to **L4.1** was 2:1. No attempt was made to make the mono-cobalt complex. An evaluation of the column fractions is in Table 4-3.

Each fraction was taken to dryness under vacuum and further analysis performed on the resulting solid. The first three fractions dried to give $[Co(tacn)Cl_3]$. Fraction 2 and 3 also had an impurity that was shown by NMR spectrometry to be **L4.13**. The most definitive feature of the spectra, to assign it to **L4.13**, is that in the non-aromatic region, the peak for the benzylic methylene group is twice as big as the peaks for the carbon and hygrogen atoms next to the primary amine. Fraction 4 and 5 are **L4.1,** in the NMR spectra the peak for the benzylic methylene group is the same size as the

peak for the carbon and hydrogen atoms next to the primary amine. No cobalt complexes were made in this synthesis.

Table 4-3 Evaluation of Column Fractions for **L4.1**

Fraction	Concentration	Colour of solution	Colour of product	Yield
1	1 M	Purple	Blue	0.016 g
2	2 M	Purple	Blue/Green	0.034 g
3	3 M	Cherry Red	Blue/Green	0.043 g
4	3 M	Orange	Yellow	0.098 g
5	4 M	Yellow	Orange/brown	0.16 g
6	5 M	Yellow	Brown	0.13 g

Attempt at Complexes of 1,3-bis({2-pyridylmethyl}aminomethyl)benzene (L4.4)

The synthesis for the **L4.4** cobalt complex followed the general synthesis that was described above. Due to the unsuccessful attempts to make the di-cobalt complexes the mono-cobalt complex was the aim of the synthesis and then if promising the reaction would have been tried again in hopes to make the di-cobalt complex. The ratio of $[Co(tacn)Cl_3]$ to **L4.4** was 1:1. A Dowex column was used to separate the reaction mixture and nine bands were seen and collected. Unfortunately, most of the fractions collected were a mixture of different compounds. An evaluation of the fractions is in Table 4-4.

Table 4-4 Evaluation of Column Fractions for **L4.4**

Fraction	**Concentration of HCl**	**Colour before reducing volume**	**Colour of dried product**
1	0 M	Red	Blue
2	1 M	Purple	Blue
3	2 M	Cherry Red	Blue
4	3 M	Orange	Yellow
5	4 M	Red	Red
6	5 M	Orange/Brown	Brown
7	6 M	Pale Yellow	Brown
8	6 M	Yellow	Brown
9	6 M in ethanol	Yellow	Brown

In this case the colour of the product refers to the colour of the majority of the product. Quite often there were specks of other colours present, an indication that the separation of the fractions on the column was not entirely successful or there was decomposition of the products on the column or during evaporation of the eluant. No cobalt complex of **L4.4** was isolated.

The first three fractions, when brought to dryness did contain $[Co(tacn)(Cl)_3]$. There was also impurity of $[Co(tacn)_2]^{3+}$. The impurity of $[Co(tacn)_2]^{3+}$ is present in all fractions throughout and in a greater amount than in the synthesis of the **L4.1**, **L4.2** and **L4.3** cobalt complex synthesis. There was also (2-aminomethyl)pyridine in the first three fractions, which is one of the starting materials for the synthesis for **L4.4** and **L4.5**. The sample batch of **L4.4** ligand that was used in the experiment was re-

examined and there was no starting material impurity in the ligand that was added to the cobalt complex synthesis. Fraction 4 and 5 contained, apart from $[Co(tacn)_2]^{3+}$, $[Co(tacn)(ampy)Cl]^{2+}$ with fraction 4 also containing some paramagnetic material, most likely a cobalt(II) species. Fractions 6-9 contained a degraded form of the ligand which, from the evidence in the NMR spectra was concluded to contain an aldehyde **L4.14** Figure 4-14. In both the ^{1}H and ^{13}C NMR spectra there is a loss of symmetry compared with the original ligand spectra. There are more peaks in the aromatic region. As well as that there is an additional peak at 10.0 ppm in the ^{1}H NMR spectrum and 195 ppm in the ^{13}C NMR spectrum. These peaks are consistent with the presence of an aldehyde.

Figure 4-14 Aldehyde Fragment from Degradation of **L4.4**

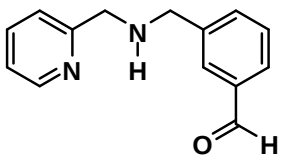

L4.14

Attempt at Complexes of 1,4-bis((2-pyridylmethyl)aminomethyl)benzene (L4.5)

The synthesis for the **L4.5** cobalt complex followed the general synthesis that was described above for **L4.4**. The mono-cobalt complex was the aim of the synthesis and then if promising, the reaction would have been tried again in hopes to make the di-cobalt complex. The ratio of $[Co(tacn)Cl_3]$ to **L4.5** was 1:1. A Dowex column was used to separate the reaction mixture and eight bands were seen and collected. Unfortunately the column did not achieve complete separation and most of the

fractions collected were a mixture of different compounds. An evaluation of the fractions is in Table 4-5.

Table 4-5 Evaluation of Column Fractions for **L4.5**

Fraction	**Concentration of HCl**	**Colour before reducing volume**	**Colour of dried product**
1	1 M	Purple	Blue
2	2 M	Purple	Blue
3	3 M	Cherry Red	Green
4	4 M	Orange	Red
5	5 M	Pale Yellow	Orange
6	6 M	Yellow	Orange/brown
7	6 M	Yellow	Brown
8	6 M in ethanol	Yellow	Brown

As in the reaction of **L4.4**, there was $[Co(tacn)Cl_3]$ isolated from the first three fractions. $[Co(tacn)_2]^{3+}$ was not present in these three fractions but was present in the fractions 4-6. Fraction 4 and 5 also contained $[Co(tacn)(ampy)Cl]^{2+}$, with fraction 4 being paramagnetic and fraction 5 being diamagnetic. Fraction 5 also contained unreacted **L4.5**. Fractions 6-8 contained the aldehyde fragment, **L4.15**, resulting from the degradation of **L4.5** (Figure 4-15). The spectra for **L4.15** are similar to that of **L4.14** with the aldehyde peak at 10 ppm in the ^{1}H NMR spectrum and 195 ppm in the ^{13}C NMR spectrum. There are differences in the spectra most notably in the aromatic region. There are fewer peaks in the aromatic region indicating that there is symmetry in the molecule. As well as the peaks for the ampy arm region there are two peaks for

the benzene ring in the ^{1}H spectrum and four peaks in the ^{13}C spectrum for the benzene ring.

Figure 4-15 Aldehyde Fragment from Degradation of **L4.5**

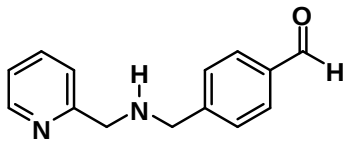

L4.15

Degradation of L4.4 and L4.5

The reaction that is thought to be taking place is outlined in Scheme 4-5 and Scheme 4-6 below. One of the secondary amines is being oxidised to an imine, followed by hydrolysis to give an aldehyde. From the NMR evidence it is clear that the fragment is not an imine. The peak is at 10 ppm in the ^{1}H NMR spectrum whereas an imine peak would be at approximately 8.5 ppm. In the ^{13}C NMR spectrum the peak is at 190 ppm which is consistent with an aldehyde. If it were an imine the peak would be at approximately 160 ppm.

Since the amine to imine reaction is an oxidation, there must also be an oxidant. The other partner in this reaction is likely to be either air (O_2) or a cobalt complex species most likely undergoing reduction from a cobalt(III) species to a cobalt(II) species. There is some evidence that the cobalt complex is involved. There was a larger amount of $[Co(tacn)_2]^{3+}$ made in the reaction of the ampy based ligands rather than the en based ligands. Cobalt(II) metal centres can undergo rapid ligand exchange reactions and the $[Co(tacn)_2]^{2+}$ complex is very stable and can be oxidised to form

$[Co(tacn)_2]^{3+}$ quite readily even just by being left open to the air. Also, the NMR shows evidence of broadening and noise characteristic of impurities of cobalt(II) species.

Scheme 4-5 Reactions involved in Ligand Degradation of **L4.4** and **L4.5**

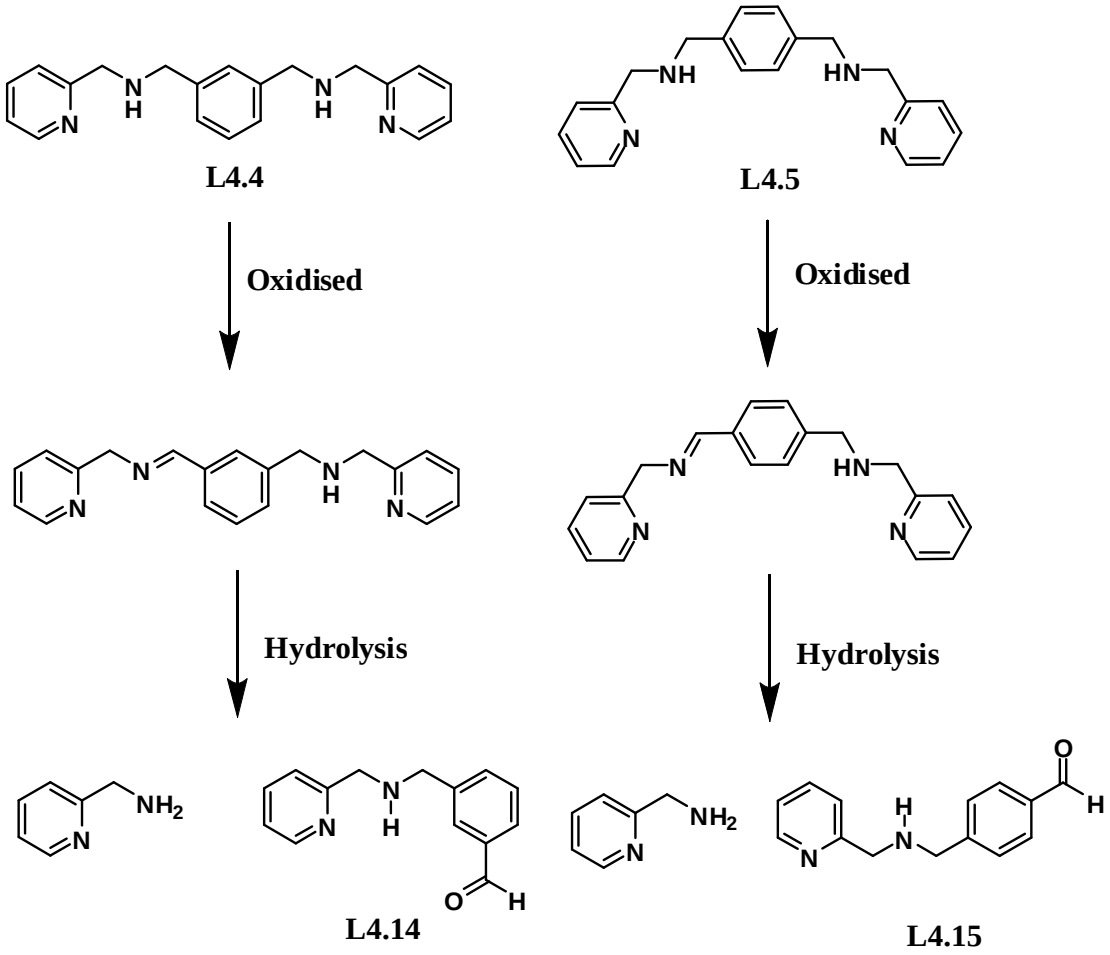

The lesser of the two **L4.4** fragments can then go on to form a $[Co(tacn)(ampy)(pyridine)Cl]^{2+}$ complex. This does not rule out the possibility that it is completely, or in part, air oxidation. Further evidence for the reaction is the isolation of ampy from the reaction mixture when there was none present in the ligand added to the reaction. This indicates a reaction was happening that involved the breakdown of the ligand. The reaction also produced $[Co(tacn)_2]^{3+}$.

Scheme 4-6 Reaction of the Cobalt Complex Involved in Ligand Degradation

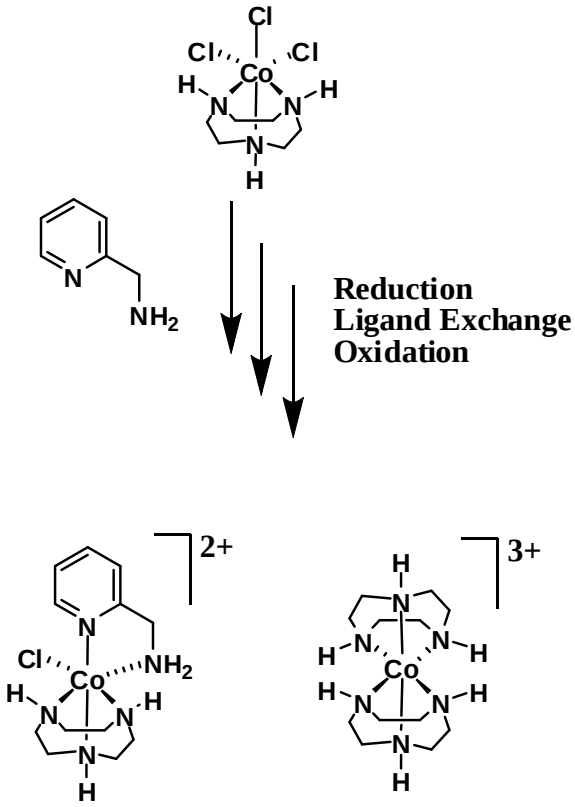

As in the reaction with **L4.4**, the cobalt complex synthesis with **L4.5** shows the presence of a redox reaction (Scheme 4-5). There are differences between the two syntheses however. First of all, the degradation does not seem as prominent in the **L4.5** synthesis as in the **L4.4** synthesis. This can be seen through the fact that some unreacted and non-degraded **L4.5** was recovered from the reaction; even though the reaction conditions were the same.

Due to the fact that **L4.5** did not degrade to the same extent a further reaction was carried out with a shorter reaction time. The pH was raised to 8 and it was heated at 80^{o}C for one hour before the pH was lowered to 3 and was reacted for a further hour. The results however were that a large portion of the [Co(tacn)Cl_3] was recovered.

Some $[Co(tacn)_2]^{3+}$ and $[Co(tacn)(ampy)Cl]^{2+}$ were also isolated as well as some of the aldehyde. Most of the ligand however was recovered un-degraded.

In light of the aims of this research, to bind two metals to the one ligand, **L4.4** and **L4.5** are unsuitable ligands for this work. They both degrade to give aldehyde products under the reaction conditions usually employed in cobalt(III) complex synthesis. Through extensive investigation, the degradation could be assigned a mechanism and the mode of the reaction could be discovered. Using this information, conditions that result in the degradation could be avoided. This is potentially time consuming and, especially with the success in the en based ligand, time could be better spent pursuing other paths.

SUMMARY

This chapter detailed the syntheses of five ligands. These ligands have the potential to bind two metal centres. The idea was to use octahedral cobalt(III) complexes to bond with the ligands and then bond three other sites on each metal of the complex with a tridentate ligand. This leaves one site on each metal to bind a fibre mimic. Due to other synthetic pursuits, a supply of $[Co(tacn)Cl_3]$ was readily available and was used as the cobalt(III) complex with the tridentate ligand already bound.

The di-cobalt complexes of **L4.2** and **L4.3** were made by the unexpected discovery of adding charcoal to the reaction mixture. They were characterised by ^{1}H and ^{13}C NMR spectrometry and elemental analysis. Unfortunately, because of time constraints further progress was not made with these complexes. The mono-cobalt complexes of

L4.2 and **L4.3** were also made and characterised by ^{1}H and ^{13}C NMR spectrometry and elemental analysis. The mono-cobalt complex of **L4.3** was taken further along the reaction pathway and a carboxylic acid was coordinated to the cobalt complex. This complex was characterised by ^{1}H and ^{13}C NMR spectrometry.

Attempts were made to coordinate the pendant arm of the mono-cobalt complex of **L4.3**. This was tried in a number of ways with many different metal salts and metal complexes. To date, no material has been obtained that could be characterised.

The syntheses of the cobalt(III) complexes of **L4.1**, **L4.4** and **L4.5** were also attempted. It is unclear why the complexation of **L4.1** did not work and this reaction should be repeated again in case it was an anomaly of the one reaction. Ligands **L4.4** and **L4.5** degraded under the reaction conditions to produce aldehydes **L4.14** and **L4.15** respectively, but it might be possible to make the desired complex a different way.

Chapter Five

Xylene Bridged

Bis(1,4,7-triaza-cyclonon-1-ylmethyl)

based ligands

Chapter 5

Xylene Bridged Bis(1,4,7-triaza-cyclonon-1-ylmethyl) based ligands.

INTRODUCTION

As mentioned in previous chapters, the ligands that are of interest have two separate binding domains. Three ligands were identified for study where their binding domains were based on the nine membered ring 1,4,7-triaza-cyclononane (tacn) (Figure 5-1). They were 1,2-, 1,3-, 1,4-bis(1,4,7-triaza-cyclonon-1-ylmethyl)benzene (**L5.1**, **L5.2**, and **L5.3** respectively).[32] They each contain two tacn rings with a benzene ring spacer. They are all known compounds and the syntheses have been described in the literature.[32] These ligands have many characteristics which make them of interest to study in the context of the project aims.

The criteria for the ligands in this project were that they were capable of coordinating two metal ions and also leave a possible site to introduce a fibre mimic on each metal centre. The tacn rings provide three nitrogen donor atoms and can coordinate to three sites on a metal ion in a facial manner. This would leave three vacant sites on each octahedral metal atom to bond other ligands. Ideally, two of these sites will be taken

up with a bidentate ligand, such as 2,2´-bipyridine (bpy). The remaining site will be used to bind a fibre mimic.

Figure 5-1 Ligands Described in this Chapter

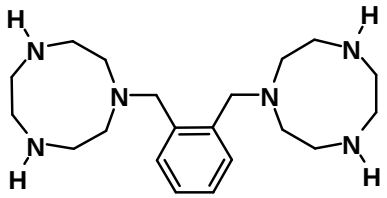

L5.1

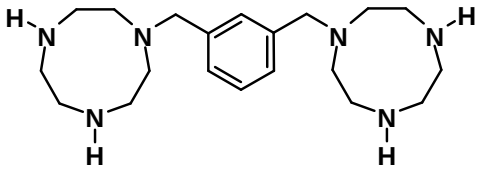

L5.2

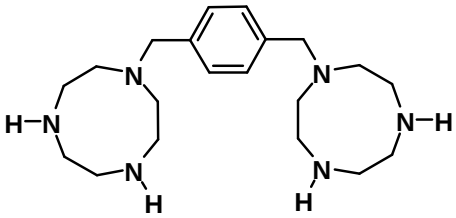

L5.3

With the coordinating arms protruding from the benzene spacer, variation can be introduced by changing the relative positions of the two arms around the benzene ring. In this way, the distance between the fibre mimics (carboxylic acid groups) could be varied to a degree. In **L5.1**, the two binding arms are close and can both lie on one side of the ring, as seen in Figure 5-2. This means that they could both coordinate to the same octahedral metal atom. Unfortunately, if that happens there would not be any coordination sites left for possible fibre mimics. **L5.3**, however, has the two binding arms far away from each other. Due to this, the binding arms cannot both bond to the same metal atom. This helps in providing vacant sites for fibre mimics. **L5.2** has an intermediate distance between the two binding arms.

Figure 5-2 Possible Complex of **L5.1**

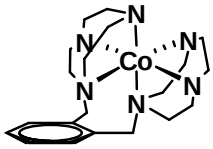

Previous Research

A literature search was performed using both the Cambridge Crystallographic Database (CCD) and Scifinder Scholar. The results for the search from the Cambridge Crystallographic Database (CCD) are presented as a table and then discussed for each of the ligands. Additional references found through Scifinder Scholar are discussed in the paragraph following the table.

For the columns in the tables, **Metal(s)** refers to metals bonded directly to the ligands; they are listed with their oxidation states. **Formula** is the formula for isolated complexes including solvent molecules and counterions. **Number of refs** refers to the number of entries in the database and the paper is referenced. Occasionally there is more than one entry from the one paper. **Coord. number** is the total number of donor atoms attached to the metal centre. **Geometry** is listed using IUPAC polyhedral symbols (where *OC*-6 means octahedral, and *TBPY*-5 means trigonal bipyramidal).[114] **Bridged** is referring to whether the metal atoms are bridged by another ligand in addition to the ligand of interest. A highlighted row indicates an image of the crystal structure from the CCD is included below the table (the image is of the complex only, no solvent molecules or counterions are included).

Table 5-1 Results for the CCD Search for Complexes with **L5.1**

1,2-Bis(1,4,7-triaza-cyclonon-1-ylmethyl)benzene, L5.1					
Metal(s)	**Formula**	**No of refs**	**Coord. number**	**Geometry**	**Bridged**
Cu^{II}, Cu^{II}	$[Cu_2(\mathbf{L5.1})Br_4]\cdot DMF$	1[32]	5, 5	*TBPY*-5 *TBPY*-5	No
2(Cu^{II}, Cu^{II})	$[Cu_4(\mathbf{L5.1})_2Cl_4.(\mu\text{-}Cl_2](PF_6)_2$	1[115]	5, 5	*TBPY*-5 *TBPY*-5	Yes – chloride, between the two dimers
Cu^{II}	$[Cu(\mathbf{L5.1})](ClO_4)_2\cdot H_2O$	1[32]	6	*OC*-6	N/A
Zn^{II}	$[Zn(\mathbf{L5.1})](ClO_4)_2\cdot H_2O$	1[116]	6	*OC*-6	N/A
Ni^{II}	$[Ni(\mathbf{L5.1})](ClO_4)_2\cdot H_2O$	1[32]	6	*OC*-6	N/A

Figure 5-3 Crystal Structure of $[Cu_2(\mathbf{L5.1})Br_4]\cdot DMF$

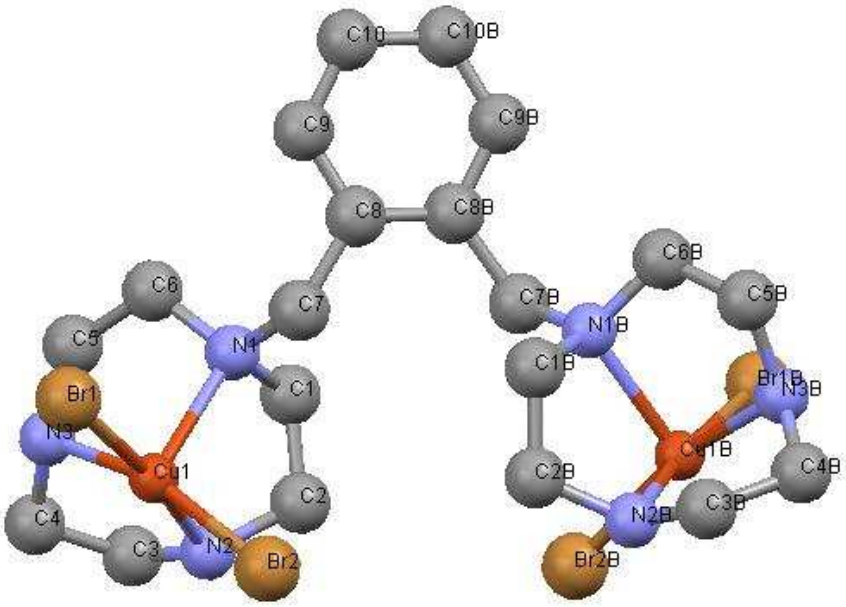

A literature search of ligand **L5.1** produced results that have complexes with di-copper(II),[32, 117] mono-copper(II),[32] mono-zinc(II),[116] di-nickel(II)[32] and mono-nickel(II).[32, 118] The CCD had five relevant entries (Table 5-1). Three of these were copper complexes, one was a mono-zinc complex and the other was a mono-nickel complex. The mono-copper, mono-nickel and mono-zinc complexes were all octahedral and bound by both of the 1,4,7-triazacyclonone (tacn) rings in a sandwich fashion. This means that ligand **L5.1** takes up all the binding sites so there was nowhere to introduce another ligand. There are no free coordination sites to add an acid. Complexes like these are unsuitable for the photolysis experiments of the kind intended in this research.

Table 5-2 Results for the CCD Search for Complexes with **L5.2**

1,3-Bis(1,4,7-triaza-cyclonon-1-ylmethyl)benzene, L5.2					
Metal(s)	**Formula**	**No of refs**	**Coord. number**	**Geometry**	**Bridged**
Cu^{II}, Cu^{II}	$[Cu_2(\mathbf{L5.2})(OH)_2(\mu\text{-}O_3POPhNO_2)](ClO_4)\cdot H_2O$	1[117]	5, 5	*TBPY*-5 *TBPY*-5	Yes - mono(4-nitrophenyl) phosphate
Cu^{II}, Cu^{II}	$[Cu_2(\mathbf{L5.2})(Cl)_2]$	1[119]	5, 5	*TBPY*-5 *TBPY*-5	No
Cu^{II}, Cu^{II}	$[Cu_2(\mathbf{L5.2})(\mu\text{-}OH)_2](BPh_4)\cdot CNCH_3$	1[120]	6, 6	*OC*-6 *OC*-6	Yes - hydroxide
Ni^{II}, Ni^{II}	$[Ni_2(\mathbf{L5.2})(ImH)_4(H_2O)_2](ClO_4)_4\cdot 3H_2O$	1[121]	6, 6	*OC*-6 *OC*-6	No

Figure 5-4 Crystal Structure of $[Cu_2(\mathbf{L5.2})(OH)_2(\mu\text{-}O_3POPhNO_2)](ClO_4)\cdot H_2O$

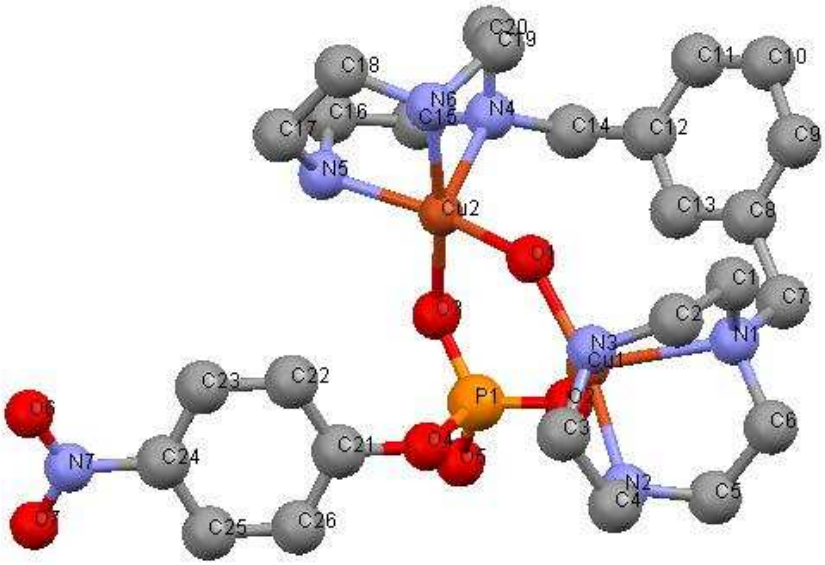

The other two copper complexes have two copper atoms; one bound to each arm of the ligand. One complex has bound bromide ligands (Figure 5-3). In the other complex there are two ligand complexes that are bridged by chloride ions. In both these cases, there are coordination sites that are taken up by ligands that could be exchanged for fibre mimics.

A literature search of ligand **L5.2** came back with results of complexes with di-copper(II),[32, 117, 121, 122] and di-nickel(II).[32, 121] The CCD had four relevant entries (Table 5-2). Three were of di-copper complexes and the fourth was a di-nickel(II) complex. The metal atoms in the di-copper complexes adopt a trigonal bipyramidal or octahedral geometry, with a site to introduce another ligand. Auxiliary ligands of interest are those that bind to the metal centre *via* an oxygen atom. These ligands are of interest because the fibre mimics that are to be used are carboxylic acids and it is useful to know whether there are instances of the ligands **L5.1**, **L5.2** or **L5.3** bound to the same metal as oxygen bound ligands. In the case of **L5.2** two examples of oxygen

bound ligands were observed. One was the mono(4-nitrophenyl)phosphate ion, pictured in Figure 5-4, which bridges the two copper centres in one of the complexes. In another complex hydroxide bridges the two copper centres. This supports the idea that these ligands are viable for making complexes useful to this study. The di-nickel complex has two octahedral nickel centres with each metal centre with three sites on each metal bound to **L5.2**, two sites have imidazole molecules coordinated and the remaining site has a water molecule.

A related ligand from the literature is **L5.5**, Figure 5-5.[123-126] This ligand has two pentadentate sites and has the ability to bind two octahedral metals, leaving only one free site on each metal. In the literature, the di-metal complexes of this ligand were reported with di-nickel(II),[125] di-manganese(II),[123] di-zinc(II)[124] and di-copper(II).[126] The nickel and manganese complexes are both octahedral; with five of the binding sites being taken up with **L5.5** and the sixth site an auxiliary ligand; a water molecule for the nickel complex and a chloride ligand for the manganese complex. The zinc and copper complexes are five coordinate and all the sites are taken up with **L5.5**.

Figure 5-5 Ligand **L5.5**

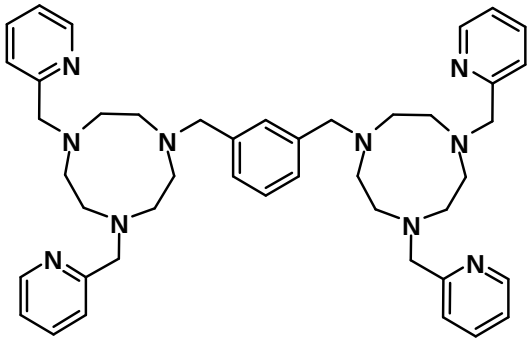

L5.5

L5.6 (Figure 5-6) is similar to **L5.5**. It has an ethane-1,2-diamine spacer group between the two tacn rings instead of the benzene ring. This ligand has had two

cobalt(III) complexes reported; one where the auxiliary ligand was a hydroxide ligand on each of the two metal centres. This complex was in equilibrium with the other complex which had both of the metal centres bridged by the one hydroxide group occupying the auxiliary sites on both of the metal centres.

Figure 5-6 Ligand **L5.6**

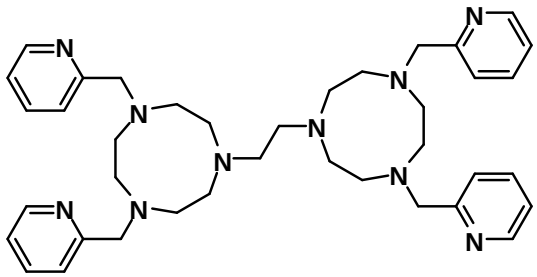

L5.6

Table 5-3 Results for the CCD Search for Complexes with **L5.3**

1,3-Bis(1,4,7-triaza-cyclonon-1-ylmethyl)benzene, L5.3					
Metal(s)	**Formula**	**No of refs**	**Coord. number**	**Geometry**	**Bridged**
Cu^{II}, Cu^{II}	$[Cu_2(\mathbf{L5.3})Cl_4]$	2[117, 119]	5, 5	*TBPY*-5 *TBPY*-5	No
Zn^{II}, Zn^{II}	$[Zn_2(\mathbf{L5.3})DMF_2(H_2O)_4]$ $(ZnCl_4)_2$	1[116]	6, 6	*OC*-6 *OC*-6	No
Ni^{II}, Ni^{II}	$[Ni_2(\mathbf{L5.3})(H_2O)_6]$ $(ClO_4)_4 \cdot 4(H_2O)$	1[32]	6, 6	OC-6 *OC*-6	No

Figure 5-7 Crystal Structure of $[Zn_2(\mathbf{L5.3})DMF_2(H_2O)_4](ZnCl_4)_2$

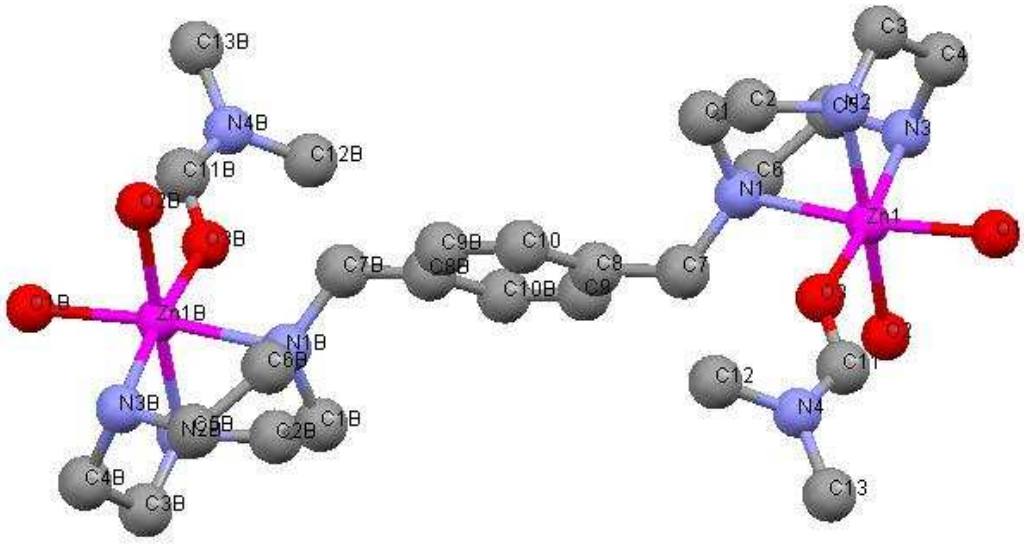

A literature search for ligand **L5.3** produced results of complexes with di-copper(II),[32, 117, 119, 122, 127, 128] di-zinc(II)[116] and di-nickel(II).[32] The CCD had four relevant entries (Table 5-3); two for di-copper complexes and one of each for di-zinc and di-nickel complexes. The di-copper structures have a trigonal bipyramidal geometry. The di-zinc complex (Figure 5-7) and the di-nickel complex have octahedral geometries and a coordination site in which to introduce another ligand.

Ligand **L5.7** (Figure 5-8) has four tacn rings on a benzene core. They are in a 1,2,4,5-relationship. This means that it displays all the relationships that the three ligands **L5.1**, **L5.2** and **L5.3** have. With this ligand you would expect to see the same types of binding modes seen for **L5.1**, **L5.2** and **L5.3**. The rings in a 1,2- relationship should be able to make sandwich complexes. The rings in a 1,3- relationship should be able to bind two metal centres that are bridged by additional ligands. There is also the possibility that all of the tacn rings can each bind a single metal atom. This is exactly what is seen to happen.

Figure 5-8 Ligand **L5.7**

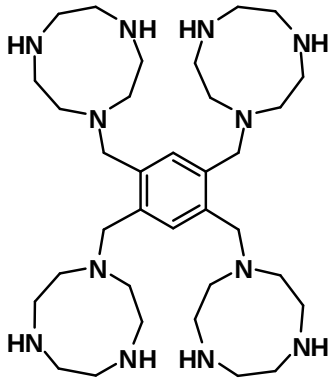

L5.7

L5.7 has been observed to bind 2-4 metal atoms.[118, 129-131] Complexes have been made with nickel(II) and copper(II). Three different nickel(II) complexes have been reported. One has two octahedral nickel atoms each coordinated to two tacn rings in a 1,2- relationship to each other to form a sandwich type complex. Another nickel(II) complex has three octahedral nickel atoms; two of the metal centres are bound by one tacn ring. Both metal centres have water molecules on the other three sites. The other metal centre is bound by the two remaining tacn rings in a sandwich type fashion. The third nickel(II) complex is tetranuclear, with each tacn ring binding one metal atom and the remaining sites on each metal are taken up by three water molecules.

Three different copper(II) complexes have been reported with **L5.7**. They are all very similar. Each complex is tetranuclear and each tacn ring binds one metal. The copper atoms are all five coordinate with the remaining two sites taken up with a bridging ligand that connects the copper atoms that are bound to the tacn rings in a 1,3-relationship to each other. The bridging ligands are hydroxide, methoxide or azide. The scope of this work means that this ligand would not be suitable but it is an excellent source of inspiration.

From the results of the literature search it is apparent that a wide range of complexes have been made with the ligands **L5.1**, **L5.2** and **L5.3** and compounds similar to them.

It is rather curious that cobalt complexes of the xylene bridged ligands have not been reported previously, especially seeing that a few of the research groups that have reported on the complexes work with cobalt(III) complexes on a regular basis. Cobalt(III) complexes are commonly made with amine donor groups and these ligands have amine donor groups. They are based on tacn whose cobalt(III) complex with various other auxiliary ligands has been reported in the literature. Cobalt(III) complexes have been studied at length in the past, from the time of Fremy in 1852[132] and was investigated extensively by Werner[133, 134] and is still considered one of the best complexes to use in the development of theories and used in model systems.

RESULTS AND DISCUSSION

Ligand Synthesis

Shown in Scheme 5-1 are the syntheses undertaken to obtain **L5.1**, **L5.2** and **L5.3**. The multi-step syntheses can be broken up into two major parts: the formation of the cycle and the adding of the aryl group.

Scheme 5-1 Overview to make **L5.1**, **L5.2** and **L5.3**

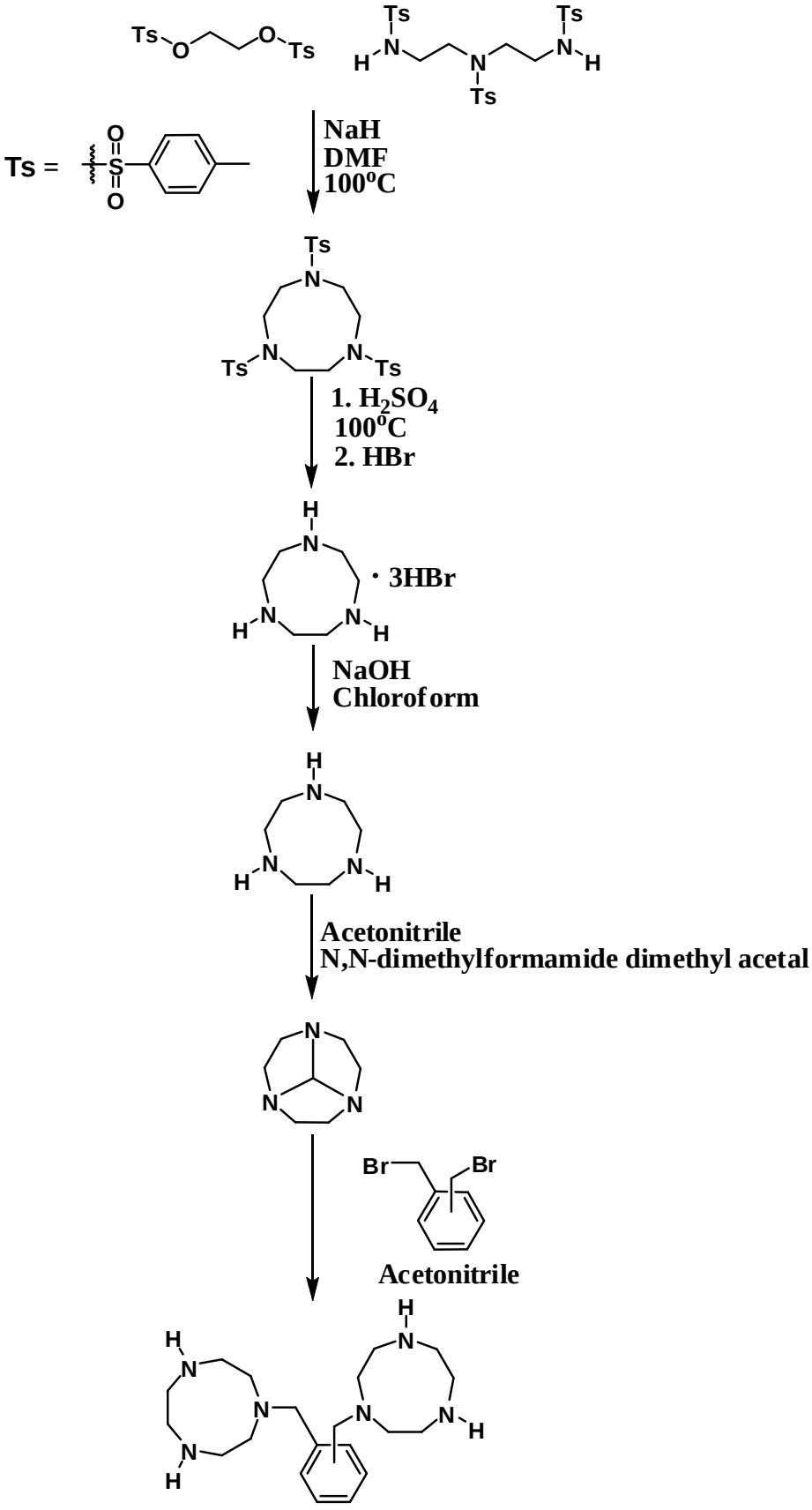

L5.1 L5.2 L5.3

The starting materials to make the backbone of the tacn ring are ethane-1,2-diol (glycol) and N-(2-aminoethyl)ethane-1,2-diamine (dien). The dien can not be reacted as it is. This is because in the reaction the nitrogen atom is deprotonated and undergoes a nucleophilic reaction with the activated glycol. If the dien is used as it is there are five protons that can be removed. This could lead to the primary amines reacting twice over with glycol molecules or the secondary amine could react with a glycol molecule. A way around all these possible unwanted reactions is to employ a protecting group. The p-toluenesulfonyl (Ts) group is a standard amine protecting group and takes care of both of the problems. The middle amine forms a secondary sulfonamide on tosylation and would not react with the glycol derivative because it no longer has an acidic proton. The Ts groups also prevent the end amines, which became primary sulfonamide with an acidic proton, from reacting more than once.

Scheme 5-2 Synthesis of tacntt

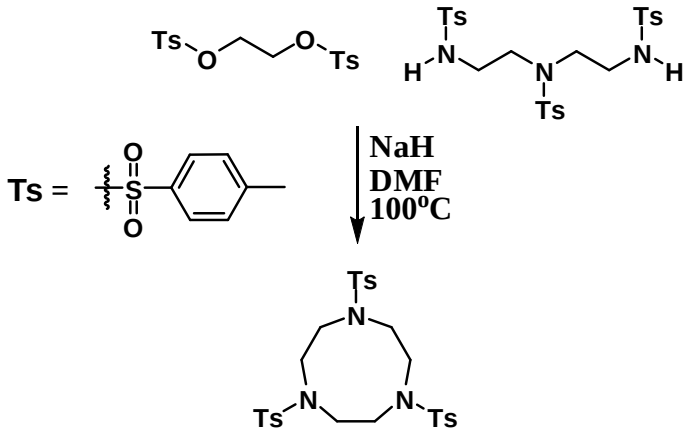

The reaction was carried out under basic conditions which the Ts group can withstand. The synthesis in Scheme 5-2 was the more successful of the two methods employed in the synthesis of N,N',N''-tris(*p*-toluenesulfonyl)-1,4,7-triazacyclononane

(tacntt). The other method[135] uses a different base (K_2CO_3) and was performed at a higher temperature (120^oC).

The K_2CO_3 synthesis had limited and varied results, with yields ranging from 0-68%. This synthesis was inconsistent at giving results. The main problem with this synthesis is thought to be contamination by water. Water reacts with the K_2CO_3 making it an ineffective base unable to deprotonate dientt and the water also reacts with the N,N',-di(*p*-toluenesulfonyl)-1,2-ethanediol (endt) to form 1,2-ethanediol. The main evidence for the contamination of water was condensation that appeared in the necks of the three necked flask when the solution was heated above 100^oC. With a boiling point of 152^oC, it is unlikely to be DMF at that temperature and pressure.

The DMF was dried over 4 Å molecular sieves for at least a week prior to the reaction and was vigorously agitated every day with the molecular sieves being changed every three days. The glassware and starting materials were dried in a 60^oC oven for at least 24 hours. Even after these measures, the reaction was unreliable. Different reaction conditions were tried with longer drying periods and methods with mixed results. The NaH synthesis[136] was found to be a better method with crude yields always above 90% and purified yields between 80-95%. NaH is used as the base to deprotonate dientt, it also reacts with water. This provides an additional built-in method for ensuring that the DMF is dry before the addition of endt.

The protecting group was then removed in sulfuric acid (Scheme 5-3). The sulfuric acid deprotection is a common method for the deprotection of Ts groups. Temperature control is important to this reaction. If the temperature rises much above 100^oC the

reaction is unsuccessful and no product is produced. If the temperature is 90^{o}C or less the deprotection does not go to completion and the yield is significantly lower than the average.

Scheme 5-3 Synthesis of the Tacn Salt

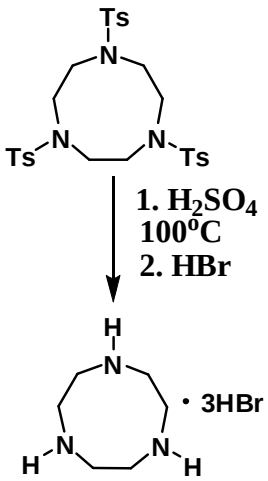

The synthesis of the tricycle (Scheme 5-4) must start with the free amine and not the salt. The HBr salt of tacn was changed to the free amine by neutralising it with a 50% NaOH solution and extraction with chloroform.

The aryl group is added by reacting through a tricycle. Using the tricycle prevents each ring from reacting with more than one aryl group. The reaction to add the aryl groups to the tacn is a nucleophilic addition with the tricycle acting as the nucleophile. Once one aryl group is added to the tricycle the resulting product is positively charged making it not as good a nucleophile. Then the synthesis breaks off into the three branches depending on which of the three ligands is to be synthesised. For **L5.1** α,α'-Dibromo-*o*-xylene is used, for **L5.2** α,α'-Dibromo-*m*-xylene is used and for **L5.3** α,α'-Dibromo-*p*-xylene is used.

Scheme 5-4 Making the Reactive Tricycle

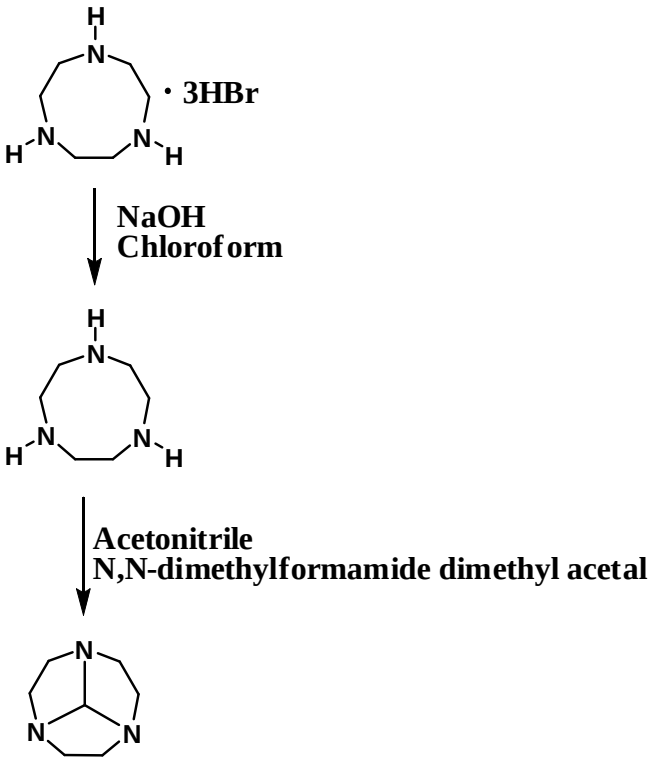

Scheme 5-5 Synthesis of **L5.1, L5.2, L5.3**

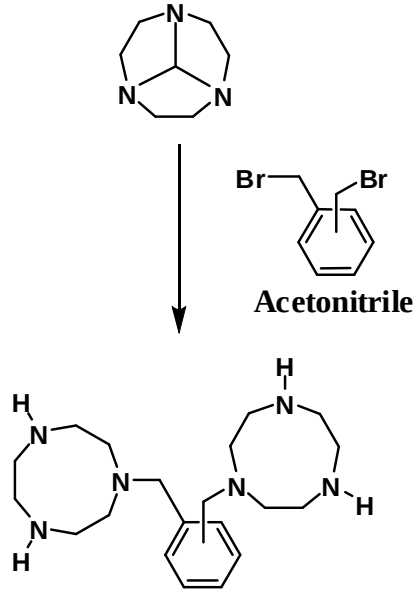

L5.1 L5.2 L5.3

There are symmetry elements in the ligands which are highlighted in Figure 5-9. The mirror planes, indicated by dashed lines, relate one half of the molecule to another. In each case the symmetry relates the two tacn rings to one another and the two halves of each tacn ring are also equivalent.

Figure 5-9 Symmetry Elements seen in the Ligands

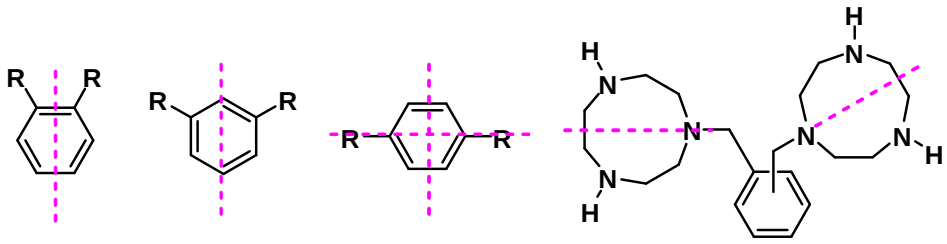

With the 1,2- substituted benzene ring the mirror plane runs through the middle of the ring dissecting through the sides. This means that each carbon atom is equivalent to one other and there would be three peaks in the aromatic region of the ^{13}C NMR spectrum. In the 1,3- substituted benzene ring the mirror plane runs through the middle of two atoms. This means that two carbons are equivalent and two carbon atoms are unique. This would be represented in the aromatic region of the ^{13}C NMR spectrum by four peaks. In the 1,4- substituted benzene ring there are two mirror planes; one running through the sides and the other perpendicular running through two atoms. This means that four carbon atoms are equivalent to each other and the other two carbon atoms are equivalent to each other. There are two peaks in the aromatic region of the ^{13}C NMR spectrum; one for four equivalent carbon atoms and the other for two equivalent carbon atoms.

For the tacn rings, it has already been shown in Figure 5-9 that the two rings in each molecule are equivalent. There is more symmetry. There are six carbon atoms in each

ring; however each carbon atom is equivalent to another carbon atom in that ring. Going by this it is expected that there will be three peaks for the tacn rings instead of six. Similarly, with the ^{1}H NMR spectra, there are twelve hydrogen atoms in each tacn ring, but, each hydrogen atom is equivalent to the hydrogen attached to the same carbon atom and also to the hydrogen atoms related by the mirror plane. Consequently, in the ^{1}H NMR spectra there are only three peaks with each peak representing four hydrogen atoms in the same tacn ring and eight hydrogen atoms overall.

The ligands were isolated as the HBr salts and were characterised by ^{1}H and ^{13}C NMR spectrometry. The numbering system for the carbon atoms is shown in Figure 5-10. The non-quaternary aromatic carbon atoms have one attached hydrogen atom referred to by the number of the carbon atom it is attached to and then ‘a’ for example the hydrogen atom attached to carbon atom 2 would be 2a. The non-aromatic carbon atoms have two attached hydrogen atoms and they are referred to by the number of the carbon it is attached to and then ‘a’ or ‘b’ for example the hydrogen atoms attached to carbon atom 7 would be 7a and 7b. Equivalent centres are separated by a / for example 7a/7b means they are represented by the same peak in the spectrum.

Figure 5-10 NMR numbering

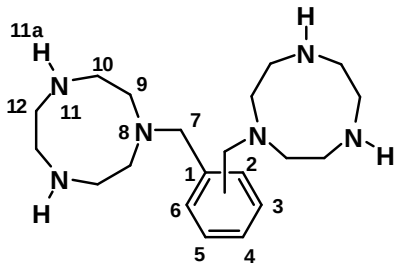

L5.1 L5.2 L5.3

The ^{1}H NMR spectra of all three ligands show four peaks between 2.5 – 4.0 ppm. These are the three peaks of the tacn ring and that assigned to the benzylic methylene hydrogen atoms. The peaks for 9a/9b and 10a/10b are both seen as triplets with integrals relating to eight hydrogen atoms. The peak for 12a/12b is a singlet with an integral relating to eight hydrogen atoms. The peak for 7a/7b is a singlet with an integral relating to four hydrogen atoms. In the aromatic region, the number of peaks differs for all the three ligands. For **L5.1** the 1,2- substituted ligand, there are two peaks (3a/6a and 4a/5a). For **L5.2**, the 1,3- substituted ligand, there are three peaks (2a and 4a/6a and 5a). For **L5.3**, the 1,4- substituted ligand there is one peak for the four chemically equivalent hydrogen atoms (2a/3a/5a/6a).

In the ^{13}C NMR spectra of all three ligands, four peaks between 40 – 60 ppm are seen. These are the three peaks for the tacn ring and one peak for the benzylic methylene carbon atoms. Three of them are the same height which will be the three peaks associated with the carbon atoms in the tacn ring. The fourth one is half the height and is further downfield, as would be expected for a benzylic carbon atom. In the aromatic regions of the spectra the number of peaks differs, reflecting the different substitution pattern. For **L5.1,** the 1,2- substituted ligand, there are three peaks. One small one that is the quaternary carbon atoms (1/2) and two larger ones the same size as each other (3/6 and 4/5). For **L5.2**, the 1,3- substituted ligand, there are four peaks. One is a large peak corresponding to the two tertiary carbon atoms (4/6) and the three smaller peaks which are due to the quaternary carbon atoms (1/3) and the two single carbon atoms (2 and 5). For **L5.3**, the 1,4- substituted ligand, there are two peaks. One is a small peak that is assigned to the two quaternary carbon atoms (1/4) and the other is a large peak which is assigned to the other four aromatic peaks (2/3/5/6).

Complex Synthesis

Once the ligands **L5.1**, **L5.2** and **L5.3** were synthesised, efforts were made to prepare the cobalt(III) complexes. The initial reaction route taken is outlined in Scheme 5-6 and employs coordination chemistry with many precedents in the literature.[113, 137-139] In general terms, there are four possible outcomes from the synthesis; the desired neutral dicobalt complex (**I**), the neutral monocobalt complex (**II**), a charged mononuclear sandwich complex (**III**), and a charged multinuclear sandwich complex (**IV**) which will be referred to as a polymer complex.

The ability of the ligand to form the mononuclear sandwich complex (**III**), where both arms of the one ligand is bound to the same cobalt metal, depends on the substitution. As mentioned in the beginning of this chapter both **L5.1** and **L5.7** form sandwich type complexes by taking advantage of the 1,2- substitution relationship. No such complexes have been reported for **L5.2** or **L5.3**. However, there could be a possibility of a polymeric complex with two arms of different ligand atoms coordinating to the same metal atom (**IV**). There is a chance that they could form a dimer or a polymer with two ligands on the same metal. This outcome is minimised by keeping the concentration of the ligand low and adding it dropwise over a long period of time. As ligand is added an orange precipitate forms. The reaction is performed in aqueous solution and the dinuclear and mononuclear species are neutral while the sandwich and polymer species are charged. It is likely that if charged complexes are made they will stay in the solution and are filtered out when the solid is collected.

Scheme 5-6 Synthesis of Cobalt Complexes of **L5.1**, **L5.2** and **L5.3**

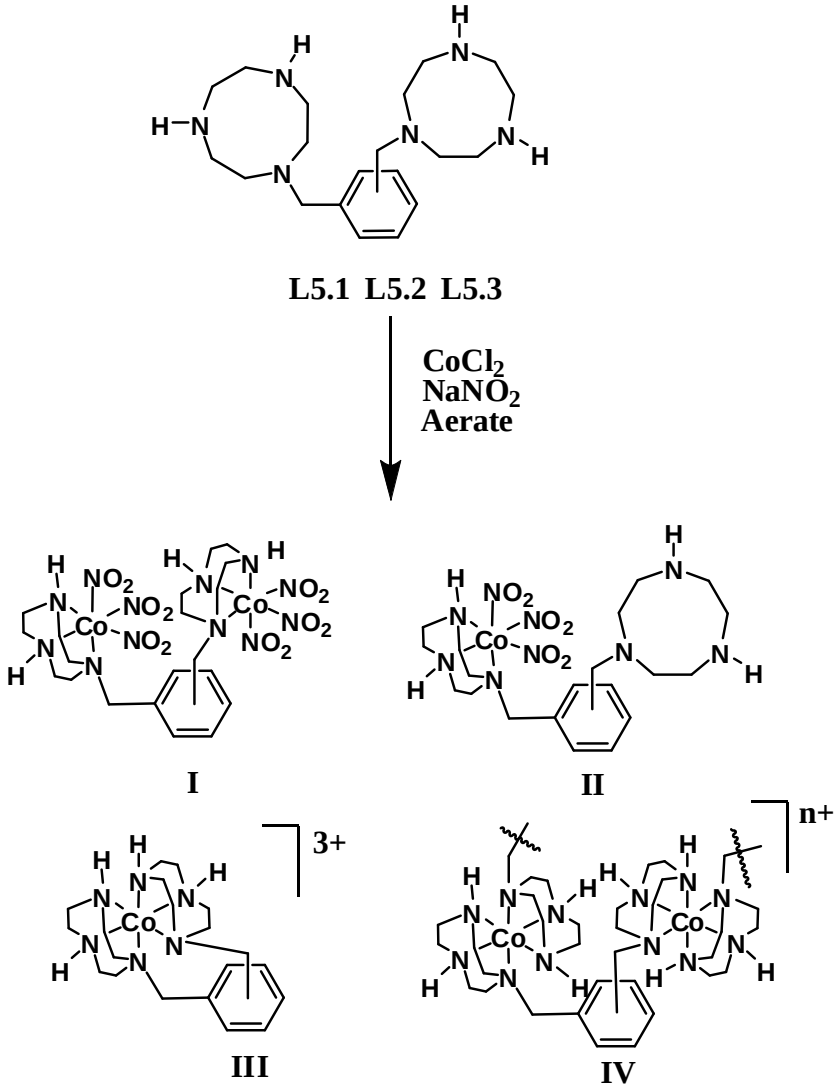

The low solubility of these complexes has made them difficult to characterise. The ^{1}H and ^{13}C NMR spectra were run in DMSO-d6. The peaks in the ^{1}H NMR spectra were all broad and this, with poor signal-to-noise ratios, means it is hard to work out what are real peaks. Some of the peaks had a bump on the shoulder and the peaks could easily be masking other peaks that cannot be seen. Despite this, some information can be obtained. There are two clear regions of peaks on all the spectra. In the ^{1}H NMR spectra there are peaks in a non-aromatic region between 2.2-4.8 ppm and an aromatic region between 7.0-7.6 ppm. In the ^{13}C NMR spectra there are peaks in a non-

aromatic region between 40-60 ppm and an aromatic region between 120-140 ppm. These peaks provide evidence that the ligand is still in the isolated solid in some form. The number of peaks from each ligand complex is seen in Table 5-4 below.

Table 5-4 NMR Peak Counts for the Cobalt Nitrite Complexes

Ligand in Complex	**^{1}H NMR spectra**	**^{13}C NMR spectra**
L5.1	9 non-aromatic 2 aromatic	29 non-aromatic 18 aromatic
L5.2	18 non-aromatic 8 aromatic	29 non-aromatic 16 aromatic
L5.3	8 non-aromatic 3 aromatic	25 non-aromatic 8 aromatic

Based on experience gained during this project, the chemical shift that is expected for a carbon atom next to a coordinated secondary amine, is approximately 50 ppm. In all the ^{13}C NMR spectra of the complexes, the non-aromatic peaks start from approximately 40 ppm. It is clear from this that there are carbon atoms next to non-coordinated secondary amines (like those in the free ligand). There are also peaks in the 50-60 ppm range which are normally assigned to carbon atoms next to coordinated secondary and tertiary amines in these kinds of systems. From this evidence it is apparent that there is some mononuclear species or a mixture containing free ligand. This latter possibility can be discounted based on the high solubility of the ligand in water. In all the cases more peaks were seen than were expected or could be accounted for in a pure sample of the mononuclear complex. If there was no

symmetry in the molecule the highest number of aromatic peaks you would expect to see is six. In all the spectra more than six aromatic peaks were observed. In the non-aromatic region the highest number of peaks you would expect to see in an asymmetric complex of these ligands is 12. Given the number of peaks were more than double what was expected in the aromatic region in all cases, it is possible that there is a mixture of dinuclear and mononuclear complexes.

There is another possible explanation for the large number of peaks in the NMR spectra. That is linkage isomerisation and ligand exchange. It could be possible that the nitrite ligands are bound to the metal centre in different ways.[140] They could be bound through the nitrogen atom or through the oxygen atom. Examples are known where the isomerisation can take place in basic or acidic conditions.[141-143] While it is unusual for a solid to be isolated displaying both examples of N-bonded and O-bonded nitrite ligands, it has been observed in solution.[144] There are examples where the isomerisation takes place in DMSO and it results in an unequal mixture of N-bonded and O-bonded isomers.[145] Another possibility is that the complex is exchanging ligands with the solvent. DMSO can bind to the metal centre through the oxygen. As there are six nitrite ligands this leads to a range of possible complexes with a different number of DMSO ligands bound. A decision was made to investigate the mononuclear complexes further to see if the reaction routes were viable in the advent that dinuclear complexes of these ligands were made in the future.

The elemental analyses of the complexes were obtained. From the NMR spectra, it is already known that the samples were not pure. The main point of the elemental analysis was to get an idea of the ratios of ligand to cobalt metal in the complex. The

ratios of the elements analysed for carbon, hydrogen, nitrogen and cobalt content did not come out to an integer ratio of ligand to cobalt metal, which was expected. For the cobalt complex of **L5.1** the ratios were $C_{40}H_{70}N_{16}Co$ (Found: C 40.6; H 6.0; N 19.26; Co 5.5%) this is approximately equal to one cobalt metal per two ligand molecules. For the cobalt complex of **L5.2** the ratios were $C_{22}H_{39}N_{10}Co$ (Found: C 39.5; H 5.9; N 21.3; Co 9.0%) this is approximately equal to one cobalt metal per ligand molecule. For the cobalt complex of **L5.3** the ratios were $C_{17}H_{31}N_{8}Co$ (Found: C 35.7; H 5.6; N 19.2; Co 11.3%) this is approximately equal to one cobalt metal per ligand molecule. In the cobalt complex of **L5.1** the analysis suggest a $\mathbf{ML_2}$ type structure. In the cobalt complex for **L5.2** there is less cobalt metal present than what you would expect for a straight mononuclear complex. This suggests that there could be some $\mathbf{ML_2}$ present or a polymeric structure of some kind. The **L5.3** cobalt complex has more cobalt metal than is expected for a straight mononuclear complex. This could be an indication of some dinuclear species present.

Changing the Auxiliary Ligands

Originally the next step in the synthesis was to replace the nitrite ligands with chloride ligands through treatment with HCl (Scheme 5-7). The reaction conditions were first tried with $[Co(tacn)(NO_2)_3]$ to help tune the reaction conditions without using the precious sample. That reaction has been reported previously in the literature.[146] However, when the reaction was tried with the ligand complexes the usual conditions resulted in significant degradation of the complexes and an alternative route had to be devised.

Scheme 5-7 Ligand Exchange of Complexes with **L5.1**, **L5.2** and **L5.3** Replacing Nitrite with Chloride

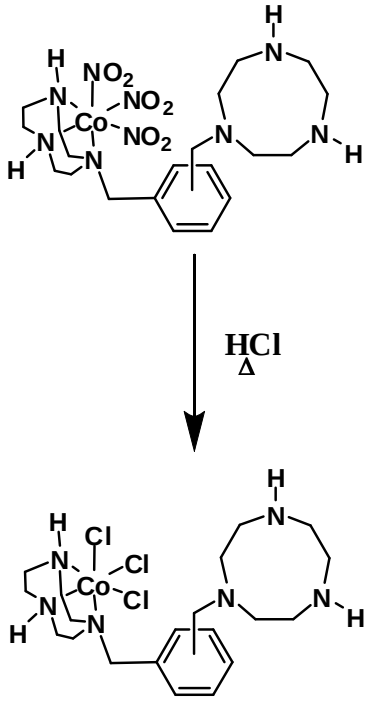

The altered synthesis can be seen in Scheme 5-8. The nitrite ligands were replaced with trifluoromethanesulfonate (Tf) ligands. This was done by adding the minimum amount of trifluoromethanesulfonic acid to a ground up powder of the complex. This was then heated under vacuum. Immediately after the addition of the acid the orange powder turned purple and dissolved and an orange gas was liberated. The reaction mixture was poured slowly into diethyl ether and a precipitate formed. The precipitates were all purple and they were all hygroscopic and had to be kept in a vacuum desiccator. The reaction conditions were again first tried out with $[Co(tacn)(NO_2)_3]$. The resulting purple powder obtained from the $[Co(tacn)(NO_2)_3]$ and Tf acid synthesis was not only not hygroscopic but was also insoluble in the common solvents used.

Scheme 5-8 Ligand Exchange Complexes of **L5.1**, **L5.2** and **L5.3** Replacing Nitrite Ligands for Tf

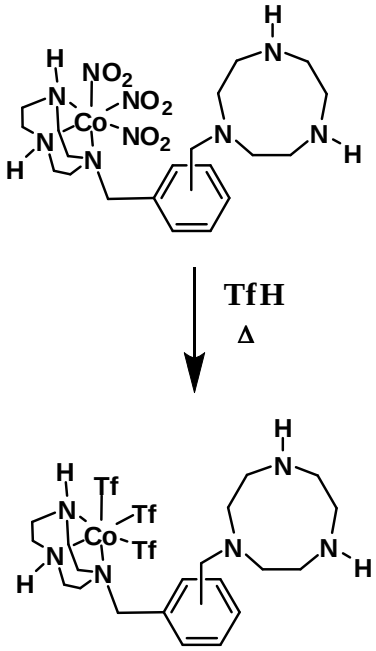

Both the ^{1}H and ^{13}C NMR spectra were run in D_2O. Tf ligands are usually easily replaced by other ligands. Due to this, there is a good chance that when the samples are made up for analysis the D_2O replaces the Tf ligands on the complex. Despite this, the complex will be referred to as the Tf complex. The ^{1}H NMR spectra of the Tf complexes are less complicated than of the NO_2 complexes. This supports the notion that different bonding modes of the NO_2 ligand may be responsible for some of the complexity in the spectra. The peaks are still broad but not to the extent that they were. There is still some information that can be obtained from the spectra. Again there are two regions of peaks, the aromatic region from 7.2-7.8 ppm and non-aromatic region from 2.6-4.2 ppm. There are often peaks relating to residual diethyl ether at 1.18 ppm and 3.45 ppm.

The ^{13}C NMR spectra for the complexes contained a lot of noise. The only spectrum that reliable information could be obtained from was that of the **L5.2** complex. In the

aromatic region there were three definite peaks that could be distinguished from the noise. They are at 138.1, 132.8 and 120.3 ppm. There could be other smaller peaks hidden in the noise. In the non-aromatic region there are eight distinct peaks ranging from 44.0-62.0 ppm. This is the number of peaks that would be expected in this region for the Tf mononuclear complex and some of the peaks have shifted downfield from that of the ligand salt. This evidence proves that in the **L5.2** complex at least, there is a mononuclear complex of the ligand.

In the ^{13}C NMR spectrum of the **L5.2** complex there is evidence of Tf being present. This is seen in the 1 : 3 : 3 : 1 arrangement of the peaks at 128.7 : 124.5 : 120.3 : 116.1 ppm. This splitting pattern is seen because of fluorine atoms being NMR nuclei that split other peaks. As there are three fluorine atoms the signal is split three times causing the pattern seen. Because there is only one of these patterns in the spectra it implies that all the Tf in the solution is in the same environment. This would not be the case if they were still coordinated to the complex.

Further Reactions with the Mononuclear Complexes

In preparation for making the dinuclear species, a synthesis to add 2,2´-bipyridine (bpy) to the Tf complex was attempted. The Tf complex was dissolved in ethanol and excess bpy was added and it was left to stir. The resulting solution was added to diethyl ether and a precipitate formed. The precipitate was filtered and then heated with HCl to exchange the Tf ligand for a chloride ligand and it was then taken to dryness.

The reaction to add bpy was unsuccessful. This could be due to the conditions when trying to exchange the Tf for a chloride. The conditions used in the experiment are very similar to the conditions used for the original nitrite ligand exchange to chloride ligands that resulted in a breakdown of the ligand.

SUMMARY

The synthesis of the di-cobalt complex of the ligands **L5.1**, **L5.2** and **L5.3** was unexpectedly complex from a relatively simple, tried and true, methodology. Indeed, the wide range of precedents for successful preparation of cobalt(III) complexes in this way, for some time, blinded us to the possibility that mono-cobalt complexes may actually be formed in these reactions. Even talking with experts in this field the possibility of mono-cobalt complexes was never raised. Through elemental analysis and extrapolating back from further reactions it was determined that the mono-cobalt complexes of the ligands were probably made.

It was recognised that the difficulty in producing di-cobalt complexes with these ligands were strikingly similar to the problems encountered with the ligands in **Chapter 4**. The ligands in **Chapter 4** can be made on a rather large (> 3 g) scale in a week, whereas the ligands in this chapter take at least two weeks to get less than half that amount. Due to these considerations this work was put on hold.

Now, with the success in **Chapter 4** of making the di-cobalt(III) complexes, the work on these complexes can be revisited. The breakthrough of adding charcoal to stimulate

the reaction was not discovered in time to be applied to these ligands within the scope of this research but it is possible that with this new information the mononuclear cobalt complexes of the ligands, **L5.1**, **L5.2** and **L5.3,** could be reacted with a compound analogous to the one used in **Chapter 4**.

The mono-cobalt complexes of the ligands were initially made with auxiliary ligands of NO_2. These complexes were in most part insoluble and hard to characterise. This may be complicated by the linkage isomerisation of the nitrite ligands. The nitrite ligands were replaced by Tf. Trying to replace the nitrite ligands with chloride ligands and trying to make the bpy complexes resulted in a degradation of the ligand. It was found that mild conditions were needed and overly acidic conditions need to be avoided with these complexes and ligands.

Chapter Six

Conclusion and future work

Chapter 6

Conclusion and future work

Research is a living entity and there is hardly ever a decisive end when the work is done and no more can be achieved. This work is an example of that. A new laser system was designed and setup. The rates of photodecarboxylation were measured and lower limit rates were able to be reported. Bis(bidentate) and bis(tridenate) ligands with xylene spacers were made and the characteristic of only wanting to bind one cobalt(III) metal centre was observed. The discovery of how to make the di-cobalt complexes of the bis(bidentate) ligands was a significant achievement. This knowledge can now be applied to the bis(tridentate) systems in the hope that success will breed success.

From the work in **Chapter 2**, in the laser flash photolysis studies, some answers can be drawn on the rate of the reaction. A lower limit of the reaction rate was set at 2 x 10^7 s^{-1} for the $[Co(bpy)_2(gly)]^{2+}$ and $[Co(tpa)(gly)]^{2+}$ complexes; and 5 x 10^6 s^{-1} for the $[Co(tpa)(aib)]^{2+}$ complex, where bpy is 2,2'-bipyridine; gly is glycinate; tpa is tris(2-pyridylmethyl)amine; and aib is aminoisobutyrate. This was the limit set by the sensitivity of the equipment. The numbers that were obtained had the effect of putting to rest some differing opinions of what was happening in the system. The reporting of the rate to be 4.0 x 10^3 s^{-1} made by Natarajan and co-workers[26] and also by Lewis[27] had been disproved. In both of these cases the suspicion in that the measurements

made were characteristic for the apparatus rather than the reactions being studied. This experimental work backs up what had been observed by Telfer[17] with his work with a radical clock, from which it was inferred that if there was a radical reaction it was occurring at a faster rate than 10^8 s^{-1}. A more definitive rate could be obtained with an experimental set up with faster response time. The mechanism could also be explored through using different substituents as the R groups of the amino acidate

From the work in **Chapter 3**, in the steady state photolysis the premise was to see if two species with opposite charges will react together after they had both undergone photodecarboxylation. The two reacting species, $[Co(bpy)_2(gly)]^{2+}$ and $[Co(EDTA)]^-$, where EDTA is ethane-1,2-diamine-N,N,N',N'-tetraacetate, were subjected to steady state photolysis separately. In these reactions the previously reported photodecarboxylation occurred.[26, 58] The two complexes were then subjected to steady state photolysis together. There was a marked difference from when they were reacted separately to when they were reacted together. This is evidence that the two species are interacting in the experiment.

Furthermore, in the bulk photolysis experiment a pink product was isolated that was not present in the reaction of the two complexes separately. This product has not been fully characterised yet but on concentrating the fraction eluted from the column, it precipitated from solution. Unfortunately, the solid was unable to be dried and the exact composition is still unknown. This is a good sign that it may be possible to obtain X-ray quality crystals from slow evaporation of a suitable solvent. Another approach to this work is to try this experiment with a range of compounds in hopes

that patterns may arise in the characterisation data to allow for elucidation of the products by more sporting methods.

The cationic complex can be varied in a number of ways. One is to change the auxiliary ligands (bpy) and another is to change the amino acid derived ligand group. An example of changing the auxiliary ligand would be to increase the denticity of the ligand. The bpy ligands are bidentate; or, if they were changed to a tetradentate ligand, such as tpa it may be less likely to disassociate. The acid group could be changed in many ways by changing the R groups on the amino acid, or another way is to incorporate the acid group into a polydentate ligand such as the acid N,N-(2-pyridylmethyl)glycinate (dpa) Figure 6-1. This is a tetradetate ligand and again it may prevent the dissociation of the acid group after the reaction has occurred. The coupling product from using the dpa complex would be vastly different from the expected gly product. Having the added binding groups would mean that if a coupling product was produced then there would be more binding sites that could bond to an octahedral metal centre. This could lead to a bridging species or a hypodentate complex.

Figure 6-1 Examples of Changing the Cationic Species in the Steady State Photolysis

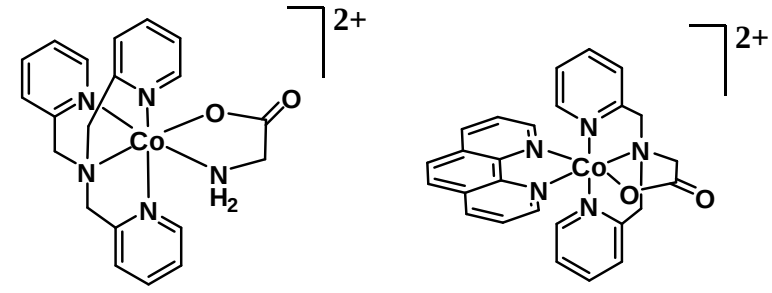

[Co(tpa)(gly)]$^{2+}$ **[Co(dpa)(phen)]$^{2+}$**

Not much variation to the $[Co(EDTA)]^-$ complex can be made because all of the coordination sites on the metal centre are bound by the ligand. In the preparation of Na[Co(EDTA)], there is an intermediate product of $Ba[Co(EDTA)]_2$. This is then reacted on further with Na_2SO_4 to make the insoluble $BaSO_4$, which precipitates in solution, and Na[Co(EDTA)]. The $Ba[Co(EDTA)]_2$ salt could be used directly and if the $[Co(bpy)_2(gly)]SO_4$ salt was used then, theoretically, when the two components are added in the solution together $BaSO_4$ would form an insoluble powder and the only two ions in the solution would be the positive and negative ions that are hoped to react together.

One surprising outcome of this research was in the attempts to make di-cobalt complexes. Eight ligands were made, that, for all intents and purposes, should be able to bind two metal atoms. They either preferred to make the mono-cobalt complexes or no complex at all. This was not expected especially seeing that six of these ligands have been reported in the literature as binding two metal atoms, although, admittedly not cobalt atoms.

The work with the bis(bidentate) ligands, covered in **Chapter 4**, the work is at an exciting stage and the next few steps in the pathway are mapped out. The di-cobalt(III) complexes with **L4.2** and **L4.3** have been made and characterised with the coordinated chloride ligand. The chloride can be exchanged for a Tf using the method that was used to make the mono-cobalt(III) analogue. If the di-cobalt(III) complexes behave in a similar way to the mono-cobalt(III) analogue it is only a simple reaction to exchange the Tf ligand to the acid (Figure 6-2). Alternatively, the chloride could be exchanged for the acid directly.

Figure 6-2 Di-cobalt complexes of **L4.2** and **L4.3** with a Carboxylic Acid Attached

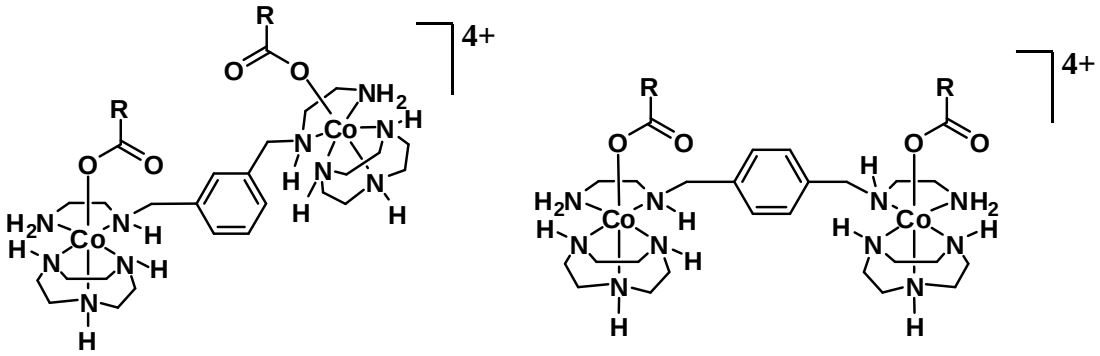

$[Co_2(tacn)_2(L4.2)(ROO)_2]^{4+}$ $[Co_2(tacn)_2(L4.3)(ROO)_2]^{4+}$

As in the reaction for the mono-cobalt acid complex, acetic acid would probably be used first to ensure the reaction conditions where correct. The reason this is used is because the NMR spectra are simple and it is easy to tell whether there are coordinated acid or not especially when there is excess acid used.

No cobalt(III) complexes were made with **L4.1** for unknown reasons. The ligand does have the potential problem of bonding both arms to the same metal atom. This could be avoided by introducing the cobalt metal to **L4.1** when it is already bound by a ligand taking up four sites of the octahedral metal ion. This leaves only two possible sites for the bidentate ligand to bond. The two sites would have to be cis- to one another, such as in $[Co(EDDA)(NO_2)_2]^-$ in Figure 6-3, (where EDDA is ethane-1,2-diamine-N,N'-diacetate). Preparation of the ethane-1,2-diamine (en) complex has been reported before and it is conceivable that using a similar method would produce the desired complex.[147]

Figure 6-3 $[Co(EDDA)(NO_2)_2]^-$

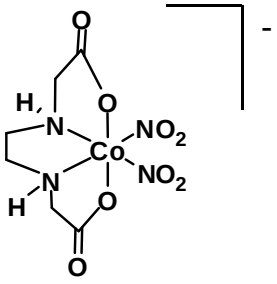

For the bis(bidentate) ligands based on ampy, **L4.4** and **L4.5**, the degradation under the reaction conditions makes it likely they will not be pursued in the course of this research. Although some groups do investigate the degradation of ligands, it does not fall within the bounds of what is being tried to be achieved.

From the work in **Chapter 5**, the information discovered from the work with the ligands in **Chapter 4** can now be applied to ligands **L5.1**, **L5.2** and **L5.3** in **Chapter 5**. The problem of making di-cobalt(III) complexes can be approached in two ways. The first way is to take the already made mono-cobalt(III) complex and react it with an equimolar amount of cobalt(III) complex starting material with some charcoal and proceed in an analogous manner that worked for the ligands in **Chapter 4**. Alternatively, other methods of adding cobalt could be explored.

A better starting material in this case would be one where the auxiliary bi(dentate) ligand was already built in to the complex such as 1,10-phenanthroline (phen) or bpy group already bonded to the cobalt(III) complex (both of which are known literature compounds),[148]as shown in Figure 6-4.

Figure 6-4 Possible Starting Materials for the Synthesis of Cobalt(III) Complexes of **L5.1**, **L5.2** and **L5.3**

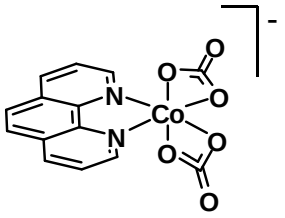

$[Co(phen)(CO_3)_2]^-$

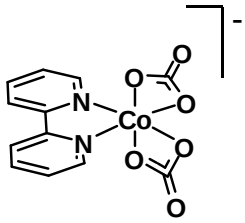

$[Co(bpy)(CO_3)_2]^-$

There is also a wealth of literature compounds that can bond two metal atoms; one such ligand it **L6.1** (Figure 6-5). It has seven potential donor atoms, three on each half of the molecule and a propylene spacer with an OH group off the middle carbon atom.[149] Ligands of this type with the OH group in between two binding centres have been known to facilitate bridging of the metal atoms in the complex with both the OH in the ligand and with additional ligands. This ligand has had metal complexes reported with di-iron(III), di-zinc(II) and di-copper(II) metal centers.[150-154]

Figure 6-5 L6.1

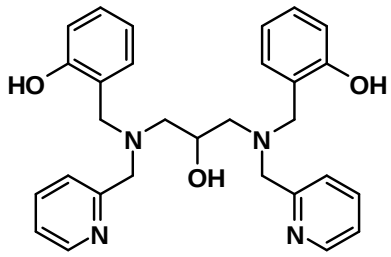

L6.1

Chapter Seven

Experimental

Chapter 7

Experimental

GENERAL EXPERIMENTAL

Starting materials and solvents were obtained commercially and used in syntheses without further purification, unless otherwise stated. Ethane-1,2-diamine (en) was dried over KOH pellets. DMF was dried with 4Å molecular sieves which were changed every few days for a week.

1-Dimensional ^{1}H and ^{13}C NMR spectra were recorded on a Varian UNITY-300 spectrometer. 2-Dimensional ^{1}H and ^{13}C NMR spectra were recorded on a Varian INOVA-500 spectrometer. If consideration of the peak height and chemical shift of signals in ^{1}H and ^{13}C NMR spectra did not allow full assignment of the spectrum, COSY or NOESY experiments were used to assist in assigning the ^{1}H NMR spectrum and then HSQCAD was used to assign the ^{13}C NMR spectrum. ^{1}H NMR chemical shifts are referenced to residual solvent resonance or to TMS or TMPS as an internal reference. ^{13}C NMR chemical shifts are referenced to the bulk solvent resonance or to TMS or TMPS as an internal reference. At the beginning of the synthesis for each compound there is a diagram where the numbers on it are referred to in the reporting of the NMR data. The peaks of the NMR spectra are reported in ppm and are set out

with the solvent and internal reference in brackets and followed by the list of peaks. After each peak the number of equivalent nuclei and the corresponding atoms on the diagram are reported in brackets.

Infrared spectra (400-4000 cm^{-1}) were obtained using a Shimadazu 8201PC Series FTIR spectrometer that was interfaced with an Intel 486 PC operating Shimadzu HyperIR software. Spectra were obtained using the diffuse reflectance method, in solid KBr. Microanalyses were performed at the University of Otago. UV/vis spectra were recorded on a Varian CARY Probe 50 UV-vis Spectrophotometer.

The resins used for column chromatography were all commercially obtained from Aldrich, Sigma or Alfa Aesar. The Cationic Sephadex resin used was CM Sephadex C-25 (carboxymethyl Sephadex). The Anionic Sephadex resin was DEAE Sephadex A-25 (diethylaminoethyl Sephadex). Two types of cationic Dowex was used in this research and they were Dowex 50W-x2 and Dowex 50W-x4. The columns were packed by wetting and expanding the resin in distilled water and filling the column. The column was then stoppered and agitated and left to settle to allow for uniform packing. The measuring of the column was performed on the resin after it had been washed with distilled water and stopped expanding. Column dimensions are reported in cm (length x diameter). The Sephadex was cleaned after each use by running high concentrations (higher than the concentration of the last eluant) of NaCl through the column followed by rinsing with distilled water until the resin stopped expanding. The Dowex was cleaned after each use by running 6 M HCl in ethanol through the column followed by rinsing through with water until the resin stopped expanding. If the Dowex was still discoloured the resin was removed from the column and placed in a

beaker with 4 M HCl and 50% H_2O_2. The slurry was stirred until effervescence ceased. The resin was reloaded on to the column and was washed with water until the pH was neutral and the resin stopped expanding.

CHAPTER 2 FLASH PHOTOLYSIS STUDIES

CAUTION: Perchlorate salts of metal complexes containing organic ligands are potentially explosive and should be handled with care and in small quantities.

The compounds used were those already synthesised by Telfer and Otter. They used literature preparations and reagent grade chemicals from commercial sources. $[Co(bpy)_2(gly)](ClO_4)_2$,[17, 155] $[Co(bpy)_2(CH_2NH_2)](ClO_4)_2$,[17] $[Co(tpa)(gly)](ClO_4)_2$,[156] $[Co(tpa)(CH_2NH_2)](ClO_4)_2$,[156] $[Co(tpa)(aib)](ClO_4)_2$.[156]

Method and Experimental Setup

The cell is glass with the dimensions of 22 mm x 22 mm x 24 mm as shown in Figure 2-5. It was painted with two windows for the analysing beam to pass through at each end and a further window along one side to assist in visually monitoring certain aspects of the experiment such as filling. The cell was painted with black acrylic paint on all sides and the bottom of the cell both inside and outside. The cell was repainted approximately every three weeks. A small plate of copper (20 mm x 20 mm) was placed on the bottom inside the cell.

The laser being used in these experiments was a Lumonics EX744 Pulsemaster excimer using a Kr/F gas fill. This produces a pulse of UV radiation at a wavelength of 248 nm. It generates a pulse of light of approximately 40 ns duration. The output power has a maximum of 450 mJ per pulse. The maximum output power decreases over time as the gas fill degrades.

A schematic of the cell and surrounding set up is shown in Figure 2-4. The laser pulse is reflected by a 248 nm mirror into the cell from above. It passes through a slit which limits the flash to an area of 18 mm x 18 mm which lies in the centre of the cell. This minimises the scattering of light by the meniscus formed at the cell edge.

The analysing beam was generated by an Applied Photophysics flash system bulb which emits white light at a steady state. It passed through a slit and then the cell followed by another slit and a UV cut-off filter. The analysing beam then passed to an Applied Photophysics monochromator. The monochromator was placed so that the slit lies horizontal to match up with the horizontal slit in the cell. The slit on the monochromator was opened to 1-2 mm. The monochromator was set to a wavelength where there is an increase in absorbance as the reaction progresses. A detection wavelength of 410 nm was used for all the compounds.

The monochromator has a built in photomultiplier component where the light is converted to an electronic signal that can be read by the rest of the equipment. The signal is then sent through a pre-amp. The voltage on the pre-amp was set to a low setting of 350 V. The signal is then transferred to a Tektronix TDS 3032 oscilloscope. The data is displayed graphically as voltage *vs* time.

CHAPTER 3 STEADY STATE PHOTOLYSIS

CAUTION: Perchlorate salts of metal complexes containing organic ligands are potentially explosive and should be handled with care and in small quantities.

$[Co(bpy)_2(gly)](ClO_4)_2$,[17, 155] was synthesised by Telfer and Otter from reagent grade chemicals. H[Co(EDTA)] was synthesised by Hartshorn.[157] $Ba[Co(EDTA)]_2$ and Na[Co(EDTA)] were prepared by using literature preparations.[158]

NMR Scale Photolysis

D_2O solutions of $[Co(bpy)_2(gly)](ClO_4)_2$ (~5 mg, ~7.3 x 10^{-6} mols), Na[Co(EDTA)] (~2.6 mg, ~7.3 x 10^{-6} mols) or both, were placed in 5 mm NMR tubes and submerged in an ice-water quartz bath. The solutions were irradiated for 60 minutes with filtered light (254 nm Pyrex transmission filter, Corning 7-54) from a 200 W high pressure mercury lamp. Following photolysis, the solutions were acidified with DCl and ^1H and ^{13}C NMR spectra obtained immediately.

Large Scale Photolysis

A 1 L aqueous solution of $[Co(bpy)_2(gly)](ClO_4)_2$ (~0.6 g/L), Na[Co(EDTA)] (~0.3 g/L) or both were photolysed in 200 mL batches with an immersable Jelight PS-3004-30 mercury lamp for 80 minutes. The solutions were kept cool by standing the reaction vessel in an ice bath and having a magnetic stirrer constantly agitate the solution. The batches were combined and chromatographed either down a CM Sephadex C-25 (25 x 3 cm) column, a DEAE (diethylaminoethyl) Sephadex A-25 (25

x 3 cm) column, or both. In the case where both columns were employed the cationic column was used to separate the mixture first, followed by the anionic column.

Both the cationic and anionic columns were eluted with 0.2 M $NaClO_4$. The fractions collected and were reduced in volume to ~20-50 mL. By that time a precipitate had usually formed. The solids were filtered off and the filtrates were placed into evaporating dishes.

CHAPTER 4 XYLENE BRIDGED BIS(BIDENTATE) SYSTEMS

CAUTION: Perchlorate salts of metal complexes containing organic ligands are potentially explosive and should be handled with care and in small quantities.

The following were synthesised using literature preparations with little to no change: $[Cu_2(\mathbf{L4.8})](ClO_4)_4$,[100] N,N',- di(p-toluenesulfonyl)1,2-ethanediol (endt),[159] N,N',N''-tri(p-toluenesulfonyl)N1-(2-aminoethyl)ethane-1,2-diamine(dientt),[135, 136] $[Co(tacn)Cl_3]$.[113] $[Co(tacn)(NO_2)_3]$,[113] and 5,5-bis(4-amino-2-azabutyl)-1,9-diamino-3,7-diazanonane (**L4.6**).[92, 100]

1,2-bis(2-aminoethylaminomethyl)benzene·4HCl (L4.1)

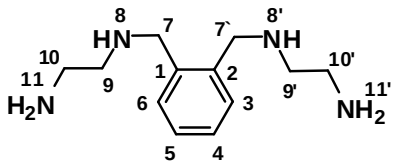

L4.1

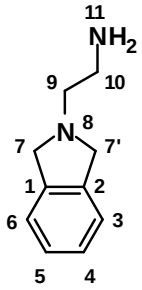

L4.13

Ethane-1,2-diamine (en) (20 mL, 17.98 g, 0.30 mol) was stirred at room temperature. α,α'-Dibromo-*o*-xylene (2.01 g, 7.63 mmol) was added portionwise over 5 hours and the solution was left to stir overnight. Excess en was removed on a rotary evaporator. The yellow residue was made up to 1 L with water, upon which it went cloudy. Dilute HCl was added until the solution was acidic, which coincided with the cloudiness disappearing. The solution was loaded on to a Dowex 50W-x2 column (30 x 5 cm). 2.25 M HCl (10 L) was used to elute any residual en. The column was then eluted with 4 M HCl (10 L), and the product was eluted in this fraction. Also in this fraction was a secondary component **L4.13**. The fractions were taken to dryness on a rotary evaporator and analysed by NMR spectrometry. The impure product is a light brown colour. Crude yield is 2.07 g which, using the NMR peaks relates to approximately 1.18 g (3.20 mmol) 40% **L4.1**·4HCl and 0.89 g (4.46 mmol) 60% **L4.13**·2HCl. NMR **L4.1**·4HCl ^{1}H NMR (D_2O; TMPS) δ 7.45-7.43 (4H, m, 3,4,5,6), 4.40 (4H, s, 7,7′), 3.48-3.65 (8H, m, 9,9′,10,10′). ^{13}C NMR (D_2O; TMPS) 134.1 (2C, 4,5), 133.6 (2C, 3,6), 132.3 (2C, 1,2), 50.9 (2C, 7,7′), 46.9 (2C, 9,9′), 38.2 (10,10′). NMR **L4.13**·2HCl ^{1}H NMR (D_2O; TMPS) δ 7.45-7.43 (4H, m, 3,4,5,6), 3.88 (4H, t, 7,7′), 3.55 (2H, d, 9), 3.02 (2H, d, 10) . ^{13}C NMR (D_2O; TMPS) δ 135.3 (2C, 1,2), 131.8 (2C, 4,5), 125.6 (2C, 3,6), 61.8 (2C, 7,7′), 53.4 (2C, 9,9′), 37.5 (2C, 10,10′).

1,3-bis(2-aminoethylaminomethyl)benzene·4HCl (L4.2)

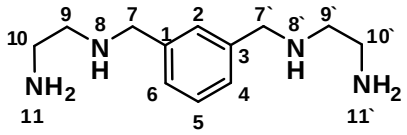

L4.2

Ethane-1,2-diamine (en) (100 mL, 89.90 g, 1.50 mol) was stirred at room temperature. α,α'-Dibromo-*m*-xylene (2.51 g, 9.51 mmol) was added portionwise over 8 hours and the solution was left to stir overnight. A white precipitate formed during this time which was filtered off. Excess en was removed on a rotary evaporator. The yellow residue was made up to 1 L with water. Dilute HCl was added until the solution was just acidic. The solution was loaded on to a Dowex 50W-x2 column (30 x 5 cm). 2.25 M HCl (10 L) was used to elute any residual en. The product was eluted with 4 M HCl (10 L). The product was a brown oil and unsuitable for elemental analysis. For the yield calculations it is assumed that the ligand was protonated, with chloride counterions. Yield of **L4.2**·4HCl 2.38 g (6.42 mmol) 67.5%. Experimental NMR **L4.2**·4HCl ^{1}H NMR (D_2O; TMPS) δ 7.6 (4H, m, 2,4,5,6), 4.4 (4H, s, 7,7′), 3.5 (8H, m, 9,9′,10,10′). ^{13}C NMR (D_2O; TMPS) δ 134.0 (2C, 6,4), 133.9 (1C, 2), 133.4 (2C, 1,3), 133.0 (1C, 5), 53.9 (2C, 7,7′), 46.5 (2C, 9,9′), 38.2 (2C, 10,10′).

1,4-bis(2-aminoethylaminomethyl)benzene·4HCl (L4.3)

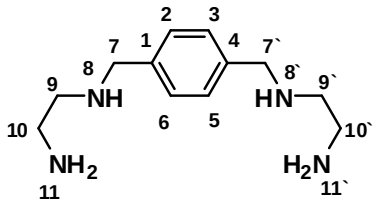

L4.3

Ethane-1,2-diamine (en) (50 mL, 39.48 g, 0.66 mol) was stirred at room temperature. α,α'-Dibromo-*p*-xylene (1.75 g, 6.61 mmol) was added portionwise over 10 hours and

the solution was left to stir overnight. A white precipitate formed during this time. All of the mixture was placed on a rotary evaporator to remove excess en. The yellow residue was made up to 1 L with water. Dilute HCl was added until the solution was acidic. The solution was loaded on to a Dowex 50W-x2 column (30 x 5 cm). 2.25 M HCl (10 L) was used to elute any residual en as the en·2HCl salt. The product was eluted with 4 M HCl (10 L). The product was a pale yellow powder. Yield **L4.3**·5HCl 2.04 g (3.76 mmol) 56.8%. mp > 350^{o}C. Experimental NMR **L4.3**·5HCl ^{1}H NMR (D_2O; TMPS) δ 7.48 (4H, d, 2,3,5,6), 4.25 (4H, s, 7,7′), 3.40-3.30 (8H, dm, 9,9′,10,10′). ^{13}C NMR (D_2O; TMPS) δ 131.8 (2C, 1,4), 130.6 (4C, 2,3,5,6), 51.0 (2C, 7,7′), 43.8 (2C, 9,9′), 35.4 (2C, 10,10′). (Found: C, 35.7; H, 6.4; N, 13.8. Calc for $C_{12}H_{27}Cl_5N_4$: C, 35.6; H, 6.7; N, 13.8%)

1,3-bis((2-pyridylmethyl)aminomethyl)benzene·4HCl (L4.4)

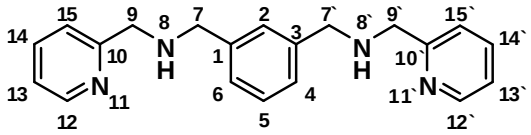

L4.4

2-Aminomethylpyridine (20 mL, 20.98 g, 0.125 mol) was stirred at room temperature. α,α'-Dibromo-*m*-xylene (2.64 g, 9.99 mmol) was added portionwise over 2 hours and the solution was left to stir overnight. The orange solution was made up to 1 L with water, upon which it went cloudy. Dilute HCl was added until the solution was acidic which coincided with the cloudiness disappearing. The solution was loaded on to a Dowex 50W-x2 column (30 x 5 cm). 2.25 M HCl (10 L) was run through the column to collect the excess 2-aminomethylpyridine as the HCl salt. The product eluted with 4 M HCl (10 L). A small amount of product came off in 6 M HCl and 6 M HCl/Ethanol. The product was a brown oil unsuitable for elemental analysis. For yield

calculations it is assumed that the product was protonated with chloride counterions. Yield of **L4.4**·4HCl 2.16 g (4.65 mmol) 46.5%. NMR **L4.4**·4HCl ^{1}H NMR (D_2O; TMPS) δ 8.88 (2H, d, 12,12′), 8.60 (2H, t, 14,14′), 8.16 (2H, d, 15,15′), 8.01 (2H, t, 13,13′), 7.66 (4H, m, 2,4,5,6), 4.76 (4H, s, 9,9′), 4.54 (4H, s, 7,7′). ^{13}C NMR (D_2O; TMPS) δ 149.3 (2C, 12,12′), 148.0 (1C, 1), 146.7 (2C, 14,14′), 134.5 (1C, 2), 134.4 (2C, 4,6), 133.8 (1C, 5) 133.2 (2C, 10), 130.6 (2C, 13,13′), 130.3 (2C, 15,15′), 54.0 (2C, 9,9′), 50.0 (2C, 7,7′).

1,4-bis((2-pyridylmethyl)aminomethyl)benzene·5HCl·0.25H_2O (L4.5)

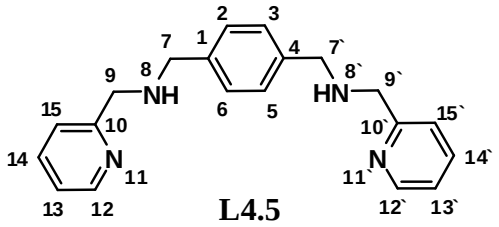

L4.5

2-Aminomethylpyridine (17.57 g, 0.16 mol) was stirred at room temperature. α,α'-Dibromo-*p*-xylene (4.29 g, 0.016 mol) was added portionwise over 2 hours and the solution was left to stir for 1 hour. On addition of the α,α'-Dibromo-*p*-xylene the solution went from yellow to orange, and after stirring it developed into a deep red colour. When the solution was made up to 1 L with water it went cloudy. Dilute HCl was added until the solution was acidic which coincided with the cloudiness disappearing. The solution was loaded on to a Dowex 50W-x2 column (30 x 5 cm). 2.25 M HCl (10 L) was used to elute the excess 2-aminomethylpyridine, it was isolated as the HCl salt. The product was eluted with 4 M HCl (10 L). Yield 2.84 g (6.12 mmol) 38.2%. m.p. 248-251^{o}C. Experimental NMR **L4.5** ^{1}H NMR (D_2O; TMPS) δ 8.81 (2H, d, 12,12′), 8.47 (2H, t, 14,14′), 8.02 (2H, d, 15,15′), 7.97 (2H, t, 13,13′), 7.63 (4H, s, 2,3,5,6), 4.69 (4H, s, 9,9′), 4.50 (4H, s, 7,7′). ^{13}C NMR (D_2O;

TMPS) δ 148.8 (2C, 10), 147.8 (2C, 14,14′), 147.7 (2C, 12,12′), 134.4 (1C, 1,4), 133.6 (4C, 2,3,5,6) 129.9 (2C, 15,15′), 129.9 (2C, 13,13′), 53.7 (2C, 9,9′), 50.6 (2C, 7,7′). (Found: C, 48.1; H, 5.6; N, 11.1. Calc for $C_{20}H_{27.5}Cl_5N_4O_{0.25}$: C, 47.5; H, 5.5; N, 11.1%)

N, N', N"-tris(*p*-toluenesulfonyl)-1, 4, 7-triazacyclononane (tacntt)

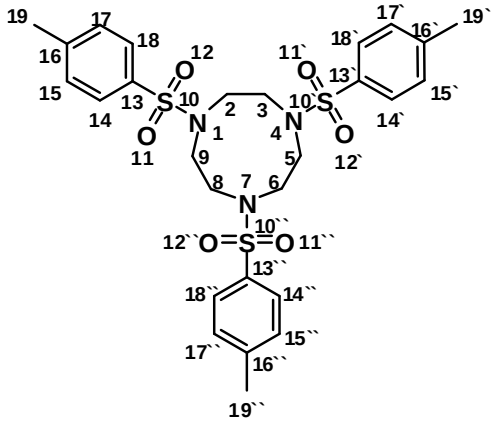

Synthesis based on a literature preparation with significant changes.[136] Dientt (28.30 g, 0.05 mol) in dry DMF (550 mL) was stirred. NaH (8 g) was added. After the main effervescence the solution was brought to 100°C. A solution of endt (18.5 g, 0.05 mol) in dry DMF (200 mL) was added over 2 hours. The now yellow solution was stirred at 100°C overnight. The solution was then cooled and excess NaH was filtered off. The solution was added gradually to ice cold water (4 L) which caused a white precipitate to form. This was filtered off, washed with water and dried at 100°C. Crude yield 27.5 g (0.046 mol) 92.6%, m.p. 169-170°C. Recrystallised from chloroform/ethanol. Yield 24.6 g (0.041 mol) 82.8%. ^{1}H NMR ($CDCl_3$; TMS) δ 7.71 and 7.33 (6H each, d, either 14,14′,14″,18,18′,18″ or 15,15′,15″,17,17′,17″), 3.44 (12H, s, 2,3,5,6,8,9), 2.43 (9H, 19,19′,19″). ^{13}C NMR($CDCl_3$; TMS) δ 143.6 (3C, 13,13′,13″), 134.3 (3C,

16,16′,16″), 129.7 and 127.3 (6C each, either 14,14′,14″,18,18′,18″ or 15,15′,15″,17,17′,17″), 51.6 (6C, 2,3,5,6,8,9), 21.3 (3C, 19,19′,19″).

Tacn.3HBr

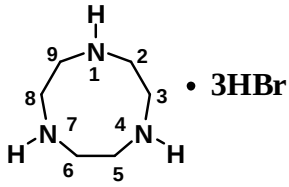

• 3HBr

Based loosely on literature a preparation.[113, 136] Tacntt (29.37 g, 0.49 mol) was added portionwise to concentrated H_2SO_4 (50 mL). The now black solution was heated to 100^{o}C and stirred for three days. The solution was cooled and added to a stirring solution of dry ethanol (100 mL) and dry diethyl ether (60 mL). The temperature was kept under 20^{o}C. A further dry diethyl ether (100 mL) was added and the solution was cooled to 0^{o}C on an ice bath. A grey viscous, tacky solid formed on the bottom of the flask and the supernatant was decanted off with care. The solid was dissolved in the minimum amount of hot water and filtered. To the filtrate conc. HBr was added until no more precipitation was observed. The mixture was collected in the fridge overnight. The solid was collected by vacuum filtration and washed with ethanol. The product was a white grainy solid. Yield 12.67 g (0.034 mol) 69.4%, m.p. 299-301^{o}C. ^{1}H NMR(D_2O; TMPS) δ 3.56 (12H, s, 2,3,5,6,8,9) ^{13}C NMR(D_2O; TMPS) δ (6C, 2,3,5,6,8,9)

CHAPTER 4 XYLENE BRIDGED BIS(BIDENTATE) SYSTEM COMPLEXES

$[Co(tacn)(H_2L4.2)Cl]Cl_4$

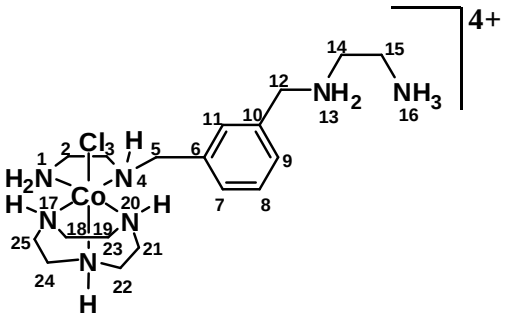

L4.2 (2.21 g, 6.00 mmol) and $[Co(tacn)Cl_3]$ (1.61 g, 5.46 mmol) were placed in a 100 mL roundbottom flask with water (30 mL). The pH was raised to 8 and the mixture was heated at 80^{o}C for 1 hour. The colour at the end of this time was a deep red/purple. The pH was lowered to 3 with HCl and the reaction mixture was heated at 80^{o}C for a further hour. A Dowex 50W-x2 (15 x 3 cm) column was used to separate the mixture and eight bands were seen and collected.

The product was a tacky pink solid $[Co(tacn)(H_2$**L4.2**$)Cl]Cl_4 \cdot 2H_2O \cdot 3.5HCl$ (1.14 g, 1.93 mmol) 35.4%. m.p. >350^{o}C ^{1}H NMR (D_2O; TMPS) δ 7.58-7.62 (4H, m, 7,8,9,11), 4.40 (4H, s, 5,12), 3.37-3.67 (20H, m, 2,3,14,15,18,19,21,22,24,25). ^{13}C NMR (D_2O; TMPS) δ 132.7-137.6 (6C, 6,7,8,9,10,11), 57.3 (1C, 5), 57.1 (1C, 12), 52.6-55.8 (7C, 2,18,19,21,22,24,25), 46.6 (1C, 14), 45.9 (1C, 2), 38.2 (1C, 15). (Found: C, 28.7; H, 6.4; N, 13.4%. Calc for $C_{18}H_{46.5}Cl_{8.5}CoN_7O_2$: C, 28.7; H, 6.2; N, 13.1%).

Fraction	Colour of dried product	Product
1	Blue	$[Co(tacn)Cl_3]$
2	Blue	$[Co(tacn)Cl_3]$
3	Blue/Green	$[Co(tacn)Cl_3]$
4	Yellow	$[Co(tacn)_2]Cl_3$
5	Brown	Unknown
6	Brown	Unknown
7	Purple	$[Co(tacn)(H_2\mathbf{L4.2})Cl]^{4+}$
8	Purple	$[Co(tacn)(H_2\mathbf{L4.2})Cl]^{4+}$

$[Co_2(tacn)_2(L4.2)Cl_2]Cl_4$

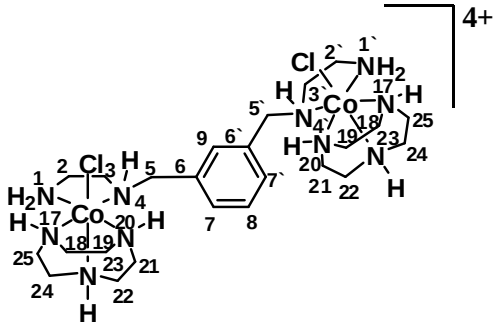

L4.2 (0.50 g, 1.27 mmol) and $[Co(tacn)Cl_3]$ (0.76 g, 2.55 mmol) were placed in a 50 mL roundbottom flask with water (25 mL). The pH was raised to 8 with sodium hydroxide and activated charcoal (1 g) was added. The reaction mixture was heated at 80^{o}C for four hours. The pH was lowered to 3 with HCl and the reaction was heated at 80^{o}C for a further two hours. The solution was cooled to room temperature and filtered to remove the charcoal. The solution was then made up to 1 L with water and loaded onto a 50W-x2 (15 x 3 cm) Dowex column and eluted with increasing concentrations of HCl.

Fraction	Colour of dried product	Product
1	Blue	$[Co(tacn)Cl_3]$
2	Blue/Green	$[Co(tacn)Cl_3]$
3	Yellow	$[Co(tacn)_2]Cl_3$
4	Purple	$[Co_2(tacn)_2(\mathbf{L4.2})Cl_2]^{4+}$ / $[Co(tacn)(H_2\mathbf{L4.2})Cl]^{4+}$
5	Purple	$[Co_2(tacn)_2(\mathbf{L4.2})Cl_2]^{4+}$

The product was a tacky purple solid $[Co_2(tacn)_2(\mathbf{L4.2})Cl_2]Cl_4{\cdot}0.5CH_3OH{\cdot}8HCl$ 0.55 g (0.488 mmol) 38.4%. ^{1}H NMR (D_2O; TMPS) δ 7.63 (1H, d, 8), 7.52 (2H, d, 7,7′), 7.25 (1H, s, 9), 4.09 (4H, s, 5,5′), 2.44-3.72 (32H, m, 2,2′,3,3′,18,18′,19,19′,21,21′,22,22′,24,24′,25,25). ^{13}C NMR(D_2O; TMPS) δ 137.2 (2C, 7,7′) 134.3 (1C, 9 or 8), 133.4 (2C, 6,6′), 132.2 (1C, 8 or 9), 57.5 (2C, 5,5′), 52.6-55.7 (14C, 3,3′,18,18′,19,19′,21,21′,22,22′,24,24′,25,25′), 46.0 (2C, 2,2′). $[Co_2(tacn)_2(\mathbf{L4.2})Cl_2]Cl_4{\cdot}0.5CH_3OH{\cdot}8HCl$ (Found: C, 26.4; H, 5.6; N, 12.4. Calc for $C_{24.5}H_{62}Cl_{14}Co_2N_{10}O_{0.5}$: C, 26.3; H, 5.6; N, 12.5).

$[Co(tacn)(H_2L4.3)Cl]Cl_4$

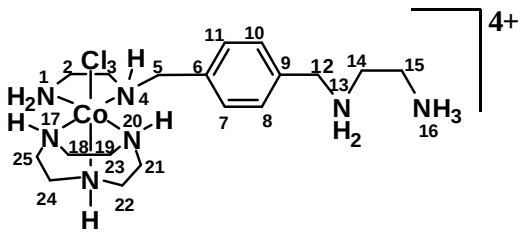

L4.3 (1.57 g, 3.88 mmol) and $[Co(tacn)Cl_3]$ (1.12 g, 3.80 mmol) were placed in a 100 mL roundbottom flask with water (30 mL). The pH was raised to 8 and heated at 80^{o}C

for 1 hour. The colour at the end of this time was a deep red. The pH was lowered to 3 and the reaction mixture was heated at 80^{o}C for a further 1.5 hours. A Dowex 50W-x2 (15 x 3 cm) column was used to separate the mixture and six bands were seen and collected.

Fraction	**Colour of dried product**	**Product**
1	Blue	[Co(tacn)Cl_3]
2	Blue	[Co(tacn)Cl_3]
3	Blue/Green	[Co(tacn)Cl_3]
4	Yellow	[Co(tacn)$_2$]Cl_3
5	Purple	[Co(tacn)(H_2**L4.3**)Cl]$^{4+}$
6	Brown	**L4.3**

Fraction 5 is the product. The fraction was reduced in volume on a rotary evaporator. When the solution was nearing dryness methanol (30 mL) was added, which resulted in formation of a light pink precipitate. The solid was filtered and washed with a little methanol. The filtrate was taken to dryness also and yielded a dark pink/purple glass. It was the product with different cocrystallised solvent molecules. Light pink solid [Co(tacn)(H_2**L4.3**)Cl]Cl_4·2H_2O·3HCl and by elemental analysis (Found: C, 32.6; H, 7.0; N, 14.9. Calc for $C_{18}H_{44}Cl_6CoN_7O_2$: C, 32.7; H, 6.8; N, 14.8) The filtrate that was taken to dryness is a dark pink/purple glass [Co(tacn)(H_2**L4.3**)Cl]Cl_4·5HCl and by elemental analysis (Found: C, 31.2; H, 6.3; N, 14.0. Calc for $C_{18}H_{42}Cl_8CoN_7$: C, 30.9; H, 6.1; N, 14.0). Yield light pink powder [Co(tacn)(H_2**L4.3**)Cl]Cl_4·2H_2O·3HCl 0.94 g (1.42 mmol) 37.4%. m.p. >350^{o}C Yield dark pink/purple glass [Co(tacn)(H_2**L4.3**)Cl]Cl_4·5HCl 0.32 g (4.70 mol) 12.4%. m.p. >350^{o}C ^{1}H NMR (D_2O;

TMPS) δ 7.54 - 7.58 (4H, 7,8,10,11), 4.38 (4H, 5,12), 2.69-72 (20H, 2,3,14,15,18,19,21,22,24,25). ^{13}C NMR(D_2O; TMPS) δ 138.0 (1C, 6), 137.1 (1C, 9), 133.7 (2C, 7,11 or 8,10), 133.6 (2C, 7,11 or 8,10), 57.1 (1C, 12), 55.6 (1C, 5), 52.5-55.0 (7C, 3,18,19,21,22,24,25), 46.4 (1C, 14), 45.8 (1C, 2), 38.1 (1C, 15).

$[Co_2(tacn)_2(L4.3)Cl_2]Cl_4 \cdot 5HCl \cdot 2H_2O \cdot 1.5CH_3OH$

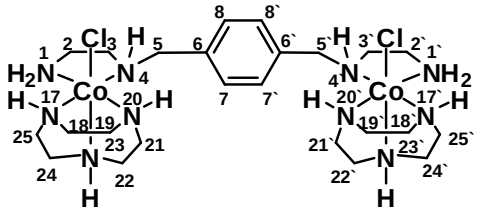

L4.3 (0.46 g, 1.27 mmol) and $[Co(tacn)Cl_3]$ (0.75 g, 2.55 mmol) were placed in a 50 mL roundbottom flask with water (25 mL). The pH was raised to 8 with sodium hydroxide and 1 g activated charcoal was added. The reaction mixture was heated at 80^{o}C for four hours. The pH was lowered to 3 with HCl and the reaction was heated at 80^{o}C for a further two hours. The solution was cooled to room temperature and filtered to remove the charcoal. The solution was then made up to 1L with water and loaded on to a Dowex 50Wx2 (15 x 3 cm) column which was eluted with increasing concentrations of HCl.

Fraction	**Colour of dried product**	**Product**
1	Blue	$[Co(tacn)Cl_3]$
2	Blue/Green	$[Co(tacn)Cl_3]$
3	Yellow	$[Co(tacn)_2]Cl_3$
4	Purple	$[Co(tacn)(H_2$**L4.3**$)Cl]Cl_4$
5	Purple	$[Co_2(tacn)_2($**L4.3**$)Cl_2]Cl_4$

Yield purple powder $[Co_2(tacn)_2(\mathbf{L4.3})Cl_2]^{4+}$ 0.28 g (0.261mmol) 20.5%. m.p. >350^oC ^1H NMR (D_2O; TMPS) δ 7.55 (4H, s, 7,7′,8,8′), 4.36 (4H, s, 5,5′), 2.76–3.15 (8H, m, 2,2′,3,3′, 18,18′,19,19′,21,21′,22,22′,24,24′,25,25). ^{13}C NMR(D_2O; TMPS) δ 137.2 (2C, 6,6′), 133.4 (4C, 7,7′,8,8′), 57.7 (2C, 5,5′), 52.6-55.7 (14C, 3,3′,18,18′,19,19′,21,21′,22,22′, 24,24′,25,25′), 46.0 (2C, 2,2′). $[Co_2(tacn)_2(\mathbf{L4.3})Cl_2]Cl_4 \cdot 5HCl \cdot 2H_2O \cdot 1.5CH_3OH$ (Found: C, 28.5; H, 6.4; N, 13.0. Calc for $C_{25.5}H_{67}Cl_{11}Co_2N_{10}O_{3.5}$: C, 38.4; H, 6.3; N, 13.0).

$[Co(tacn)(L4.3)(Tf)]^{2+}$

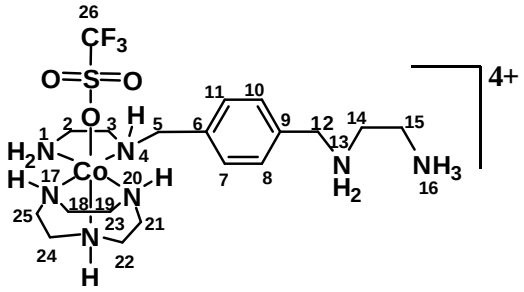

$[Co(tacn)(H_2\mathbf{L4.3})Cl]Cl_4$ (0.78 g, 1.18 mmol) was placed in a 250 mL roundbottom flask. Trifluoromethanesulfonic acid was added dropwise until all of the solid had dissolved. The reaction was stirred and warmed at 70^oC for two hours under vacuum. After this time the solution was added slowly to vigorously stirring dry diethyl ether. A pink precipitate formed. The solid was collected by suction filtration and was dried in a vacuum desiccator. The solid is hygroscopic and time exposed to the air should be minimal. Yield 0.94 g. Product was used without further characterisation or purification.

[Co(tacn)(H_2L4.3)(CH_3COO)]$^{4+}$

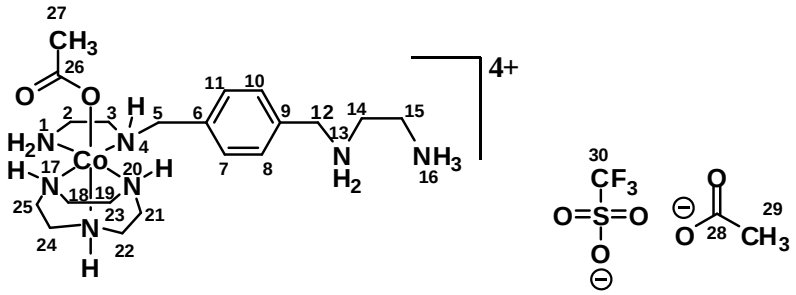

[Co(tacn)(**L4.3**)(Tf)]$^{2+}$ (0.94 g) was placed in a 50 mL conical flask with dry analytical grade acetone (20 mL). Excess sodium acetate (2 g) was added, which does not dissolve in acetone. The slurry was stirred overnight. During this time all the acetone evaporated. The complex was redissolved in acetone and the excess sodium acetate was filtered off. Yield 0.91 g. ^{1}H NMR (D_2O; TMPS) δ 7.53 - 7.60 (4H, 7,8,10,11), 4.37 (4H, 5,12), 2.69-3.57 (20H, 2,3,14,15,18,19,21,22,24,25) 2.27 (3H, 27), 2.09 (big peak 3H, 29). ^{13}C NMR(D_2O; TMPS) δ 188.4 (1C, 26), 183.6 (1C, 28), 137.8 (1C, 6), 137.1 (1C, 9), 133.6 (2C, 7,11 or 8,10), 133.4 (2C, 7,11 or 8,10), 128.6:124.4:120.2:116.0 (1:3:3:1 ratio, 1C, 30), 57.0 (1C, 12), 56.0 (1C, 5), 52.2-54.2 (7C, 3,18,19,21,22,24,25), 46.7 (1C, 14), 45.2 (1C, 2), 38.3 (1C, 15), 27.3 (1C, 27), 25.6 (1C, 29).

L4.14

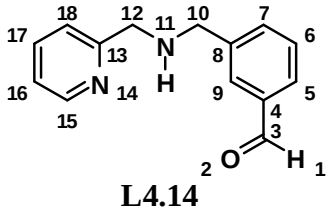

L4.14

L4.4 (2.24 g, 4.83 mmol) and [Co(tacn)Cl_3] (1.41 g, 4.83 mmol) were placed in a 100 mL roundbottom flask with water (30 mL). The pH was raised to 8 and heated at 80^{o}C overnight. The colour at the end of this time was purple. The pH was lowered to 3 and

the reaction mixture was heated at 80^{o}C for a further hour. A Dowex 50W-x2 (15 x 3 cm) column was used to separate the mixture and nine bands were seen and collected.

Fraction	**Colour of dried product**	**Product**
1	Blue	$[Co(tacn)Cl_3]$ / $[Co(tacn)_2]Cl_3$
2	Blue	$[Co(tacn)Cl_3]$ / $[Co(tacn)_2]Cl_3$
3	Blue	$[Co(tacn)Cl_3]$ / $[Co(tacn)_2]Cl_3$
4	Yellow	$[Co(tacn)(ampy)Cl]^{2+}$ / $[Co(tacn)_2]Cl_3$
5	Red	$[Co(tacn)(ampy)Cl]^{2+}$ / $[Co(tacn)_2]Cl_3$
6	Brown	**L4.14 /** $[Co(tacn)_2]Cl_3$
7	Brown	**L4.14 /** $[Co(tacn)_2]Cl_3$
8	Brown	**L4.14**
9	Brown	**L4.14**

Due to the products not being pure, a yield could not be determined. ^{1}H NMR (D_2O; TMSP) δ 9.99 (1H, s, 1), 8.88 (1H, d, 15), 8.61 (1H, t, 17), 8.14 (1H, d, 18), 8.08 (1H, s, 9), 8.05 (1H, t, 16), 7.90 (1H, d, 7), 7.88 (1H, d, 5), 7.74 (1H, t, 6), 4.78 (2H, s, 12), 4.27 (2H, s, 10). ^{13}C NMR was unable to be referenced due to the TMPS peaks being obscured by noise.

L4.15

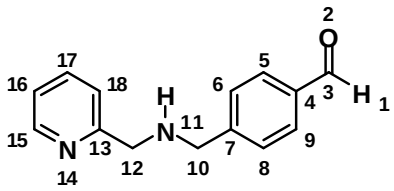

L4.15

L4.5 (2.24 g, 4.83 mmol) and [Co(tacn)Cl_3] (1.43 g, 4.83 mmol) were placed in a 100 mL roundbottom flask with water (30 mL). The pH was raised to 8 and heated at 80^{o}C overnight. The colour at the end of this time was purple. The pH was lowered to 3 and the reaction mixture was heated at 80^{o}C for a further 1.5 hours. A Dowex 50W-x2 (15 x 3 cm) column was used to separate the mixture and eight bands were seen and collected.

Fraction	**Colour of dried product**	**Product**
1	Blue	[Co(tacn)Cl_3]
2	Blue	[Co(tacn)Cl_3]
3	Green	[Co(tacn)Cl_3]
4	Red	$[Co(tacn)(ampy)Cl]^{2+}$ / [Co(tacn)$_2$]Cl_3
5	Orange	$[Co(tacn)(ampy)Cl]^{2+}$ / [Co(tacn)$_2$]Cl_3
6	Orange/brown	**L4.15 /** [Co(tacn)$_2$]Cl_3
7	Brown	**L4.15**
8	Brown	**L4.15**

Due to the products not being pure, a yield could not be determined. ^{1}H NMR (D_2O; TMSP) δ 9.82 (1H, s, 1), 8.75 (1H, d, 15), 8.53 (1H, t, 17), 8.01 (1H, d, 18), 7.97 (1H,

t, 16), 7.36 – 7.57 (4H, m, 5, 6, 8, 9), 4.64 (2H, s, 12), 4.37 (2H, s, 10). ^{13}C NMR was unable to be referenced due to the TMPS peaks being obscured by noise.

CHAPTER 5 XYLENE BRIDGED BIS(1,4,7-TRIAZA-CYCLONON-1-YLMETHYL) BASED LIGANDS

The following were synthesised using literature preparations with little to no change: N,N',-di(*p*-toluenesulfonyl)-1,2-ethanediol (endt),[159] N,N',N''-tris(*p*-toluenesulfonyl)N′-(2-aminoethyl)ethane-1,2-diamine (dientt),[135, 136] 1,4,7-triazatricylclo[5.2.1.04,10]decane,[160] 1,2-Bis(1,4,7-triazacyclonon-1-ylmethyl)benzene (**L5.1**),[32] 1,3-Bis(1,4,7-triazacyclonon-1-ylmethyl)benzene (**L5.2**),[32] 1,4-Bis(1,4,7-triazacyclonon-1-ylmethyl)benzene (**L5.3**).[32] N,N',N''-tris(*p*-toluenesulfonyl) 1, 4, 7- triazacyclononane (tacntt) and tacn·3HBr are described above under **Chapter 4 Ligands**.

1, 4, 7- triazacyclononane (tacn)[i]

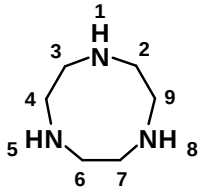

[i] In the literature, the synthesis for 1,4,7-triazatricylclo[5.2.1.04,10]decane[160] X. Zhang, W.-Y. Hsieh, T. N. Margulis, and L. J. Zompa, *Inorganic Chemistry*, 1995, **34**, 2883. does not include this step which is necessary to get the free amine of the tacn salt.

Tacn·3HBr salt (6.72 g, 18.0 mmol) was added to 50% sodium hydroxide solution 50 mL and stirred overnight. The solution was placed in a separating funnel. The ligand was extracted with chloroform (7 x 50 mL). The chloroform extracts were collected and combined and the solution was dried with magnesium sulfate. The magnesium sulfate was filtered off and the solvent was removed on a rotary evaporator. The product was a yellow oil. Yield 1.97 g (15.3 mmol) 84.8%. ^{1}H NMR ($CDCl_3$; TMS) δ 2.53 (12H, 2,3,5,6,8,9) ^{13}C NMR($CDCl_3$; TMS) δ 46.4 (6C, 2,3,5,6,8,9).

$[Co_n(L5.1)_n(NO_2)_n]$

This synthesis is based on a literature preparation.[113] $Co(NO_3)_2·6H_2O$ (0.61 g, 2.08 mmol) and $NaNO_2$ (0.70 g, 10.2 mmol) were dissolved in buffer solution (7.1 mL) (a bulk buffer solution was made and consists of NaOH (7.12g), acetic acid (20.5 mL) and water (178 mL)) and aeration was begun. The HBr salt of **L5.1** (1.00 g, 1.15 mmol) and NaOH (0.33 g) was dissolved in water (7.1 mL) and was added dropwise to the aerating solution. A precipitate formed immediately. Aeration was continued for a further 1 hour. The orange solid was collected by suction filtration, washed with water and dried in the oven. Yield 0.15 g (Found: C, 40.6; H, 6.0; N, 19.0; Co, 5.5%).

$[Co_n(L5.2)_n(NO_2)_n]$

This synthesis is based on a literature preparation.[113] $Co(NO_3)_2·6H_2O$ (0.62 g, 2.13 mmol) and $NaNO_2$ (0.70 g, 10.1 mmol) were dissolved in buffer solution (7.1 mL) (a bulk buffer solution was made and consists of NaOH (7.12g), acetic acid (20.5 mL) and water (178 mL)) and aeration was begun. The HBr salt of **L5.2** (1.08 g, 1.24 mmol) and NaOH (0.30 g) was dissolved in water (7.1 mL) and was added dropwise

to the aerating solution. A precipitate formed immediately. Aeration was continued for a further 1 hour. The orange solid was collected by suction filtration, washed with water and dried in the oven. Yield 0.61 g (Found: C, 39.6; H, 6.0; N, 21.3; Co 9.0%)

$[Co_n(L5.3)_n(NO_2)_n]$

This synthesis is based on a literature preparation.[113] $Co(NO_3)_2 \cdot 6H_2O$ (0.6458 g, 2.21 mmol) and $NaNO_2$ (0.68 g, 9.72 mmol) were dissolved in buffer solution (7.1 mL) (a bulk buffer solution was made and consists of NaOH (7.12g), acetic acid (20.5 mL) and water (178 mL)) and aeration was begun. The HBr salt of **L5.3** 1.01 g (1.11 mmol) and NaOH 0.27 g was dissolved in water 7.1 mL and was added dropwise to the aerating solution. A precipitate formed immediately. Aeration was continued for a further 1 hour. The orange solid was collected by suction filtration, washed with water and dried in the oven. Yield 0.62 g (Found: C, 35.7; H, 5.7; N, 19.3; Co, 11.3%).

$[Co_n(L5.1)_n(Tf)_n]$

$[Co_n(\mathbf{L5.1})_n(NO_2)_n]$ (1.13 g) was placed in a 10 mL roundbottom flask. To it was added Trifluoromethanesulfonic acid (~5 mL). The orange powder turned purple. The stirred solution was heated at 40^oC under vacuum with a water aspirator. An orange gas was given off during this time. After three hours the viscous solution was added slowly to vigorously stirred dry diethyl ether. A purple, hygroscopic precipitate was present. The purple solid was collected by suction filtration and dried in a vacuum desiccator. Yield 0.97 g.

$[Co_n(L5.2)_n(Tf)_n]$

$[Co_n(\mathbf{L5.2})_n(NO_2)_n]$ (0.53 g) was placed in a 10 mL roundbottom flask. To it was added Trifluoromethanesulfonic acid (~3 mL). The orange powder turned purple. The stirred solution was heated at 40^oC under vacuum with a water aspirator. An orange gas was given off during this time. After four hours the viscous solution was added slowly to vigorously stirred dry diethyl ether. A purple, hygroscopic precipitate was present. The purple solid was collected by suction filtration and dried in a vacuum desiccator. Yield 1.62 g. ^1H NMR (D_2O; TMSP) δ 7.59-7.38 (m), 3.97 (m), 3.66 (m), 3.28 (m), 3.06 (m). ^{13}C NMR(D_2O; TMSP) δ 138.1, 135.2, 134.5, 132.8, 120.7, 128.7 : 124.5 : 120.3 : 116.1 (1:3:3:1 ratio, Tf), 60.2, 59.2, 54.1, 53.7, 49.9, 46.1, 44.7, 44.3.

$[Co_n(L5.3)_n(Tf)_n]$

$[Co_n(\mathbf{L5.3})_n(NO_2)_n]$ (0.63 g) was placed in a 10 mL roundbottom flask. To it was added Trifluoromethanesulfonic acid (~3 mL). The orange powder turned purple. The stirred solution was heated at 40^oC under vacuum with a water aspirator. An orange gas was given off during this time. After four hours the viscous solution was added slowly to vigorously stirred dry diethyl ether. A purple, hygroscopic precipitate was present. The purple solid was collected by suction filtration and dried in a vacuum desiccator. Yield 0.74 g.

Appendix

Appendix 1

X-Ray Crystallography

Table A1.1-A1.3 lists the crystal data and X-ray experimental details for the three fully refined crystal structures discussed in this thesis. Throughout the text, selected bond lengths and angles are discussed and listed under the appropriate figures, while the remaining distances and angles, as well as atomic coordinates, anisotropic displacement factors and hydrogen atom coordinates are available on request from the Department of Chemistry, University of Canterbury.

The data for the crystal structures reported in this thesis were collected on two different X-ray diffractometers. Both detectors used graphite monochromatised Mo Kα (λ = 0.71073 Å) radiation.

The first diffractometer used was a Siemens CCD area detector mounted on a P4 four-circle diffractometer. Data collection and cell determination was performed with SMART and data reduction with SAINT. This diffractometer was used to collect the data for crystal structure of H_4(**L4.3**)$(SO_4)_2$ (Table A1.1)

The second diffractometer used was a Bruker-Nonius APEX II system. Data collection, cell determination and data reduction were all performed with the APEX software package. This diffractometer was used to collect the data for the crystal structures of Na[Co(EDTA)]·6(H_2O) and Ba[Co(EDTA)]$_2$·8(H_2O).

All structures had intensities corrected for Lorentz and polarization effects and for absorption using SADABS.[161] All structures were solved by direct methods using SHELXS and refined on F^2 using all data by full-matrix least squares procedures using SHELXL-97.[162] All non-hydrogen atoms were refined with anisotropic displacement parameters. Hydrogen atoms were included in calculated positions with isotropic displacement parameters 1.2 times the isotropic equivalent of their carrier carbon atoms.

Table A1.1 Crystal Data and Structure Refinement for Na[Co(EDTA)]

Compound		Na[Co(EDTA)]
Empirical Formula		C_{10} H_{12} N_2 O_{12} Na Co
Formula weight		434.14
Temperature (K)		96(2) K
Crystal System		Orthorhombic
Space group		Pna21
Unit cell dimensions:	a (Å)	6.4450(3)
	b (Å)	18.9325(9)
	c (Å)	13.4979(6)
	α (^{o})	90
	β (^{o})	90
	γ (^{o})	90
Volume (Å^3)		1647.01(13)
Z		4
Density (calculated (Mg/m^3)		1.751
Absorption coefficient (mm^{-1})		1.136
F(000)		880
Crystal size (mm^3)		0.70 x 0.12 x 0.06
Theta range for data collection (^{o})		1.85 to 30.83
Reflections collected		20554
Independent reflections [R(int)]		4913 [0.0578]
Completeness to theta (^{o}/%)		30.83 / 97.6
Data / restraints / parameters		4913 / 1 / 235
Goodness-of-fit of F^2		1.144
Final R_1 [I>2sigma(I)]		0.0516 [0.1302]
wR_2 (all data)		0.1448
Largest diff. peak and hole (e.Å^{-3})		1.324 and -0.905

Table A1.2 Crystal Data and Structure Refinement for $Ba[Co(EDTA)]_2$

Compound		$Ba[Co(EDTA)]_2$
Empirical Formula		$C_{20}\ H_{40}\ N_4\ O_{24}Co_2\ Ba$
Formula weight		975.76
Temperature (K)		296(2)
Crystal System		Monoclinic
Space group		P2(1)
Unit cell dimensions:	a (Å)	6.5241(2)
	b (Å)	12.8373(5)
	c (Å)	19.5103(7)
	α (^{o})	90
	β (^{o})	95.452(2)
	γ (^{o})	90
Volume ($Å^3$)		1626.63(10)
Z		2
Density (calculated (Mg/m^3)		1.992
Absorption coefficient (mm^{-1})		2.309
F(000)		980
Crystal size (mm^3)		0.65 x 0.28 x 0.17
Theta range for data collection (^{o})		2.10 to 25.05
Reflections collected		32163
Independent reflections [R(int)]		5734 [0.0301]
Completeness to theta (^{o}/%)		25.00 / 99.9
Data / restraints / parameters		5734 / 18 / 508
Goodness-of-fit of F^2		1.093
Final R_1 [I>2sigma(I)]		0.0149 [0.0397]
wR_2 (all data)		0.0400
Largest diff. peak and hole ($e.Å^{-3}$)		1.047 and -0.526

Table A1. 3 Crystal Data and Structure Refinement for **L4.3**

Compound		**L4.3**
Empirical Formula		$C_{12}\ H_{32}\ N_4\ O_{11}\ S_2$
Formula weight		472.56
Temperature (K)		93(2)
Crystal System		Monoclinic
Space group		P21/n
Unit cell dimensions:	a (Å)	9.4616(9)
	b (Å)	15.6099(15)
	c (Å)	14.0886(14)
	α (^{o})	90
	β (^{o})	101.923
	γ (^{o})	90
Volume (Å^3)		2035.9(3)
Z		4
Density (calculated (Mg/m^3)		1.542
Absorption coefficient (mm^{-1})		0.326
F(000)		1008
Crystal size (mm^3)		0.76 x 0.24 x 0.24
Theta range for data collection (^{o})		2.38 to 25.05
Reflections collected		5533
Independent reflections [R(int)]		2791 [0.0243]
Completeness to theta (^{o}/%)		25.00 / 77.7
Data / restraints / parameters		2791 / 0 / 310
Goodness-of-fit of F^2		1.046
Final R_1 [I>2sigma(I)]		0.0331 [0.0921]
wR_2 (all data)		0.0964
Largest diff. peak and hole (e.Å^{-3})		0.333 and -0.302

References

References

1 L. R. Milgrom, 'The colours of life : an introduction to the chemistry of porphyrins and related compounds', Oxford University Press, 1997.

2 R. M. Christie, 'Colour Chemistry', The Royal Society of Chemistry, 2001.

3 J. Clayden, 'Organic chemistry', Oxford University Press, 2001.

4 D. R. Waring and G. Hallas, 'The Chemistry and application of dyes', Plenum Press, 1990.

5 K. W. Bentley, 'The natural pigments', Interscience Publishers, 1960.

6 K. Venkataraman, 'The chemistry of synthetic dyes : Edited by K. Venkataraman', Academic Press, 1952.

7 F. Mayer and A. H. Cook, 'Chemie der organischen Farbstoffe
The chemistry of natural coloring matters : the constitutions, properties, and biological relations of the important natural pigments', Reinhold publishing corporation, 1943.

8 E. Puketapu-Hetet, 'Maori weaving with Erenora Puketapu-Hetet', Pitman Publishing, 1989.

9 E. J. W. Barber, 'Prehistoric Textiles', Prinston University Press, 1991.

10 R. Te Kanawa, S. Thomsen, G. Smith, I. Miller, C. Andary, and D. Cardon, *Dyes in History and Archaeology*, 2002, **18**, 47.

11 W. Arbeit, 'Tapa in Tonga', Palm Frond Productions, 1994.

12 K. E. James, 'Making Mats and Barkcloth in the Kingdom of Tonga', Australia, c1988.

13 Pliny The Elder, 'Natural History', 1938-1963.

14 A. F. Kendrick, 'Catalogue of Textiles from Burying-grounds in Egypt', H. M. Stationary Office, 1922.

15 G. J. Smith, I. J. Miller, and V. Daniels, *Journal of Photochemistry Photobiology*, 2005, **169**, 147.

16 N. Moore, G. Smith, R. Te Kanawa, and I. Miller, *Dyes in History and Archaeology*, 2003, **19**, 144.

[17] S. G. Telfer, 'The Photochemistry of Cobalt(III)-Aminoacidato Complexes', University of Canterbury, Christchurch, 1999.

[18] B. P. Branchaud, M. S. Meier, and Y. Choi, *Tetrahedron Letters*, 1988, **29**, 167.

[19] W. Adam, F. Kita, and R. S. Oestrich, *Journal of Photochemistry and Photobiology, A: Chemistry*, 1994, **80**, 187.

[20] M. Abe, M. Nojima, and A. Oku, *Tetrahedron Letters*, 1996, **37**, 1833.

[21] W. Adam and B. Walther, *Tetrahedron*, 1996, **52**, 10399.

[22] J. Perez-Prieto, M. C. Morant-Minana, R. E. Galian, and M. A. Miranda, *Photochemistry and Photobiology*, 2006, **82**, 231.

[23] G. Smith, R. T. Kanawa, I. Miller, and G. Fenton, *Dyes in History and Archaeology*, 2005, **20**, 89.

[24] A. L. Poznyak and V. I. Pavlovskii, *Angewandte Chemie International Edition in English*, 1988, **27**, 789.

[25] A. L. Poznyak and L. V. Stopolyanskaya, *Zhurnal Neorganicheskoi Khimii*, 1995, **40**, 1122.

[26] E. Natarajan and P. Natarajan, *Inorganic Chemistry*, 1992, **31**, 1215.

[27] M. G. Lewis, 'The Photochemistry and Kinetic Studies of Cobalt (III) Complexes Containing Coordinated Amino Acids', Masters of Science, University of Canterbury, Christchurch, 2002.

[28] E. Constable, 'Progress in inorganic chemistry', ed. K. D. Karlin, Wiley [etc.], 1959.

[29] A. G. Blackman, *Comptes Rendus Chimie*, 2005, **8**, 107.

[30] R. L. Fanshawe, A. Mobinikhaledi, C. R. Clark, and A. G. Blackman, *Inorganica Chimica Acta*, 2000, **307**, 26.

[31] S. Nonogaki, Y. Yoneda, and S. Makishima, *Nippon Kagaku Zasshi*, 1959, **80**, 427.

[32] B. Graham, G. D. Fallon, M. T. W. Hearn, D. C. R. Hockless, G. Lazarev, and L. Spiccia, *Inorganic Chemistry*, 1997, **36**, 6366.

[33] A. W. Adamson, *Discussions of the Faraday Society*, 1960, **29**, 163.

[34] A. W. Adamson and A. H. Sporer, *Journal of the American Chemical Society*, 1958, **80**, 3865.

[35] A. L. Poznjak, V. I. Pavlovskii, E. B. Chuklanova, T. N. Polynova, and P.-K. M. A., *Monatsh. Chem*, 1982, **113**, 561.

[36] A. L. Poznjak and V. V. Pansevich, *Zh. Neorg. Khim.*, 1979, **24**, 713.

[37] V. I. Pavlovskii and A. L. Poznjak, *Zeitschrift fuer Anorganische und Allgemeine Chemie*, 1985, **25**, 447.

[38] A. L. Poznjak and V. I. Pavlovskii, *Koord. Khim*, 1987, **13**, 1381.

[39] A. L. Poznjak and V. V. Pansevich, *Russian Journal of Inorganic Chemistry*, 1991, **36**, 1425.

[40] P. Natarajan and G. Ferraudi, *Inorganic Chemistry*, 1981, **20**, 3708.

[41] E. Natarajan and P. Natarajan, *Inorganica Chimica Acta*, 1989, **155**, 1.

[42] A. L. Poznjak and V. I. Pawlowski, *Zeitschrift fuer Anorganische und Allgemeine Chemie*, 1982, **485**, 225.

[43] D. Meyerstein and H. A. Schwarz, *Journal of the Chemical Society, Faraday Transactions 1: Physical Chemistry in Condensed Phases*, 1988, **84**, 2933.

[44] D. C. Woska and B. B. Wayland, *Inorganica Chimica Acta*, 1998, **270**, 197.

[45] Y. Sorek, H. Cohen, and D. Meyerstein, *Journal of the Chemical Society, Faraday Transactions 1: Physical Chemistry in Condensed Phases*, 1989, **85**, 1169.

[46] A. Bakac and J. H. Espenson, *Journal of the American Chemical Society*, 1984, **106**, 5197.

[47] A. M. Tait, M. Z. Hoffman, and E. Hayon, *International Journal for Radiation Physics and Chemistry*, 1976, **8**, 691.

[48] T. S. Roche and J. F. Endicott, *Journal of the American Chemical Society*, 1972, **94**, 8622.

[49] C. Y. Mok and J. F. Endicott, *Journal of the American Chemical Society*, 1978, **100**, 123.

[50] J. Stubbe, *The Journal of biological chemistry*, 1990, **265**, 5329.

[51] T. Toraya, *Chemical reviews*, 2003, **103**, 2095.

[52] J. Lilie, N. Shinohara, and M. G. Simic, *Journal of the American Chemical Society*, 1976, **98**, 6516.

[53] P. Natarajan and J. F. Endicott, *Journal of the American Chemical Society*, 1972, **94**, 3635.

[54] P. Natarajan and J. F. Endicott, *Journal of Physical Chemistry*, 1973, **77**, 2049.

[55] C. H. Langford and G. W. Quance, *Canadian Journal of Chemistry*, 1977, **55**, 3132.

[56] P. Natarajan and J. F. Endicott, *Journal of the American Chemical Society*, 1973, **95**, 2470.

[57] A. L. Poznyak and V. E. Stel'mashok, *Inorganica Chimica Acta*, 1984, **83**, L59.

[58] V. E. Stel'mashok, S. A. Mechkovskii, and A. L. Poznyak, *Zhurnal Neorganicheskoi Khimii*, 1985, **30**, 391.

[59] S.-K. Kim, S.-Y. Choi, and Y.-S. Ko, *Journal of the Korean Chemical Society*, 2004, **48**, 461.

[60] A. V. Kurnoskin, *Journal of Applied Polymer Science*, 1992, **46**, 1509.

[61] N. Naujoks and A. Stemmer, *Colloids and Surfaces, A: Physicochemical and Engineering Aspects*, 2004, **249**, 69.

[62] S.-J. Park and M. Kim, *Abstracts of Papers, 230th ACS National Meeting, Washington, DC, United States, Aug. 28-Sept. 1, 2005*, 2005, COLL.

[63] J. A. Camarero, *Biophysical Reviews and Letters*, 2006, **1**, 1.

[64] D. Fiedler, H. Leung Dennis, G. Bergman Robert, and N. Raymond Kenneth, *Accounts of chemical research*, 2005, **38**, 349.

[65] V. Maurizot, M. Yoshizawa, M. Kawano, and M. Fujita, *Dalton Transactions*, 2006, 2750.

[66] T. Kusukawa and M. Fujita, *Journal of the American Chemical Society*, 1999, **121**, 1397.

[67] N.-C. Reichardt and M. Martin-Lomas, *ARKIVOC (Gainesville, FL, United States)*, 2005, 133.

[68] A. L. Poznyak and V. I. Pavlovskii, *Zeitschrift fuer Chemie*, 1981, **21**, 74.

[69] R. M. Hartshorn and S. G. Telfer, *Journal of the Chemical Society, Dalton Transactions: Inorganic Chemistry*, 1999, 3217.

[70] S. T. Spees and A. W. Adamson, *Inorg. Chem.*, 1962, **1**, 531.

[71] A. L. Poznyak and V. E. Stel'mashok, *Zhurnal Neorganicheskoi Khimii*, 1991, **36**, 1421.

[72] T.-T. Chou, F. Mei, T.-F. Tang, and J.-P. Chang, *Huaxue Xuebao*, 1965, **31**, 203.

[73] E. B. Chuklanova, T. N. Polynova, M. A. Porai-Koshits, A. L. Poznyak, and V. I. Pavlovskii, *Koordinatsionnaya Khimiya*, 1988, **14**, 103.

[74] M. Du, X. J. Zhao, and H. Cai, *Zeitschrift fuer Kristallographie - New Crystal Structures*, 2004, **219**, 463.

[75] G. G. Melikyan, A. Floruti, L. Devletyan, P. Toure, N. Dean, and L. Carlson, *Organometallics*, 2007, **26**, 3173.

[76] M. Mathews, K. S. Viswanathan, and N. R. Kunchur, *Acta Cryst.*, 1961, **14**, 1007.

[77] P. King, R. Clerac, C. E. Anson, and A. K. Powell, *Dalton Transactions*, 2004, 852.

[78] L. C. Nathan and T. D. Mai, *Journal of Chemical Crystallography*, 2000, **30**, 509.

[79] R. Q. Fang, Z. P. Xiao, P. Cao, D. H. Shi, and H. L. Zhu, *Acta Crystallographica, Section C: Crystal Structure Communications*, 2007, **C63**, m193.

[80] X.-Y. Yi, B. Liu, R. Jimenez-Aparicio, A. Urbanos Francisco, S. Gao, W. Xu, J.-S. Chen, Y. Song, and L.-M. Zheng, *Inorganic chemistry*, 2005, **44**, 4309.

[81] L. A. Zasurskaya, I. N. Polyakova, V. B. Rybakov, T. N. Polynova, A. L. Poznyak, and V. S. Sergienko, *Crystallography Reports*, 2006, **51**, 448.

[82] Z.-P. Deng, S. Gao, L.-H. Huo, and H. Zhao, *Acta Crystallographica, Section E: Structure Reports Online*, 2006, **E62**, m3230.

[83] A. R. Kennedy, J. B. A. Kirkhouse, and L. Whyte, *Inorganic Chemistry*, 2006, **45**, 2965.

[84] J. M. Harrowfield, R. P. Sharma, B. W. Skelton, P. Venugopalam, and A. H. White, *Australian Journal of Chemistry*, 1998, **51**, 775.

[85] J. R. Nitschke, D. Schultz, G. Bernardinelli, and D. Gerard, *Journal of the American Chemical Society*, 2004, **126**, 16538.

[86] L. A. Zasurskaya, A. L. Poznyak, T. N. Polynova, V. B. Rybakov, and M. A. Porai-Koshits, *Zhurnal Neorganicheskoi Khimii*, 1996, **41**, 1647.

[87] T. Yi, S. Gao, and B. Li, *Polyhedron*, 1998, **17**, 2243.

[88] H. A. Weakliem and J. L. Hoard, *Journal of the American Chemical Society*, 1959, **81**, 549.

[89] Y. Baran and G. Lawrance, *Turkish Journal of Chemistry*, 2002, **26**, 771.

[90] J. M. Harrowfield, Y. Kim, M. Mocerino, B. W. Skelton, and A. H. White, *Journal of the Chemical Society, Dalton Transactions: Inorganic Chemistry*, 1995, 2431.

[91] A. McAuley, K. Beveridge, S. Subramanian, and T. W. Whitcombe, *Journal of the Chemical Society, Dalton Transactions: Inorganic Chemistry (1972-1999)*, 1991, 1821.

[92] A. McAuley, K. Beveridge, S. Subramanian, and T. W. Whitcombe, *Canadian Journal of Chemistry*, 1989, **67**, 1657.

[93] A. A. Achilleos, L. R. Gahan, and K. A. Nicolaidis, *Australian Journal of Chemistry*, 1989, **42**, 649.

[94] A. McAuley, S. Subramanian, and T. W. Whitcombe, *Journal of the Chemical Society, Chemical Communications*, 1987, 539.

[95] A. T. Phillip, *Australian Journal of Chemistry*, 1968, **21**, 2301.

[96] J. van Alphen, *Recueil des Travaux Chimiques des Pays-Bas et de la Belgique*, 1938, **57**, 265.

[97] Z. Wang, J. Wang, M. Li, and S. Wang, in 'Manufacture of neopentyltetraethylene diamine transfer-promoting dendrimer membrane for separating CO2', Cn, 2006.

[98] L. R. Gahan, K. E. Hart, C. H. L. Kennard, M. A. Kingston, G. Smith, and T. C. W. Mak, *Inorganica Chimica Acta*, 1986, **116**, 5.

[99] H. L. Herzog, *Organic Syntheses*, 1951, **31**, 82.

[100] P. V. Bernhardt, P. Comba, L. R. Gahan, and G. A. Lawrance, *Australian Journal of Chemistry*, 1990, **43**, 2035.

[101] P. V. Bernhardt, G. A. Lawrance, and D. F. Sangster, *Polyhedron*, 1991, **10**, 1373.

[102] O. Costisor and W. Linert, *Reviews in Inorganic Chemistry*, 2000, **20**, 63.

[103] A. A. Achilleos, L. R. Gahan, K. A. Nicolaidis, and T. W. Hambley, *Journal of the Chemical Society, Chemical Communications*, 1988, 912.

[104] L. P. Klemann, in 'Bi- or polymetallic coordination complex', Us, 1986.

[105] M. R. C. Couri, M. Vieira de Almeida, A. P. S. Fontes, J. D. A. S. Chaves, E. T. Cesar, R. J. Alves, E. C. Pereira-Maia, and A. Garnier-Suillerot, *European Journal of Inorganic Chemistry*, 2006, 1868.

[106] C. Y. Ng, A. E. Martell, and R. J. Motekaitis, *Inorganic Chemistry*, 1983, **22**, 721.

[107] Y. B. Wei and P. Yang, *Chinese Chemical Letters*, 2005, **16**, 537.

[108] M. Formica, L. Giorgi, V. Fusi, M. Micheloni, and R. Pontellini, *Polyhedron*, 2002, **21**, 1351.

[109] B. D. Palmer, G. Wickham, D. J. Craik, W. D. McFadyen, L. P. G. Wakelin, B. C. Baguley, and W. A. Denny, *Anti-Cancer Drug Design*, 1992, **7**, 385.

[110] L. Casella and S. Ghelli, *Inorganic Chemistry*, 1983, **22**, 2458.

[111] D. A. Buckingham and C. R. Clark, 'Comprehensive Coordination Chemistry', ed. G. Wilkinson, Pergamon, 1987.

[112] J. Clayden, N. Greeves, S. Warren, and P. Wothers, 'Organic Chemistry', Oxford University Press, 2001.

[113] M. S. Okamoto and E. K. Barefield, *Inorganica Chimica Acta*, 1976, **17**, 91.

[114] N. G. Connelly, Royal Society of Chemistry (Great Britain), International Union of Pure and Applied Chemistry. Division of Chemical Nomenclature and Structure Representation., International Union of Pure and Applied Chemistry. Division of Inorganic Chemistry., and International Union of Pure and Applied Chemistry., 'Nomenclature of inorganic chemistry : IUPAC recommendations 2005', RSC Pub., 2005.

[115] P. Gentschev, A. A. Feldmann, M. Luken, N. Moller, H. Sirges, and B. Krebs, *Inorganic Chemistry Communications*, 2002, **5**, 64.

[116] F. H. Fry, G. D. Fallon, and L. Spiccia, *Inorganica Chimica Acta*, 2003, **346**, 57.

[117] F. H. Fry, L. Spiccia, P. Jensen, B. Moubaraki, K. S. Murray, and E. R. T. Tiekink, *Inorganic Chemistry*, 2003, **42**, 5594.

[118] B. Graham, L. Spiccia, A. M. Bond, M. T. W. Hearn, and C. M. Kepert, *Journal of the Chemical Society, Dalton Transactions*, 2001, 2232.

[119] H.-J. Wang, C.-T. Wu, and B.-S. Luo, *Jiegou Huaxue*, 1998, **17**, 119.

[120] L. J. Farrugia, P. A. Lovatt, and R. D. Peacock, *Journal of the Chemical Society, Dalton Transactions: Inorganic Chemistry*, 1997, 911.

[121] B. Graham, L. Spiccia, B. W. Skelton, A. H. White, and D. C. R. Hockless, *Inorganica Chimica Acta*, 2005, **358**, 3974.

[122] K. P. McCue, J. D. A. Voss, C. Marks, and J. R. Morrow, *Journal of the Chemical Society, Dalton Transactions: Inorganic Chemistry*, 1998, 2961.

[123] S. J. Brudenell, L. Spiccia, A. M. Bond, G. D. Fallon, D. C. R. Hockless, G. Lazarev, P. J. Mahon, and E. R. T. Tiekink, *Inorganic Chemistry*, 2000, **39**, 881.

[124] S. J. Brudenell, L. Spiccia, D. C. R. Hockless, and E. R. T. Tiekink, *Journal of the Chemical Society, Dalton Transactions: Inorganic Chemistry*, 1999, 1475.

[125] S. J. Brudenell, L. Spiccia, A. M. Bond, P. C. Mahon, and D. C. R. Hockless, *Journal of the Chemical Society, Dalton Transactions: Inorganic Chemistry*, 1998, 3919.

[126] S. J. Brudenell, L. Spiccia, A. M. Bond, P. Comba, and D. C. R. Hockless, *Inorganic Chemistry*, 1998, **37**, 3705.

[127] P. L. Holland, C. J. Cramer, E. C. Wilkinson, S. Mahapatra, K. R. Rodgers, S. Itoh, M. Taki, S. Fukuzumi, L. Que, Jr., and W. B. Tolman, *Journal of the American Chemical Society*, 2000, **122**, 792.

[128] H. Wang, M. Hu, and C. Wu, *Wuhan University Journal of Natural Sciences*, 1997, **2**, 321.

[129] A. R. Battle, B. Graham, L. Spiccia, B. Moubaraki, K. S. Murray, B. W. Skelton, and A. H. White, *Inorganica Chimica Acta*, 2006, **359**, 289.

[130] B. Graham, M. T. W. Hearn, P. C. Junk, C. M. Kepert, F. E. Mabbs, B. Moubaraki, K. S. Murray, and L. Spiccia, *Inorganic Chemistry*, 2001, **40**, 1536.

[131] B. Graham, M. J. Grannas, M. T. W. Hearn, C. M. Kepert, L. Spiccia, B. W. Skelton, and A. H. White, *Inorganic Chemistry*, 2000, **39**, 1092.

[132] E. Fremy, *Ann. Chem. Phys.*, 1852, **25**, 257.

[133] A. Werner and A. Miolati, *Zeitschrift fuer Physikalische Chemie, Stoechiometrie und Verwandtschaftslehre*, 1893, **12**, 35.

[134] G. B. Kauffmann, 'Classics In Coordination Chemistry Part I: The Selected Papers of Alfred Werner', Dover, 1968.

[135] H. Koyama and T. Yoshino, *Bulletin of the Chemical Society of Japan*, 1972, **45**, 481.

[136] G. H. Searle and R. J. Geue, *Australian Journal of Chemistry*, 1984, **37**, 959.

[137] R. M. Hartshorn and S. G. Telfer, *Dalton*, 2000, 2801.

[138] A. M. Josceanu, P. Moore, and P. Sheldon, *Revue Roumaine de Chimie*, 1998, **43**, 945.

[139] K. Yamanari, I. Fukuda, T. Kawamoto, Y. Kushi, A. Fuyuhiro, N. Kubota, T. Fukuo, and R. Arakawa, *Inorganic Chemistry*, 1998, **37**, 5611.

[140] J. L. Burmeister, *Coordination Chemistry Reviews*, 1968, **3**, 225.

[141] W. G. Jackson, *Inorganic Chemistry*, 1987, **26**, 3857.

[142] W. G. Jackson, M. L. Randall, A. M. Sargeson, and W. Marty, *Inorganic Chemistry*, 1983, **22**, 1013.

[143] W. G. Jackson, G. A. Lawrance, P. A. Lay, and A. M. Sargeson, *Inorganic Chemistry*, 1980, **19**, 904.

[144] G. B. Kauffman, *Coordination Chemistry Reviews*, 1973, **11**, 161.

[145] W. G. Jackson, G. A. Lawrance, P. A. Lay, and A. M. Sargeson, *Australian Journal of Chemistry*, 1982, **35**, 1561.

[146] D. A. House and W. G. Jackson, *Inorganica Chimica Acta*, 1998, **274**, 42.

[147] J. I. Legg and D. W. Cooke, *Inorg. Chem.*, 1965, **4**, 1576.

[148] Y. Ida, K. Imai, and M. Shibata, *Bulletin of the Chemical Society of Japan*, 1978, **51**, 2741.

[149] B. Krebs, K. Schepers, B. Bremer, G. Henkel, E. Althaus, W. Mueller-Warmuth, K. Griesar, and W. Haase, *Inorganic Chemistry*, 1994, **33**, 1907.

[150] A. Neves, S. M. D. Erthal, V. Drago, K. Griesar, and W. Haase, *Inorganica Chimica Acta*, 1992, **197**, 121.

[151] A. Neves, L. M. Rossi, I. Vencato, V. Drago, W. Haase, and R. Werner, *Inorganica Chimica Acta*, 1998, **281**, 111.

[152] A. Neves, L. M. Rossi, A. J. Bortoluzzi, A. S. Mangrich, W. Haase, and R. Werner, *Journal of the Brazilian Chemical Society*, 2001, **12**, 747.

[153] H. Adams, D. Bradshaw, and D. E. Fenton, *Journal of the Chemical Society, Dalton Transactions*, 2002, 925.

[154] E. Longhinotti, J. B. Domingos, B. Szpoganicz, A. Neves, and F. Nome, *Inorganica Chimica Acta*, 2005, **358**, 2089.

[155] A. Tatehata, *Inorganic Chemistry*, 1982, **21**, 2496.

[156] C. A. Otter and R. M. Hartshorn, *Dalton Transactions*, 2004, 150.

[157] R. M. Hartshorn, in 'Laboratory Book', 2006.

[158] S. Kirschner, *Inorganic Syntheses (McGraw-Hill Book Co., Inc., New York, N.Y.)*, 1957, **5**, 186.

[159] M. Ouchi, Y. Inoue, Y. Liu, S. Nagamune, S. Nakamura, K. Wada, and T. Hakushi, *Bulletin of the Chemical Society of Japan*, 1990, **63**, 1260.

[160] X. Zhang, W.-Y. Hsieh, T. N. Margulis, and L. J. Zompa, *Inorganic Chemistry*, 1995, **34**, 2883.

[161] G. M. Sheldrick, in 'SADABS', University of Gottingen: Germany, 1998.

[162] G. M. Sheldrick, in 'SHELXTL', University of Gottingen: Germany, 1997.